The Thesis Committee for Katherine Blom Lininger
Certifies that this is the approved version of the following thesis:

The hydro-geomorphology of the middle Araguaia River: floodplain dynamics of the largest fluvial system draining the Brazilian *Cerrado*

APPROVED BY
SUPERVISING COMMITTEE:

Supervisor:

Edgardo M. Latrubesse

Kenneth R. Young

Carlos E. Ramos Scharrón

The hydro-geomorphology of the middle Araguaia River: floodplain dynamics of the largest fluvial system draining the Brazilian *Cerrado*

by

Katherine Blom Lininger, B.A.

Thesis

Presented to the Faculty of the Graduate School of

The University of Texas at Austin

in Partial Fulfillment

of the Requirements

for the Degree of

Master of Arts

The University of Texas at Austin

August 2013

Dedication

I would like to dedicate this thesis to my husband Micah Nelson and my parents, for their continuous love, support, and patience.

Acknowledgements

I would like to thank my advisor and committee members for their guidance and support: Dr. Edgardo M. Latrubesse (advisor), Dr. Kenneth R. Young, and Dr. Carlos E. Ramos Scharrón. I would also like to thank the faculty and graduate students in the Department of Geography at the University of Texas at Austin, for their support, advice, and camaraderie. I greatly appreciated the help and support provided by Maximiliano Bayer and his family during my fieldwork experience in Brazil. The Donald D. Harrington Graduate Fellowship, the National Science Foundation Graduate Research Fellowship, the Robert E. Veselka Fellowship, and the Lozano Long Graduate Summer Field Research Grant have provided me with generous support while completing my master's degree.

Abstract

The hydro-geomorphology of the middle Araguaia River: floodplain dynamics of the largest fluvial system draining the Brazilian *Cerrado*

Katherine Blom Lininger, M.A.

The University of Texas at Austin, 2013

Supervisor: Edgardo M. Latrubesse

Located in central Brazil, the Araguaia River is the largest river flowing through the *Cerrado*, the Brazilian savanna. The thesis presented here assesses the hydro-geomorphology of the middle Araguaia River-floodplain system by characterizing flooding patterns and linking these patterns to the geomorphology of the floodplain. It also determines the response of floodplain lake morphometry and surface water connectivity to the annual flooding of the river, and describes how different floodplain geomorphologic units influence changes in open water areas in the floodplain from the dry season to the wet season.

Peak discharges along the middle Araguaia River can be reduced downstream despite large increases in drainage area and the contribution of tributary inputs. After analyzing average daily discharge measurements from 1975 to 2007 along an upstream reach and a downstream reach in the middle Araguaia River, four main flooding types are characterized based on the magnitude of the peak discharge and the pattern of peak discharge reduction that occurs as the flood wave moves downstream. Short-term losses

of channel discharge during the flooding peak and over the flooding season from November to May are estimated, with the downstream reach displaying more short-term channel loss compared to the upstream study reach. Differences in floodplain geomorphological characteristics between the two study reaches, including the proportions of distinct geomorphologic units (a lower elevation impeded floodplain, a unit dominated by paleomeanders, and a unit of accreted banks and islands), influence the patterns of peak reduction and channel loss. Short-term losses of channel discharge during flooding peaks are usually re-gained by the channel by the end of the flooding season, although in two years about 10% of the volume input into the downstream reach was lost from the channel over the flooding season.

Using satellite imagery and an open water index, changes in lake area, perimeter, and surface water connectivity with the main channel between dry season and the wet season are determined for 32 floodplain lakes. The changes in lake morphometry and connectivity are linked to how fluvial processes formed the floodplain lakes. Spatial variations in the floodplain areas that became open water from the dry season to the wet season demonstrate that distinct floodplain geomorphologic units influence the extent and location of open water areas during flooding. Floodplain lakes that expand in area and in depth and are connected to the river channel via surface water likely provide storage areas for the channel losses and peak discharge reductions observed in some of the flooding types for the middle Araguaia River.

Although there have been attempts to plan the placement of dams on the Araguaia River, the river is not impounded, allowing for the analysis of a river system with an unaltered flow regime. This thesis contributes to knowledge of a large and understudied tropical river in an ecologically sensitive region.

Table of Contents

List of Tables

List of Figures

Chapter 1: Introduction, research objectives, and background

The Araguaia River in central Brazil is the largest river draining the Brazilian savanna, or *Cerrado*. The Araguaia River is located in the tropics, and while there is a growing body of literature on tropical river systems, these systems are still understudied (Latrubesse et al. 2005). The Araguaia River is situated in a tropical wet-dry climate, and the middle Araguaia River has created an alluvial floodplain with many floodplain lakes formed by fluvial processes. During the flooding season, which spans a period of 6 months, large amounts of water are exchanged between the middle Araguaia River and its floodplain, in some cases resulting in the reduction of peak discharge downstream despite large increases in drainage area and the input of tributaries (Aquino et al. 2008; Latrubesse and Stevaux 2002; Latrubesse et al. 2005). Based on available literature, the downstream reduction in peak discharge despite increases in drainage area and tributary inputs in the middle Araguaia River is yet to be observed in other large tropical systems with similar geomorphologic and climatic characteristics. Floodplain lakes acting as storage areas presumably play a role in this peak reduction, among other potential causes. The response of floodplain lakes to the flooding season is controlled by the geomorphologic characteristics of the lakes and the hydrology of the river (Morais et al. 2005). The thesis presented here assesses the hydro-geomorphology of river-floodplain interactions by characterizing the hydrologic patterns of flooding on the middle Araguaia River and the changes in floodplain lake morphometry and open water areas in the floodplain, providing a geomorphologic context for these processes.

The Araguaia River is not dammed, but the basin as a whole has experienced rapid land clearing beginning in the early 1970s, with only about half of the native *Cerrado* ecosystem remaining (Sano et al. 2010; Klink and Machado 2005). Despite the

impacts of land use change, the lack of dams on the river provides an opportunity to understand and analyze flooding patterns and changes in floodplain water bodies in a tropical river system in which the hydrological regime has not been drastically altered by impoundments. This chapter introduces the objectives of the thesis, the reasons that these objectives are important, and the contribution the research presented here makes to knowledge of the middle Araguaia River and to tropical river-floodplain systems in general.

RESEARCH OBJECTIVES

In order to analyze flooding patterns and floodplain lakes in the middle Araguaia River, the following four objectives will be addressed:

1. Describe the characteristics of the Araguaia River, including its geomorphology, hydrology, and ecology, and provide a review of the land-use changes occurring in the watershed (Chapter 2).

2. Determine the patterns of peak discharge reduction and characterize these patterns into flooding types, estimate the volumetric reduction in discharge during peak flooding, assess whether downstream discharge reductions result in channel discharge losses over the flooding season, and relate these patterns to the geomorphologic characteristics of the floodplain (Chapter 3).

3. Assess how floodplain lakes respond to flooding through changes in lake morphometry, determine which regions of the floodplain become open water during flooding, and investigate how geomorphologic factors influence changes in floodplain lake morphometry and open water areas (Chapter 4).

4. Describe fieldwork conducted in July 2012 and future work that will determine floodplain sedimentation rates in the middle Araguaia River (Appendix).

GEOMORPHOLOGY, CHANNEL-FLOODPLAIN INTERACTIONS, AND FLOODING PATTERNS

The Araguaia River is a large tropical river located in a wet-dry climate (Latrubesse et al. 2005). During the wet season, which occurs over a period of about six months and lags slightly behind the onset of the rainy season, river discharge rises over a few months, a common hydrologic characteristic of other large river systems in tropical wet and tropical wet-dry climates (Latrubesse et al. 2005; Wohl 2007). In the Araguaia River, discharge rises slowly up to a peak discharge and then gradually declines, although within the flooding season there can be multiple peaks of the flood wave, usually with one dominant peak discharge during the wet season (Agencia Nacional de Aguas; Aquino et al. 2008). The flood wave in the Araguaia River is not a response to a single precipitation event; it is a multi-month response to the seasonal climate.

The middle Araguaia River has an anabranching pattern, which means it maintains multiple channels separated by fluvial islands (Nanson and Knighton 1996). Over time its depositional and erosional processes have created an associated floodplain, which becomes inundated with the arrival of the wet season. As described in an introductory fluvial geomorphology text book, a floodplain is "a relatively flat alluvial depositional landform that borders river channels and is periodically inundated by floodwater" (Charlton 2007, 205). Floodplain inundation is not only caused by the river reaching bankfull discharge and overtopping its banks; it can also result from groundwater inputs, overland flow from the surrounding area, direct rainfall, flow through floodplain drainage channels, flow to floodplain water bodies connected to the main channel, and water contributed from tributaries (Richey et al. 1989; Mertes et al. 1995; Mertes 1997). Flooding drives the exchange of water, nutrients, and sediments between the river and its floodplain (Junk et al. 1989; Tockner et al. 2000). The processes of flood transmission (i.e., how a flood wave moves downstream) and floodplain

inundation are complex. Floodplain and river geomorphology exert controls on flood transmission, flooded areas, and the degree of connectivity between the river and floodplain water bodies by providing the physical structure for these processes (Morais et al. 2005; Mertes et al. 1995).

Flooding hydrology also exerts controls on channel and floodplain geomorphology. Flooding increases sediment transport and influences the geomorphologic characteristics of the channel and floodplain, as the river rises up to and beyond bankfull discharge, which has been shown to do the most geomorphologic work and control channel and floodplain geomorphology (Wolman and Miller 1960). As discharges rise and sediment loads increase, lateral sedimentation and lateral accretion of bars and islands help to form the alluvial floodplain, and overbank floods above bankfull discharge create vertical accretion of finer sediments on the floodplain (Wolman and Miller 1960; Leopold et al. 1964), highlighting the importance of understanding flooding regimes.

Many frameworks for assessing spatial and temporal flooding patterns and floodplain inundation do not fully take into account geomorphologic controls, focusing mainly on hydrology and ecology. For example, the "flood pulse concept" describes the lateral exchange of nutrients, organisms, and sediment that occurs in large river-floodplain systems with regular flooding pulses, which helps sustain fish and other aquatic organisms (Junk et al. 1989). While the exchange of sediments and nutrients between the river and the floodplain is in part a result of river hydrology, the flood pulse concept and expansions on this framework (e.g., Puckridge et al. 1998; Junk 2004; Tockner et al. 2000) tend to exclude a full assessment of how geomorphologic factors control the connectivity of floodplain water bodies, the spatial and temporal characteristics of flooding, and the development of floodplain ecosystems.

There are floodplain studies of large tropical river systems that integrate geomorphology with other aspects of the floodplain system. For example, geomorphologic units specific to the Negro River floodplain along a 600 km stretch of the river in Brazil correspond with certain vegetation assemblages of the its floodplain forest, or "igapó," and influence floristic diversity, tree density, and tree heights (Montero and Latrubesse 2013). In the Paraná River floodplain, geomorphology controls vegetation type and vegetation cover (Marchetti et al. 2013) . Mertes et al. (1995) characterized the patterns of floodplain inundation between areas of the Amazon River and its floodplain with differing geomorphologic characteristics and found geomorphologic-dependent patterns in vegetation as well. The geomorphologic features controlled inundation patterns and the mixing of different types of surface water, influencing wetland vegetation.

In the middle Araguaia River floodplain, distinct geomorphologic units have been defined, including a unit dominated by paleomeanders, a unit of bars and islands that have been attached to the floodplain, and older, lower elevation floodplain unit (Latrubesse and Stevaux 2002). Studies have shown that different vegetation assemblages are associated with these geomorphologic units (Morais et al. 2008). The geomorphologic units of the Bananal Island, which is formed by the middle Araguaia River and an abandoned belt of the Araguaia River, also influence vegetation assemblages (Valente et al. 2013). All of these studies take note of the physical and historical basis for the interactions between geomorphology, hydrology, and vegetation of channel-floodplain systems.

Studies have also discussed the geomorphology of floodplain lakes and how their morphology influences theirs responses to flooding. Latrubesse (2012) characterizes the floodplain lakes of the Amazon River and its tributaries and describes their fluvial

origins. Morais et al. (2005) demonstrate that in the Araguaia River floodplain, the morphometric response of lakes to flooding can be explained in part by their geomorphologic classification based on the process of formation, and this influences environments for aquatic organisms.

The Araguaia River displays a flooding behavior yet to be documented in other large tropical rivers with similar climates and geomorphologic characteristics, in that peak discharge reduces downstream despite large increases in drainage area and the contribution of tributaries (Aquino et al. 2008). Floodplain storage, which is the transfer and storage of river discharge during flooding and has been investigated in many tropical systems (e.g., Richey et al. 1989; Alsdorf et al. 2010; Frappart et al. 2005), can occur without net reductions of channel discharge downstream. Channel losses of discharge, or transmission losses, are commonly observed in rivers in arid climates over long periods of time (i.e., years) (Knighton and Nanson 1994; Lange 2005). For example, in the upper Niger River basin in West Africa, which is located in the tropics, river discharge decreases when the river enters an inland delta (Zwarts et al. 2005). There is high rainfall during the wet season upstream, but as the river flows into the inland delta, the climate shifts to semi-arid and river discharge is lost over the long term due in part to evaporation (Zwarts et al. 2005). However, the Araguaia River does not flow through an arid region when the discharge is reduced downstream.

The reduction in peak discharge previously documented in the middle Araguaia River will be characterized as a short-term channel loss in this thesis, in part because floodplain storage could be occurring in the middle Araguaia River without a net reduction of channel discharge downstream. However, this short-term loss may be re-gained by the channel as the flood wave passes. One objective of Chapter 3 is to determine whether channel losses occur over the entire flooding period (November to

May) or only during peak discharges. In the Upper Paraguay River basin, which is located in a wet-dry seasonal climate similar to the Araguaia River basin, the Paraguay River decreases in peak discharge when it enters the Pantanal wetland because the river develops into a depositional mega-fan system (Assine and Silva 2009; Paz et al. 2010). The middle Araguaia River-floodplain system is not a depositional fan system. Although the Paraguay River is an example of peak discharge reduction during flood waves in a large tropical wet-dry system, its geomorphologic setting differs from the middle Araguaia River.

CONTRIBUTION TO EXISTING KNOWLEDGE OF THE ARAGUAIA RIVER SYSTEM

Previous research has been conducted on the geomorphology and hydrology of the middle Araguaia River, and the analyses presented in this thesis adds to this existing body of work. The different geomorphic units of the floodplain and geomorphologic processes over time have been explained, hydrologic connectivity and morphometry of some of the types of floodplains lakes has been explored, the influences of geomorphic processes on vegetation assemblages have been described, and there has been a general characterization of the flow regime along the river itself (Morais et al. 2008; Latrubesse et al. 2009; Aquino et al. 2009; Aquino et al. 2008). This thesis adds to these efforts by providing a more detailed assessment of the middle Araguaia flooding patterns, estimating the volume of discharge reductions during flooding peaks, giving estimates of changes in open water area for different geomorphic units of the floodplain and for floodplain lakes, and describing spatial patterns of floodplain inundation pathways.

Previous analyses of flood transmission patterns on the middle Araguaia River used the maximum discharge measurements for each year at different locations along the

river, establishing that the middle Araguaia River can decrease in peak discharge downstream despite large increases in drainage area and tributary inputs, with large amounts of water presumed to be transferred to the floodplain (Aquino et al. 2008). The analyses in Chapter 3 differ from these previous efforts in that 1) average daily discharge measurements are utilized to characterize peak discharge reduction and flooding patterns, 2) short-term channel losses are estimated, and 3) whether short-term losses that occur during peak discharges can been seen over the six month flooding season is determined.

Previous studies have estimated the change in the area and perimeter of some of the types of floodplain lakes and their surface water connectivity with the main river channel in the study are for this thesis (Morais et al. 2005), and the area of inundation in the wider region (beyond the geomorphologic floodplain) due to flooding (Hamilton et al. 2002). However, there are currently no estimates of open water areas during large floods over the geomorphologic floodplain of the river. Analyzing the differences in open water area between the three geomorphologically-distinct floodplain units, which are fully described in Chapter 2 and mentioned previously, provides insights into the role floodplain geomorphology plays in spatial patterns of inundation. It is possible to determine if certain units are more or less susceptible to becoming open water due to their geomorphologic characteristics. In addition, some of the floodplain lake types (e.g., oxbow lakes, lakes formed by lateral accretion, meander scroll lakes, and others) and their morphometric changes between the wet and dry season have not been explored previously. In Chapter 4, open water area changes in different geomorphologic units of the floodplain and in floodplain lakes from the dry season (1987) to the wet season (1988) are assessed and surface water pathways of flooding are explored. In addition, the influence of the geomorphology of floodplain lakes and the floodplain are discussed. The analyses of flooding hydrology in Chapter 3 are related to the assessment of floodplain

lakes and the morphology of the floodplain, demonstrating the controls that floodplain geomorphology and fluvial processes have on channel-floodplain connectivity.

Finally, there are no current estimates of floodplain sedimentation rates in the system. The Appendix describes fieldwork that was completed in 2012 that will lead to insights into how much, at what rate, and what type of sediment is deposited on the middle Araguaia River floodplain.

CONTRIBUTION TO RESEARCH ON TROPICAL RIVER-FLOODPLAIN SYSTEMS

In the past 30 years, there has been an increase in studies analyzing channel-floodplain interactions and flooding patterns in tropical river systems. Different approaches have been taken in tropical river systems, including using remote sensing technologies to determine areas of inundation and to estimate the volume of water on the floodplain (e.g., Alsdorf et al. 2010; Hamilton et al. 2002; Frappart et al. 2005; Frappart et al. 2006). Flood routing and water balance approaches have also been used to model and estimate the fluxes of water between the channel and floodplain (e.g., Richey et al. 1989; Paz et al. 2011; Trigg et al. 2009).

Bonnet et al. (2008) analyzed one segment within the Amazon River floodplain, using synthetic aperture radar from the JERS-1 satellite, observational measurements, and modeling. They determined the fluxes between the Amazon River and a floodplain lake, the Lago Grande de Curuai, over a six-year period. Richey et al. (1989) completed a water budget and used a flood routing model along a 2,000-km stretch of the Amazon River, finding that a large percentage of the river discharge (30%) was temporarily stored on the floodplain during flooding. However, the authors did not include a discussion of the geomorphology of the floodplain and its role in floodplain water storage. Subsequent

studies investigated the patterns of flooding in geomorphically-distinct regions of the river and related geomorphology to the spatial patterns of flooding. For example, Mertes et al. (1995) described the diverse way in which floodplain inundation occurs along geomorphologically different reaches, highlighting the roles of water table rise, local tributary inputs, floodplain drainage channels, and overbank flooding in the Amazon River floodplain.

Floodplain inundation in the Amazon River floodplain has also been estimated using gravity measurements to determine changes in water mass (with data from GRACE satellites, the Gravity Recovery and Climate Experiment) and other satellite data, and the results indicate that water storage on the floodplain as a percentage of river discharge may be less than previous estimates (e.g., Alsdorf et al. 2010). GRACE data has been used to measure water storage in the entire Amazon Basin, detecting changes in flooding from 2002 to 2009 (Chen et al. 2010) and to determine changes in water storage in the Congo River and its surrounding wetlands along with additional satellite data (Lee et al. 2011). The inundated area of seasonal wetlands associated with six large rivers in South America, including the seasonal wetlands of the Araguaia River, the Amazon River, the Orinoco River, the Paraguay River, the Madeira River, and the Branco River (a tributary to the Negro River), has been estimated with passive microwave remote sensing data (Hamilton et al. 2002), but Hamilton et al. did not differentiate between the geomorphologic floodplains of these rivers and the larger regions. Modeling approaches for the Upper Paraguay River basin have been used to determine the extent of inundation in the region (Paz et al. 2011) and to model the flood wave as it moves downstream (Paz et al. 2011; Bravo et al. 2012; Paz et al. 2010). Trigg et al. (2012) assess floodplain drainage networks in the Amazon River floodplain, describing the various surface pathways for water movement between the main channel and the floodplain and

classifying different areas with distinct hydro-geomorphologic characteristics. Similarly, surface pathways for water movement between the river and the floodplain in the middle Araguaia River are described in Chapter 4.

The research presented here adds to the research on tropical river-floodplains by characterizing different types of flood wave transmission and the changes in open water areas and floodplain lakes on a river-floodplain system in a tropical wet-dry climate.

BROADER IMPACTS

The increase in hydro-electric dams in Brazil gives urgency to understanding the middle Araguaia River and its flooding patterns. The Brazilian government has investigated placing a dam on the river, although this has not yet occurred (Latrubesse et al. 2005). The Tocantins River has been dammed just downstream of the Araguaia-Tocantins confluence, causing changes in flow regimes, reduction of suspended sediment load downstream of the dam, lower numbers of fishes caught by fishermen, and loss of species (Manyari and Carvalho Jr. 2007; Merona 1986). Hydro-electric development can reduce connectivity between rivers and their floodplains, limiting the geomorphologic pathways for the exchange of nutrients between the channel and diverse floodplain environments (Thoms et al. 2005). Relative to other large tropical rivers, the Araguaia River transports a high percentage of its sediment load as sand and a smaller percentage of finer silt and clay (Aquino et al. 2009), to which nutrients more readily attach (Tockner et al. 2000). Any future impoundment resulting in flow regulation and a decrease in large floods could impede the delivery to the floodplain of the relatively small amount of fine sediment that is carried by the river channel. The spatial heterogeneity of river-floodplain systems provides a variety of ecological habitats for a diverse set of species, and the geomorphology of these systems impacts the hydrology and ecology of

the river-floodplain system (Montero and Latrubesse 2013; Mertes et al. 1995; Amoros and Bornette 2002). Anthropogenic climate change is predicted to intensify the hydrological processes in the tropics more than in the temperate zones, highlighting the need to better characterize and understand rivers systems in the tropics (Wohl et al. 2012). Climate change will also likely alter river hydrology, change thermal patterns within rivers and floodplains, and affect biogeochemical processes (Hamilton 2010), also indicating the need to monitor and understand river-floodplain systems.

The Araguaia River is now the last large river in central and southern Brazil that has not been dammed or engineered in any way, although rapid land clearing of the watershed has impacted the geomorphology of the river through increasing sedimentation within the system (Latrubesse et al. 2009). Enhancing knowledge of the role of geomorphology in flood transmission, floodplain lake environments, and open water areas is an opportunity to inform future management decisions and gain a better understanding of this important river-floodplain ecosystem.

Chapter 2: The Araguaia River: overview and human impacts

This chapter provides an overview of the Araguaia River, focusing on the middle Araguaia River. A review of the land use changes caused by soy bean and cattle expansion in the Brazilian *Cerrado* is also included, with a discussion of land clearing in the Araguaia watershed and its effects on the river's hydrology and geomorphology.

STUDY AREA

The Araguaia River watershed (Figure 2.1) is approximately 377,000 km^2 in drainage area, and the river's mean annual discharge is about 6,420 m^3s^{-1} (Latrubesse and Stevaux 2002). The Araguaia River flows into the Tocantins River, and the Araguaia-Tocantins system is the 13th largest tropical river system, with the Araguaia River by itself being the 28th largest tropical river (Latrubesse et al. 2005). Situated in Brazil's central highlands, the geology of the Araguaia River watershed includes Quaternary fluvial deposits and Precambrian, Paleozoic, and Mesozoic rock units (Latrubesse and Stevaux 2002). Latrubesse and Stevaux (2002) divide the Araguaia River into three main units: upper, middle, and lower (Figure 2.1). The 450 km upper section of the river, from the headwaters to Registro do Araguaia, is geologically-controlled, flowing in a V-shaped valley without a floodplain over Paleozoic and Mesozoic sedimentary and basaltic rocks. The 500 km lower section of the river extends from Conceição do Araguaia until the river flows into the Tocantins, and also lacks an alluvial floodplain, flowing over crystalline Precambrian rocks. Both the upper and lower courses of the river lack well-developed floodplains. In contrast, the 1,160 km middle Araguaia River (representing about 55% of the river's total length), from Registro do Araguaia to Conceição do Araguaia, has a well-developed floodplain and flows on alluvial sediments (Latrubesse and Stevaux 2002).

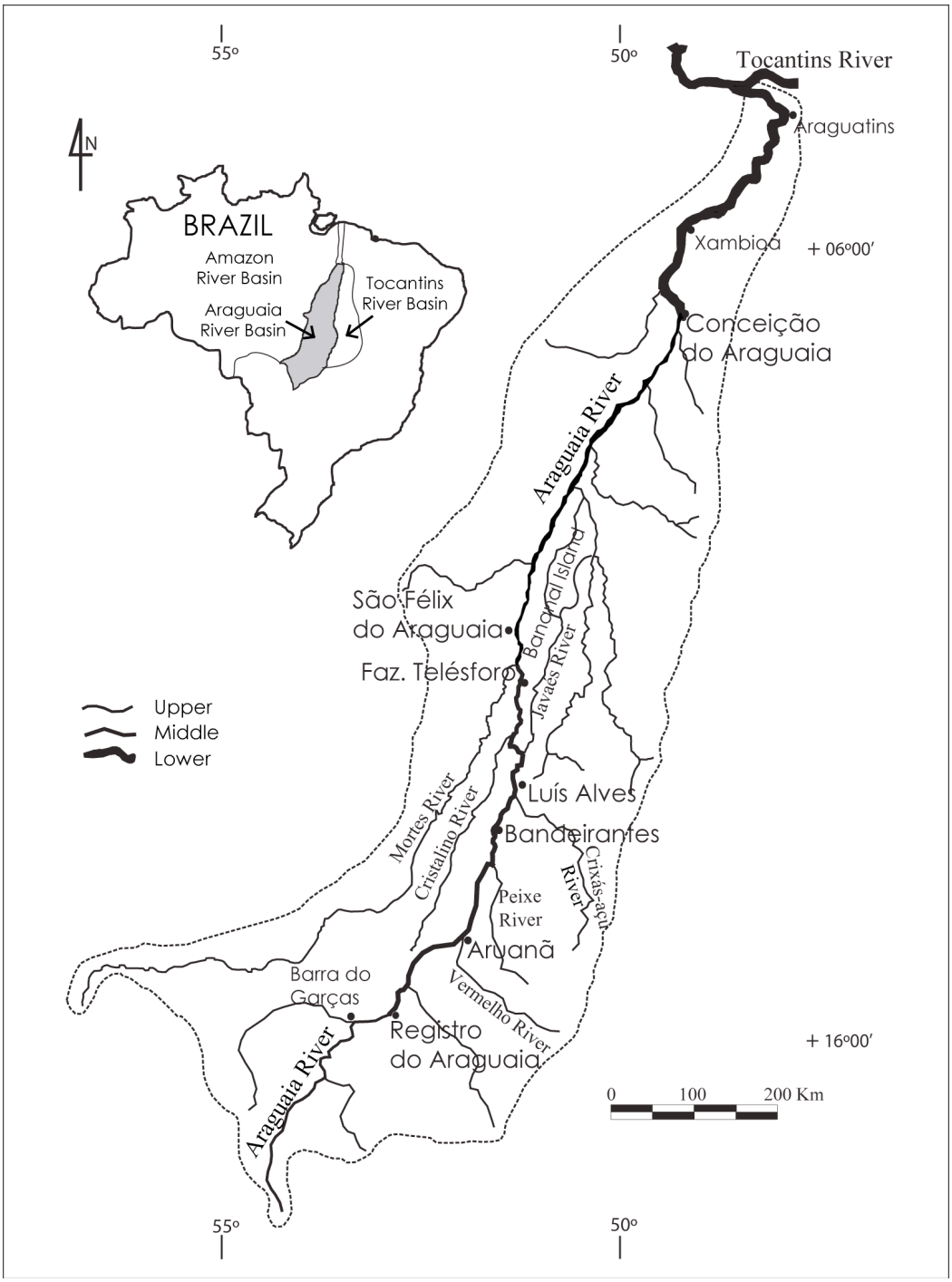

Figure 2.1. The Araguaia watershed in central Brazil. The upper section of the river is from the headwaters to Registro do Araguaia, the middle section is from Registro do Araguaia to Conceição do Araguaia, and the lower section is from Conceição do Araguaia to the confluence with the Tocantins River.

Hydrology and Climate

The region has a tropical wet-dry seasonal climate, which controls the patterns of flooding on the Araguaia River. The dry season occurs from approximately May to September and the rainy season occurs from October to April (Figure 2.2). Annual precipitation in the region ranges from 1,300 to 2,000 mm across the basin, with large seasonal variations in precipitation. On average, 95% of the annual rainfall occurs between October and April (Agencia Nacional de Aguas). Mean annual temperature ranges from 22° to 26° C (Valente and Latrubesse 2012). Peak flooding can lag slightly behind the onset of the rainy season, usually occurring during the months of November to May (Latrubesse and Stevaux 2002). The general pattern of river discharge is the same as in other tropical wet-dry rivers, with flooding occurring during the wet season and a pronounced difference between wet and dry season discharge (Latrubesse et al. 2005). The middle Araguaia River is seasonally flooded by rainwater, groundwater saturation, and river discharge. The geomorphologic characteristics of the three sections of the Araguaia River influence the hydrological regimes, with greater difference between high and low flows in the upper and lower courses compared to the middle course (see Chapter 3) (Aquino et al. 2008). At Barra do Garças, at the downstream end of the upper Araguaia River section, the peak annual flows are on average 16 times higher than the lowest annual flows (Aquino et al. 2008). From Aruanã to São Félix do Araguaia, the peak flows are 13 to 9 times the low flows, reflecting relatively lower peak flows and higher low flows along the middle section. At Conceição do Araguaia, the peaks are on average 17 times the low flows.

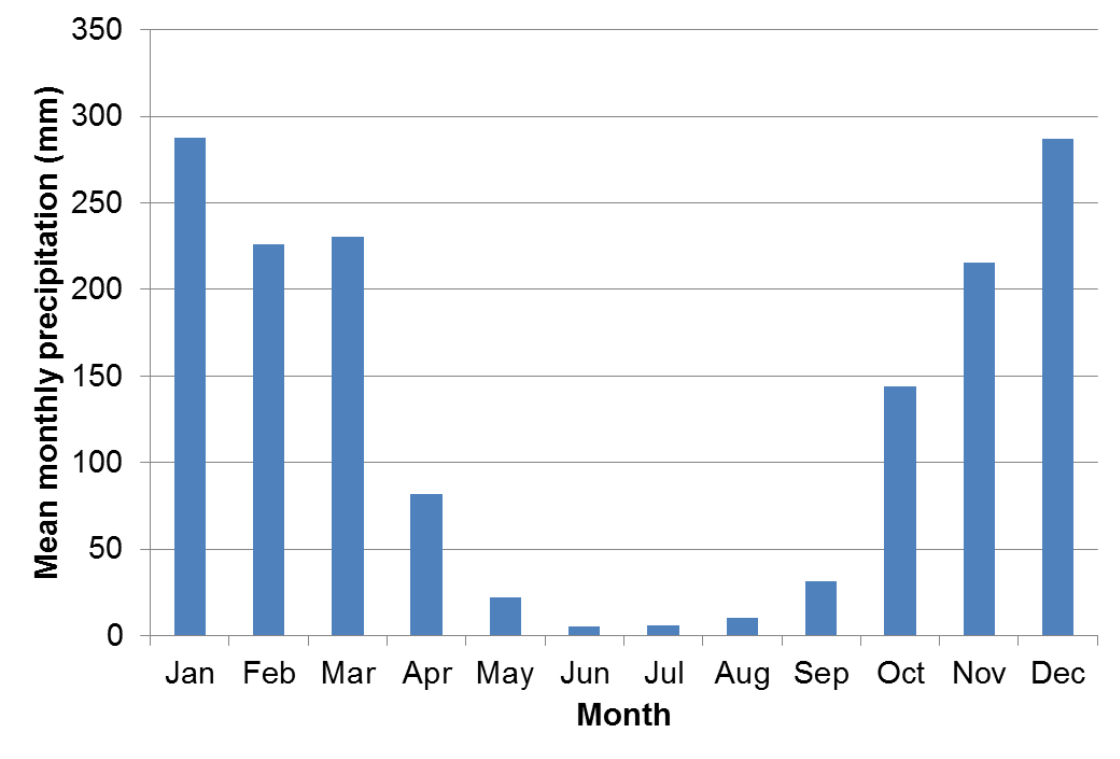

Figure 2.2. Average monthly precipitation from 1970 to 2004 at Aruanã (mm). The pattern of precipitation demonstrates the large variation between the wet season (October to April) and the dry season (May to September). Data from Agencia Nacional de Aguas.

Figure 2.3 displays the discharge records (1975 to 2007) for three gauging stations (Aruanã, Luís Alves, and Bandeirantes) in the middle Araguaia River that are used for analysis in Chapter 3 (Agencia Nacional de Aguas; discharge records were previously published by Aquino et al. 2008). The mean annual discharge, mean maximum discharge, and the bankfull discharge for each gauging station are included in each graph. The mean annual discharge and mean maximum discharge are computed for the period of record, from 1975 to 2007. Bankfull discharge data are from field data from Latrubesse (2008) for Aruanã and Luís Alves and from estimating the 1.5-year return flood using an EVI distribution at Bandeirantes (done by the author), which is one way to

estimate bankfull discharge (Dunne and Leopold 1978). Figure 2.4 shows discharge at the three gauging stations normalized by the mean annual discharge at that station. Normalized peak discharge decreases downstream from Aruanã to Luís Alves, showing that the peaks are generally reduced relative to the mean annual discharge at Bandeirantes and Luís Alves compared to Aruanã. The normalized peak discharge is particularly low at Luís Alves, as previously noted by Aquino et al. (2008).

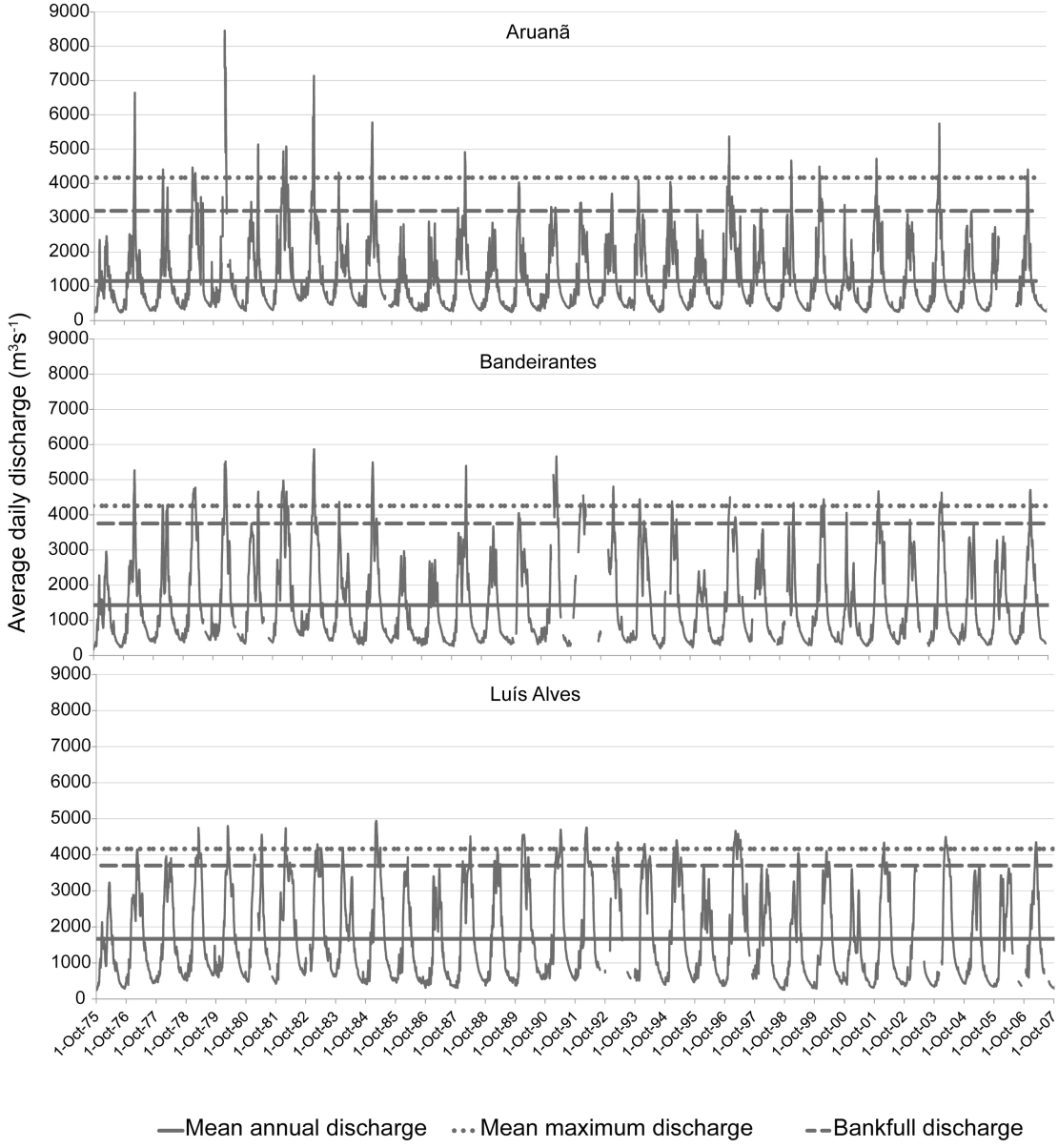

Figure 2.3. Discharge records from three gauging stations along the middle Araguaia River. The mean annual discharge, mean maximum discharge, and the bankfull discharge are included for each station. Data from Agencia Nacional de Aguas; Latrubesse (2008); these discharge data were previously published by Aquino et al. (2008).

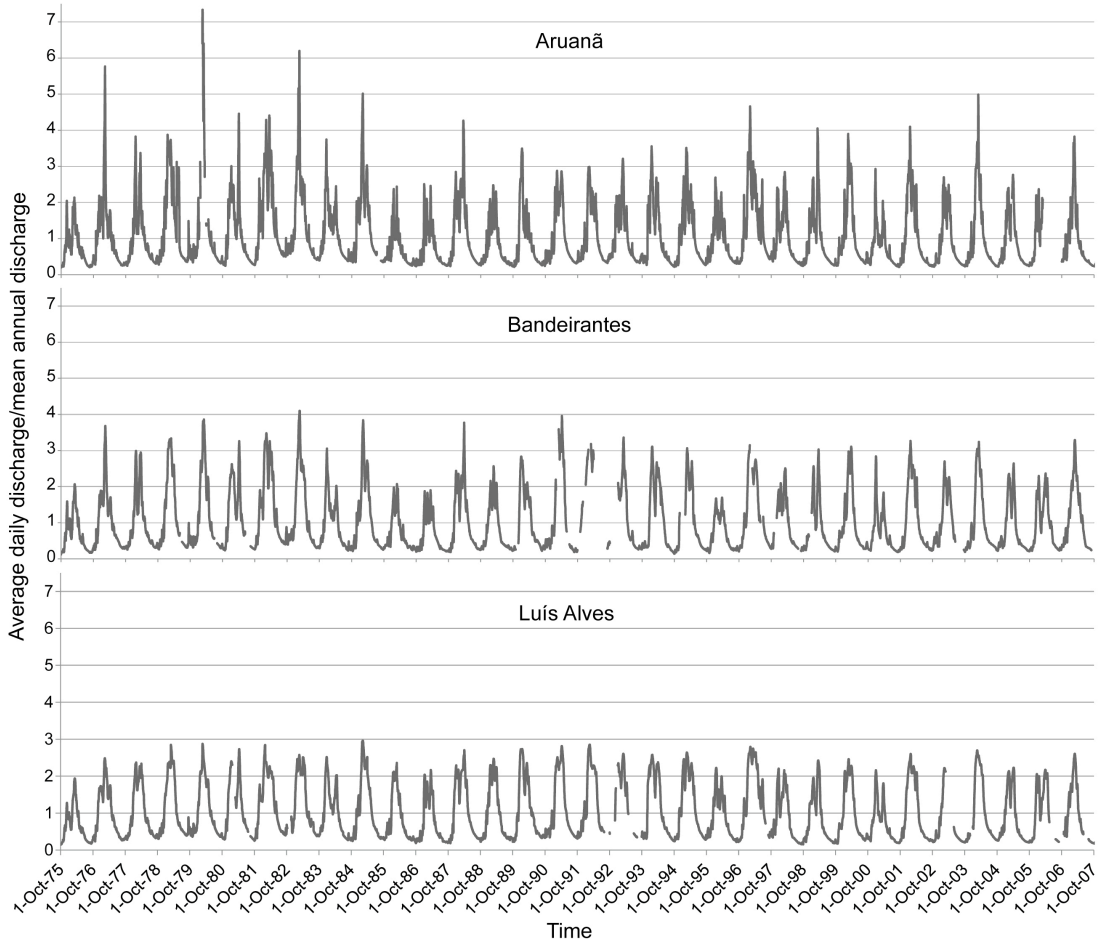

Figure 2.4. Discharges at three gaging stations normalized by the stations mean annual discharge. Data from Agencia Nacional de Aguas; these discharge data were previously published by Aquino et al. (2008).

Geomorphology of the middle Araguaia River

The middle Araguaia River is an anabranching river with a tendency to braid (Latrubesse 2008). The anabranching pattern of the middle section is typical of large, mega-rivers (Latrubesse 2008). These mega-rivers are unique because the anabranching pattern cannot be explained using geomorphologic channel characteristics developed with

data from smaller systems (Latrubesse 2008). The river transports a high proportion of sandy load (around 57%) compared to fine grain suspended sediment, which is unusual when compared to other large tropical systems (Aquino et al. 2009). A large proportion of the sandy load carried by the river travels in intermediate suspension (Latrubesse et al. 2009). Total annual loads have been estimated using field measurements and sediment transport equations to be between 6 and 8 $Mtyr^{-1}$ at Aruanã (Aquino et al. 2009; Latrubesse et al. 2009).

The middle Araguaia River floodplain, with a width ranging between 2 and 10 km, consists of three main geomorphologic units, classified by Latrubesse and Stevaux (2002) using elevation data, satellite imagery, fieldwork, and additional geographic data. The units include:

-unit I, a lower elevation backwater area containing oxbow and paleochannel lakes (the "impeded" floodplain, which is the oldest unit);

-unit II, a unit of paleomeanders and oxbow lakes; and

-unit III, a complex of accreted bars and islands that exists close to the active river channel (Latrubesse and Stevaux 2002).

Unit I, usually the furthest from the river channel, can be as much as 2 meters lower in elevation compared to unit II (Bayer 2002). The impeded floodplain has less surface water connectivity with the river channel, except in high flood periods, and is similar to lower elevation backwater areas in other tropical systems, such as the Amazon (Latrubesse and Franzinelli 2002). Unit I is made up mainly of fine sediments, reflecting the process of low-energy sedimentation occurring in this unit (Bayer 2002). This process occurs relatively slowly and has resulted in a marshy environment in unit I compared with unit II. Sediment deposits in unit II reflect its transitional location between deposition of sandy sediments of the channel and the deposition of fine suspended

sediments. The deposits in unit II are usually coarse to medium sands at the base, indicating the past influence of the active channel environment, while upper deposits in unit II can be characterized as a thin layers of sand interspersed with low-energy sediments (clay and silt) (Bayer 2002). In unit III, the sediments are mainly medium and fine sands, reflecting deposition from the high-energy channel, with interspersed layers of finer materials. Pioneer vegetation many times colonizes this unit, and deposition of finer sediments and the accumulation of organic matter in depressions between large sandy deposits near the channel bank and the floodplain facilitates colonization by providing a better substrate for vegetation (Bayer 2002).

Figure 2.5 shows the classified geomorphologic units of the middle Araguaia River floodplain near Aruanã, including a unit IV, designating the floodplains of the Araguaia tributaries (Latrubesse and Carvalho 2006). The floodplain contains many types of lakes created by fluvial processes, including abandoned channel lakes, linked abandoned channels, oxbow lakes, filled oxbow lakes, composite oxbow lakes, meander scroll lakes, composite meander scroll lakes, lakes formed by lateral accretion, blocked valley lakes, and levee lakes (Morais et al. 2005). These lakes are more fully described in Chapter 4.

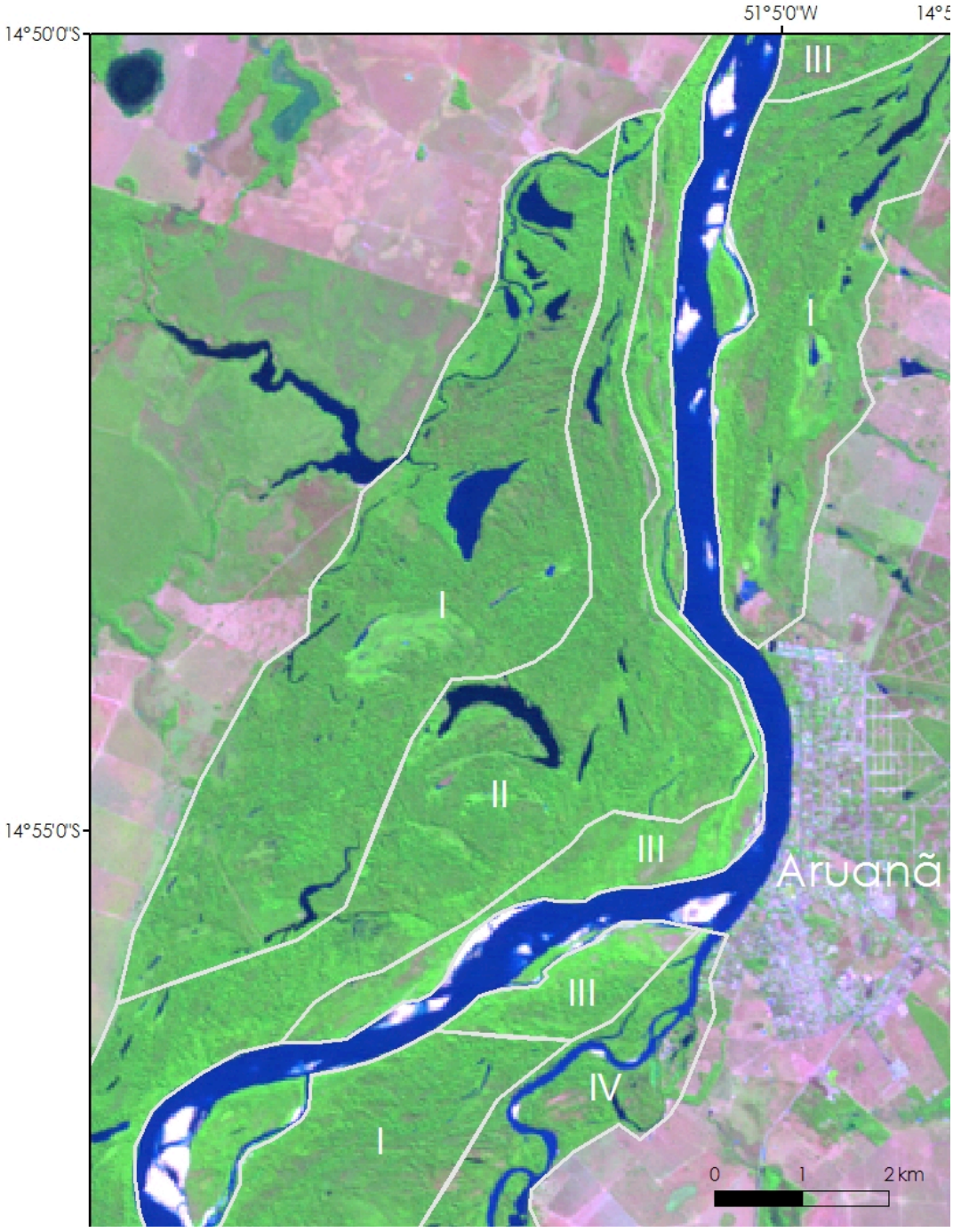

Figure 2.5. Geomorphologic units of the Araguaia Floodplain. I-Impeded floodplain; II-Paleomeander; III-Accreted islands and banks; IV-Tributary river floodplain (Latrubesse and Stevaux 2002). Background image is Landsat 5, Bands 5-4-3, 20 June 2011.

Vegetation and Ecology

Most of the Araguaia River watershed is *Cerrado*, the Brazilian savanna, although a small portion of the lower watershed is Amazonian rainforest. The *Cerrado* has been identified as a biodiversity hotspot, indicating that it is greatly threatened and has high biodiversity (Myers et al. 2000). The natural vegetation of the *Cerrado* includes forestlands, shrublands, grasslands, and wetland vegetation (Sano et al. 2010). Almost half of the plant species of the *Cerrado* are endemic to the region (Klink and Machado 2005). The Araguaia River and a previously abandoned belt, which is the under-fit Javaés River (Figure 2.1), forms a large fluvial island called the Bananal Island (Valente et al. 2013). The northern portion of this island is protected as a national park and recognized as a wetland of international importance (The Ramsar Convention on Wetlands 1997). The region is also an important area for birds, amphibians, fish, and reptiles (Klink and Machado 2005; The Ramsar Convention on Wetlands 1997).

The vegetation assemblages that make up the riparian floodplain vegetation of the middle Araguaia River are linked to the geomorphologic units, as fluvial processes exert a control on the types of vegetation (Morais et al. 2008; Latrubesse and Stevaux 2006). The vegetation of the floodplain can be characterized into four types: (1) herbaceous vegetation associated with pioneer colonization of river bars and islands; (2) a mixture of shrubs and trees associated with areas such as older, more stable islands; (3) woody vegetation and higher plant diversity in older floodplain areas (i.e., the impeded flooplain) with large trees and less channel influence; and (4) human-created pasture or cropland in the floodplain (Morais et al. 2008). Herbaceous pioneer vegetation occurs in areas more directly disturbed by flooding and deposition of sediment in bars and islands. In addition to older islands, the shrub and tree unit can be in areas of paleomeander lakes,

with varying topography, and along the banks of the river itself (Latrubesse and Stevaux 2006).

The few studies of fauna associated with the Araguaia floodplain indicate that the hydrologic patterns of annual flooding and the floodplain geomorphology greatly impact these communities. It has been established that the annual flooding cycle, floodplain inundation, and the rise and fall of floodplain lake levels control the characteristics of phytoplankton communities and the nutrient levels in the floodplain lakes (Nabout et al. 2006). During the dry season, the lakes have nutrient concentrations, while in the wet season the entrance of river water into the lakes dilutes the nutrients in the lakes (Nabout et al. 2006). The dominant species of phytoplankton is different in the wet and the dry season as well (Nabout et al. 2006). The exposure of sandy bars during the dry season are also integral for nesting habitat for the giant Amazon River turtle, *Podocnemis expansa* (Ferreira Jr. and Castro 2005). The rise and fall of lake levels in the Araguaia floodplain also impacts fish community structure and the water transparency of the lakes, and inundation of the floodplain and Bananal island region supports an extremely diverse bird community (Tejerina-Garro et al. 1998; Pinheiro 2007).

LAND-USE CHANGES AND IMPACTS IN THE ARAGUAIA RIVER WATERSHED

Since the 1970s, some estimate that approximately 55% of the land area has been converted into cash crop agriculture, pastureland, or other human uses in the Brazilian *Cerrado* as a whole (Klink and Machado 2005). Other estimates assert that about 40% of the biome has been cleared of natural *Cerrado* vegetation (Sano et al. 2010). Much of the state of Goiás, which contains most of the upper watershed of the Araguaia River, is used for pasturelands. There is also a substantial area used for soybean, corn, and sugarcane

production (Sano et al. 2010). This rapid clearing of natural vegetation has impacts on the rivers and watersheds within the region.

There are also estimates of land-use changes and clearing of natural vegetation within the Araguaia watershed specifically. Ferreira et al. (2008) use satellite imagery from the China Brazil Earth Resource Satellite (20-meter resolution) to determine land uses in the middle and upper Araguaia basin. They classify 2006 imagery into three classes: remnant vegetation, converted areas, and water bodies. Their results show that only 38.5% of the study area is still natural vegetation, while the remaining 62.5% has been impacted by humans in some way. They also analyzed a riparian buffer along the Araguaia River, noting that 44% of this buffer area is impacted by humans (Ferreira et al. 2008). Additional estimates indicate that as of 2002, about 54% of the natural *Cerrado* vegetation upstream of Aruanã was cleared or degraded by human land use (Sano et al. 2010; Coe et al. 2011).

Studies in the upper Araguaia River basin have concluded that land use changes have accelerated erosion of the land surface. Marinho et al. (2006) analyze the increase in the number of gullies in the upper Araguaia River watershed since the beginning of large-scale conversion of natural vegetation for pasture and croplands (mainly soy beans) in the 1970s. Large- and medium-scale gullies increased in number from 12 to 91 from the 1960s to 1999 in an area of 1,516 km^2 in the upper Araguaia watershed. Human activities, such as raising cattle and clearing vegetation for soybeans have accelerated the natural process of erosion in the sandy soils of the upper watershed (Castro and Queiroz Neto 2010; Marinho et al. 2006). The largest gullies are directly connected to the Araguaia River, while smaller gullies are connected to tributaries of the Araguaia (Marinho et al. 2006). Castro and Queiroz Neto (2010) discuss the histories of coffee and soy bean production in Brazil and provide evidence that soy bean production results in

greater soil erosion due to the need for crop rotation for soy bean production (Castro and Queiroz Neto 2010).

Studies have also linked the land use change and subsequent erosion in the upper watershed with geomorphologic change. Latrubesse et al. (2009) use remote sensing imagery, aerial photography, and fieldwork to document morphological changes in 10 segments of the middle Araguaia River from 1965 to 1998, from Barra do Garças to the entrance of the Cristalino River. The authors classify geomorphologic features and the depositional and erosional processes that occur over the period of study. They do not find large geomorphologic changes between 1965 and 1975; however, there are substantial geomorphologic changes from 1975 to 1998. For example, secondary channel infilling and accretion processes resulted in fewer islands by 1998, middle channel bars greatly increased in number, and the amount of lateral bars increased slightly. The authors map depositional and erosional processes and create a sediment budget using the areas and estimated thicknesses of the geomorphologic features to determine the net sedimentation between 1965 and 1998. They find that 232 million tons of sediment were deposited over the study area. The authors also estimate bed load transport by estimating dune transport and height at Aruanã at a given discharge level and applying those measurements to an empirical equation to determine bedload transport. Discharge records from Aruanã from 1971 to 1998 were used to compute annual bedload transport, finding an increase of 31% in sand transport since the 1970s. The increased sedimentation and sandy load transport are correlated with increased land clearing.

Coe et al. (2011) use ecological and hydrological models to attribute two-thirds of an observed increase of river discharge from the 1970s to the 1990s to land clearing activities in the watershed above Aruanã. Mean discharge rate in the decade of the 1970s was 25% less than the mean discharge rate in the decade of the 1990s at Aruanã, while

precipitation only increased by about 2.5% from the 1970s to the 1990s. Modeled river discharge, using precipitation datasets and changes in land cover within the watershed, was compared to observed river discharge. The model allowed for assessing the influence of changes in precipitation versus land cover on the observed increase in river discharge. The conclusion that two-thirds of the observed increase in river discharge at Aruanã can be attributed to deforestation and land clearing thus also supports Latrubesse et al. (2009) in their assertion that increased sedimentation resulted from land use changes, as the hydrologic cycle and sedimentation within rivers are linked.

Costa et al. (2003) utilize long-term data on river discharge and precipitation in the Tocantins watershed, which is adjacent to the Araguaia watershed (Figure 2.1), to compare two periods of time with significant differences in land use, 1949-1968 and 1979-1998. They find a similar response to land use change as Coe et al. (2011) discover in the Araguaia. They use agricultural census data to estimate that agricultural land increase from 30% to 50% between the time periods. Discharge in the Tocantins River increased by 24% between the two time periods, while precipitation did not significantly change. Flood season discharge also increased between the two periods (Costa et al. 2003).

The assessments of increased gully development in the upper watershed, increased river sedimentation, and increased water yield due to land use change are strong indications that land clearing has greatly impacted the watershed. However, more work should be done to analyze these changes and attribute land use changes to changes observed in hydrology and sedimentation. Assessing rates of floodplain sedimentation before the start of significant land clearing and after land clearing had begun would help determine whether land use change has increased floodplain sedimentation rates.

Research that will be done in the future to assess floodplain sedimentation rates is described in the Appendix of this thesis.

Chapter 3: Flood transmission patterns, peak discharge reduction, and estimates of channel loss in two reaches of the middle Araguaia River

As a flood wave travels downstream, the flood wave can become attenuated due to storage of water within the channel and in the floodplain (Dunne and Leopold). The geomorphologic characteristics of channels and floodplains, including floodplain lakes and floodplain channels providing storage areas, floodplain substrate, and channel slope, can cause this attenuation (Dunne and Leopold 1978; Richey et al. 1989; Woltemade and Potter 1994). Floodplain vegetation also influences this process by increasing roughness and slowing down the flood wave as it moves through the system, temporarily storing flood waters (Anderson et al. 2006). Figure 3.1 demonstrates the process of flood wave attenuation, or the smoothing and slowing of the flood wave, for a small drainage area in respond to a short-term flooding event along a river in Vermont (Dunne and Leopold 1978). It is clear in Figure 3.1 that the peaks in the flood wave at the upstream location are in response to individual precipitation pulses, and these peaks become one peak at the downstream locations (i.e., the flood wave is smoothed). The discharge per unit drainage area (the left y-axis in Figure 3.1) of the peaks decreases downstream, but the total discharge in the channel (the right y-axis in Figure 3.1) increases as the drainage area increases. Flood wave attenuation can occur without net losses in river discharge, as seen in Figure 3.1.

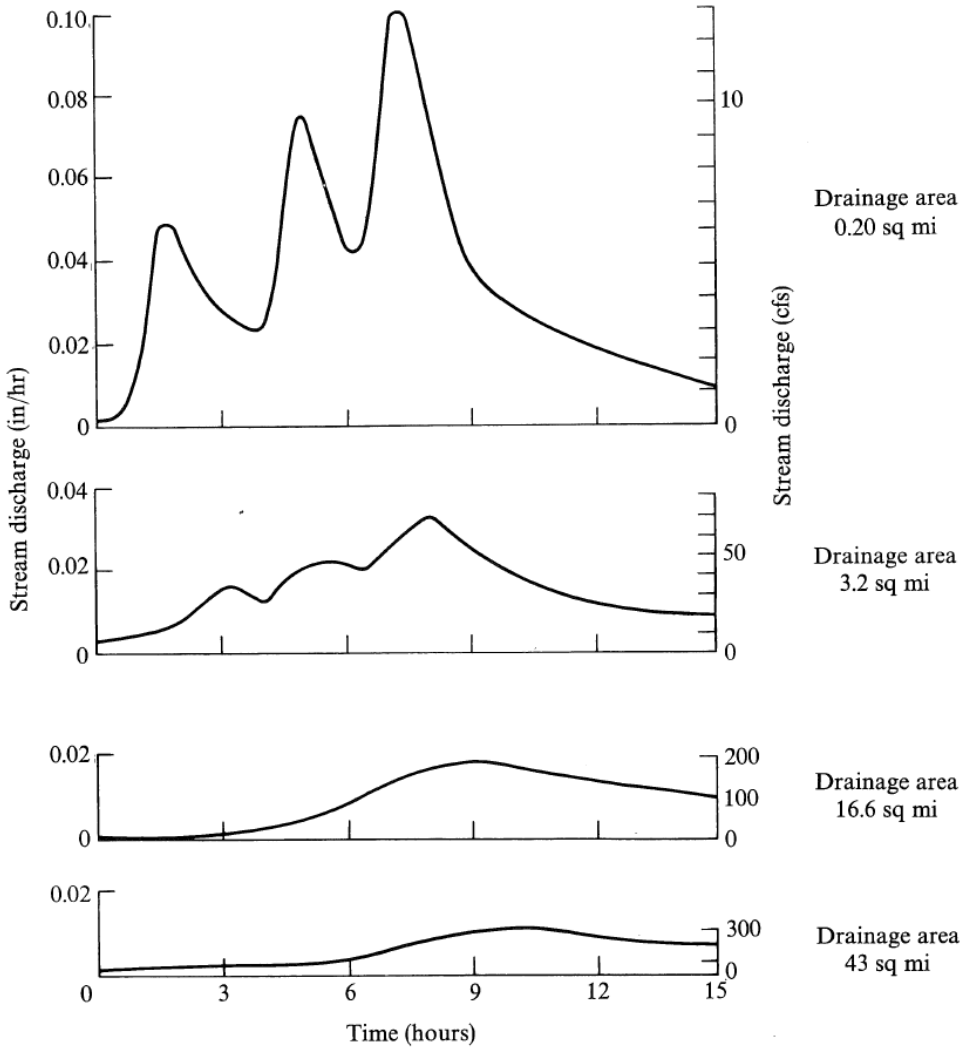

Figure 3.1. Figure 10-3 in Dunne and Leopold (1978), showing flood wave attenuation with the smoothing of the peak discharge and the reduction in discharge per unit drainage area (left y-axis), while total discharge increases with increasing drainage area.

In addition to flood wave attenuation, in the middle Araguaia River the total peak discharge can be reduced by as much as 30% as the flood wave travels downstream, indicating that the river goes through short periods of reduced channel discharge during the flooding peak despite large increases in drainage area and the input of tributary river

discharge (Aquino et al. 2008). This discharge reduction does not occur during every year, and one of the goals of this chapter is to characterize different flood years into typical flooding types. It appears that the reduction in peak discharge in the middle Araguaia River despite tributary inputs and increasing drainage area has not been documented yet in other large tropical systems with similar geomorphologic and climatic characteristics. Floodplain storage, floodplain inundation, and the smoothing and slowing of the flood wave (flood wave attenuation) have been demonstrated in the Amazon River, the Negro River, the Mekong River, and the Congo River (Richey et al. 1989; Alsdorf et al. 2010; Frappart et al. 2005; Lee et al. 2011). However, these studies do not document net channel reduction of discharge during flooding peaks, as discharge usually increases with increasing drainage area and tributary inputs, even if discharge normalized by drainage area decreases downstream, as seen in the left y-axis in Figure 3.1 (Dunne and Leopold 1978).

The Niger River is an example of a large river system displaying channel loss, but over the long term (for example, throughout the year), due to the river flowing through an inland delta in a semi-arid climate (Zwarts et al. 2005). However, the Araguaia River does not flow into an arid climate. The Paraguay River can reduce in discharge by 50% due to its entrance into the Pantanal wetland and the river becoming distributary, creating a depositional mega-fan (Assine and Silva 2009), but the geomorphologic characteristics of the middle Araguaia River floodplain are different than what is observed in the Upper Paraguay River Basin. Peak reduction of flood waves have also been modeled on a small reach scale (e.g., around 1 km of river channel) with flood waves lasting a period of hours and without tributary inputs (Sholtes and Doyle 2011). In another example, flood waves were modeled in part of the Grant River watershed, with a drainage area of 690 km^2, much smaller than the Araguaia River watershed (Woltemade and Potter 1994).

Peak discharges along the river were compared without tributary inputs in order to show absolute peak reduction for a flood wave occurring over a period of up to 50 hours (Woltemade and Potter 1994). As described in Chapter 1, the seasonal flood wave in the Araguaia River occurs over a period of time much longer than those modeled in the examples above, up to a period of 6 months instead of hours, and the Araguaia River watershed is much larger than many modeling studies investigating peak reduction.

One of the goals of this chapter is to determine the volume of the downstream reduction of discharge over the flood wave crest, which is the region of the flood wave hydrograph prior to and following the peak discharge. This volumetric reduction in discharge is different than the volume of floodplain storage during flooding, as described previously, because storage on the floodplain of river discharge during flooding can occur without reductions in discharge downstream. Thus, although peak reduction over the flood wave crest in the middle Araguaia is not the same as channel losses of discharge over the long-term, as has been observed in arid river systems (e.g., Lange 2005; Gu and Deutschman 2001; Knighton and Nanson 1994), the volume reduction in discharge during flooding peaks will be termed "channel losses over the flood wave crest". The channel losses over the flood wave crest are presumed to be short-term losses, but another goal of this chapter is to determine whether the channel losses over the flood wave crest result in channel losses over the flooding season, from November to May. This will assess whether channel losses over the flood wave crest are re-gained by the channel by the end of the flooding season. The net decrease in peak discharge with increasing drainage area along the middle portion of the Araguaia River previously has been attributed to the complex, flat floodplain and the floodplain lakes that the river has created over time (Aquino et al. 2008), and a fuller discussion of the potential

mechanisms for the estimated channel losses is discussed throughout this Chapter and in Chapter 4.

Studies of channel losses and floodplain storage many times use flow routing models, water budget approaches, and satellite imagery and other remote sensing data (Li et al. 2011; Lange 2005; Knighton and Nanson 1994; Richey et al. 1989; Alsdorf et al. 2010; Paz et al. 2011; Frappart et al. 2005). The approach taken in this chapter is to analyze peak discharge change as a percent of peak upstream discharge and as absolute change in the peak discharge rate along two reaches of the middle Araguaia River. Average daily discharge measurements from 1975-2007 are used to follow the peak discharge as it moves downstream. The peak discharge changes are used to characterize typical patterns of flood transmission and compare them to previously described models of flood transmission that were developed using yearly maximum discharges (Aquino et al. 2008). Volumetric channel losses over the flood wave crest for years in which peak discharge reduction occur are estimated using a water budget approach and are compared between two reaches of the middle Araguaia River. Volumetric channel loss over the flood wave crest, while not a measure of total floodplain storage during flooding, gives an estimate of the amount of water that could be transferred to the floodplain during the flood wave peak. This adds to knowledge of channel-floodplain connectivity on the middle Araguaia River. Estimates of volumetric channel loss over the flooding period are also made to determine whether channel losses occur over the entire flooding period or only during the flood wave crest. These methods of estimating channel losses, peak discharge reduction, and potential losses of discharge to the floodplain have been used instead of flood routing models due to a lack of tributary discharge data at the confluence of the tributaries with the middle Araguaia River and a lack of adequate elevation data for the Araguaia River floodplain.

STUDY AREA

The analysis presented in this chapter focuses on two reaches of the middle Araguaia River: a 170 km stretch between Aruanã and Bandeirantes (reach 1), and a 64 km stretch between Bandeirantes and Luís Alves (reach 2) (Figure 3.2). Gauging stations are present at Aruanã, Bandeirantes, and Luís Alves.

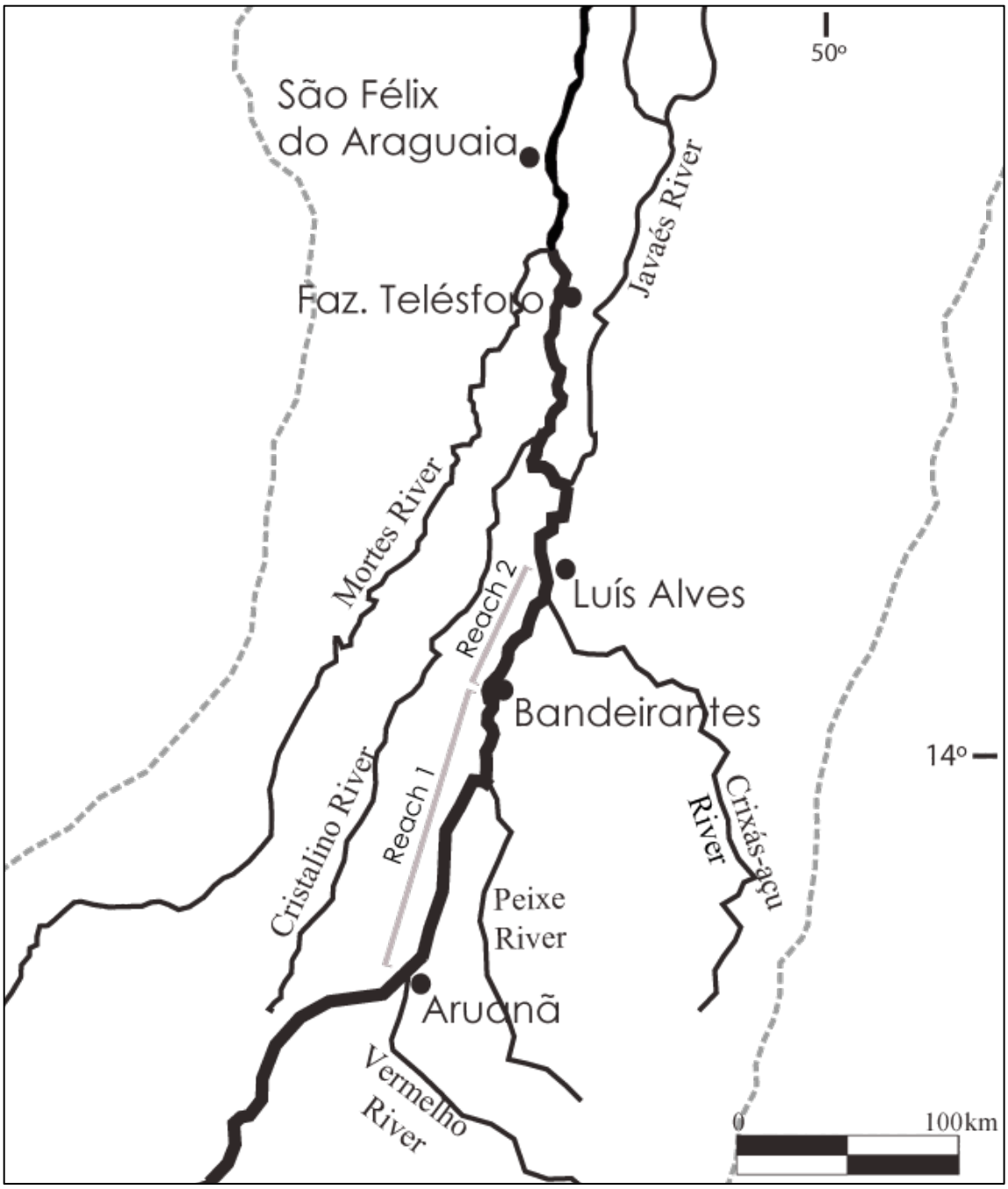

Figure 3.2. Study reaches of the Araguaia River and the location of river gauging stations at Aruanã, Bandeirantes, and Luís Alves.

Table 3.1 gives the drainage area, mean annual discharge for the period of record (1975 to 2007), bankfull discharge, and mean maximum discharge for the period of record for each gauging station, and Figure 3.3 plots these data versus drainage area for each station (Agencia Nacional de Aguas; Latrubesse 2008). The mean annual discharge increases along with increasing drainage area, but the bankfull discharge and the mean maximum discharge decreases from Bandeirantes to Luís Alves, although the bankfull discharge for Bandeirantes has been estimated using a different method than for Aruanã and Luís Alves (see Table 3.1 for description). Table 3.2 shows the mean annual discharge, bankfull discharge, and mean maximum discharge normalized by drainage area in mm yr^{-1}, showing a decrease in mean maximum discharge per unit drainage area from Aruanã to Luís Alves, which is a characteristic of flood wave attenuation (e.g., as seen in the left y-axis in Figure 3.1). There is also a slight decrease in mean annual discharge normalized by drainage area from Bandeirantes to Luís Alves.

Table 3.1. Drainage areas, mean annual discharge, bankfull discharge, and mean maximum annual discharge for three stations along the middle Araguaia River (Agencia Nacional de Aguas; Latrubesse 2008). *Indicates that the estimate of bankfull discharge was made by the author using the EVI distribution with a recurrence interval of 1.5 years (Dunne and Leopold 1978). All other estimates of bankfull discharge are from field data (Latrubesse 2008).

Station name	**Drainage Area (km^2)**	**Mean annual discharge (m^3s^{-1})**	**Bankfull discharge (m^3s^{-1})**	**Mean maximum discharge (m^3s^{-1})**
Aruanã	76,964	1156	3200	4167
Bandeirantes	92,638	1424	3755*	4256
Luís Alves	117,580	1673	3700	4165

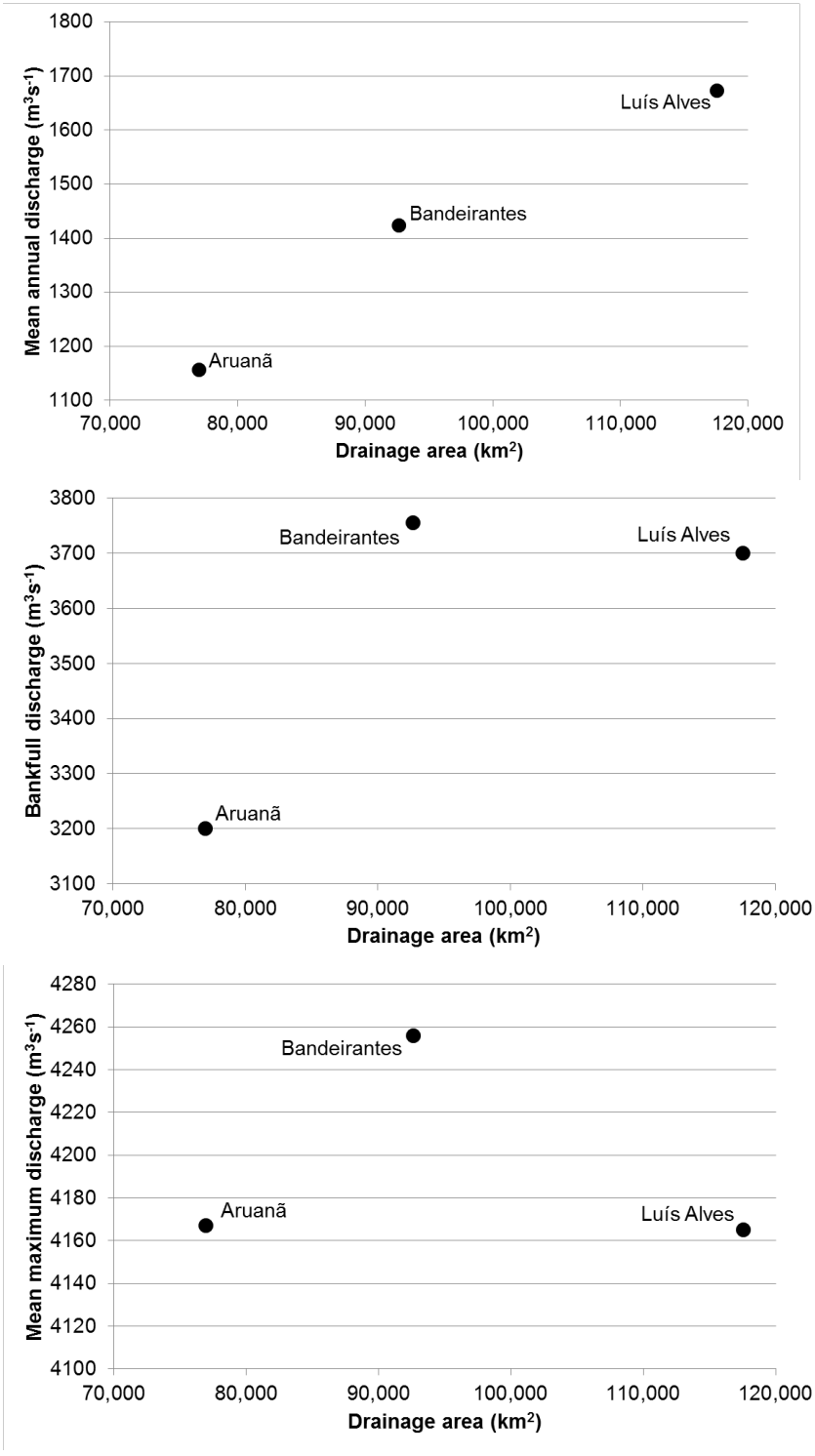

Figure 3.3. Mean annual discharge, bankfull discharge, and mean maximum discharge for the three gauging stations. The y-axis scale is different for each graph.

Table 3.2. Mean annual discharge, bankfull discharge, and mean maximum annual discharge normalized by drainage area (in mm yr^{-1}) for three stations along the middle Araguaia River (Agencia Nacional de Aguas; Latrubesse 2008). *Indicates that the estimate of bankfull discharge was made by the author using the EVI distribution with a recurrence interval of 1.5 years (Dunne and Leopold 1978). All other estimates of bankfull discharge are from field data (Latrubesse 2008).

Station name	Mean annual discharge ($mm\ yr^{-1}$)	Bankfull discharge ($mm\ yr^{-1}$)	Mean maximum discharge ($mm\ yr^{-1}$)
Aruanã	474	1311	1707
Bandeirantes	485	1278*	1449
Luís Alves	449	992	1117

One tributary flows into the Araguaia River in each reach (Table 3.3), but neither tributary has a gauging station at their confluence with the Araguaia River. The Peixe River drainage area represents about 13% of the total drainage area at Bandeirantes station, which is downstream of the confluence. The Crixas-Açu River drainage area represents about 20% of the total drainage area at the Luís Alves gauging station, downstream of the river's entrance to the Araguaia. There is a gauging station Jusanto Rio Pintado on the Crixas-Açu River upstream of the confluence with the Araguaia, with a drainage area of 18,600 km^2 (representing about 78% of the drainage area of the Crixas-Açu watershed), but there is no gauging station on the Peixe River. Both tributaries flow into the middle Araguaia River from the right bank and drain areas dominated by Pre-Cambrian rock units. They begin in hilly regions and then become meandering rivers with floodplains before entering into the Araguaia River. Table 3.4 shows the increase in drainage area along each reach, and the percentage of that drainage area increase that results from the tributary input. The tributaries provide almost all of the increase in drainage area along both reaches.

Table 3.3. Drainage areas and mean annual discharge for the tributaries in the study reaches. The mean annual discharge was estimated using a drainage area curve by Aquino et al. (2009).

Tributary	Reach	Drainage area (km^2)	Mean annual discharge (m^3s^{-1})
Peixe River	Reach 1	12,439	186
Crixas-Açu River	Reach 2	23,682	348

Table 3.4. Drainage area increases and the percentage of the drainage area increase that is due to the tributary along the study reaches.

Reach	Drainage area increase along reach (km^2)	Percent of drainage area increase along reach resulting from tributary input (%)
Reach 1	15,674	79.4
Reach 2	24,942	95.0

The three main floodplain geomorphologic units of the middle Araguaia River, unit I (the older, impeded floodplain), unit II (unit dominated by paleomeanders), and unit III (area of accreted banks and islands), are present in both reaches, making up varying areas of the floodplains in the reaches (Table 3.5).

Table 3.5. The total areas and percentages of the floodplain area in reach 1 and reach 2 by geomorphologic unit. Areas and percentages were found using ArcGIS and shapefiles of the geomorphologic units obtained from Latrubesse and Carvalho (2006) and defined by Latrubesse and Stevaux (2002).

Reach	Unit I (km^2)	Unit II (km^2)	Unit III (km^2)	Total floodplain (km^2)
Reach 1	424	277	52	753
Reach 2	87	260	12	358
Reach	**Unit I (%)**	**Unit II (%)**	**Unit III (%)**	**Total floodplain (%)**
Reach 1	56.3	36.8	6.9	67.8
Reach 2	24.2	72.5	3.3	32.2

DRAINAGE-AREA DISCHARGE RELATIONSHIPS AND MIDDLE ARAGUAIA RIVER FLOOD TRANSMISSION MODELS

The relationship between river discharge and drainage area along a river within a watershed can be fit with the following empirically-derived power function

$$Q = c * D_a^n \quad (1)$$

where Q is discharge of a given level, c is a constant that depends on the type of discharge analyzed (e.g., bankfull discharge, mean annual discharge, mean maximum annual discharge) and the specific characteristics of the watershed (e.g., climate, geology), D_a is drainage area, and n is an exponent that determines the scaling relationship between the discharge and drainage area (Dunne and Leopold 1978). Mean annual discharge along most rivers increases at about the same rate as drainage area increases, resulting in an n exponent of approximately 1 (Dunne and Leopold 1978). The relationship between mean maximum annual discharge (the mean annual flood) and drainage area in a watershed can be characterized by the power function as well, but the n exponent is usually less than 1 due to flood wave attenuation and water storage within the system (Dunne and Leopold 1978).

In the Araguaia River (including the upper, middle, and lower sections), the mean annual discharge follows this predictable pattern, with the mean annual discharge increasing at approximately the same rate as drainage area and a scaling exponent n of 0.98 (see Figure 4 in Aquino et al. 2008). The increase in mean annual discharge along with drainage area can be seen in Figure 3.3, in which the mean annual discharge downstream from Aruanã to Luís Alves. A similar relationship between mean maximum annual discharge and drainage area yields a n value of 0.82 for the entire Araguaia River

(see also Figure 5 in Aquino et al. 2008), but the measured mean maximum annual discharge from some of the gauging stations in the middle Araguaia River, including Luís Alves, deviate from the discharge-drainage area relationship, decreasing along certain reaches of the middle Araguaia (Aquino et al. 2008). This can be observed in Table 3.1 and in Figure 3.3, showing that the absolute mean maximum discharge at Luís Alves is lower than at Bandeirantes and is almost the same as at Aruanã.

Aquino et al. (2008) characterized three types of flooding that occur in the middle Araguaia River based on the magnitude peak discharge and the pattern of peak discharge reduction along the river downstream from Aruanã for 7 years. They used maximum discharge values to characterized percent reduction of peak discharge, while the present study will use average daily discharge measurements for each flood wave. In addition to the three gaging stations used for this analysis, Aquino et al. included a fourth station at Fazenda Telésforo, downstream of Luís Alves (Figure 3.2). Data from Fazenda Telésforo were not available for this analysis, as the gaging station was not maintained and the data were not available for the period of interest for the present analyses. This chapter does not analyze discharge at Fazenda Telésforo, thus in the discussion of flooding types the results from this chapter will be compared to the descriptions of floods between Aruanã, Bandeirantes, and Luís Alves.

Type A floods have major flood peaks along the course of the middle Araguaia River (for example, 7139 m^3s^{-1} at Aruanã) and peak discharge reductions of about 30% from Aruanã to Luís Alves and Aruanã to Fazenda Telésforo (example years are 1980 and 1983). The authors stated that the reduction in peak discharge in type A floods likely occurs because floodplain lakes linked to the channel near Aruanã provide storage areas for river discharge. Type B floods do not have major flood peaks (Aquino et al. characterize these peaks as between 4,000 m^3s^{-1} and 5,000 m^3s^{-1}) and have small increases

in peak discharge along the middle course of the river, with no peak discharge reduction (example years given are 1977, 1978, and 1979). Another characteristic of this flood type is the maintenance of a similar discharge or a small loss in discharge between Luís Alves and Fazenda Telésforo. The loss in discharge between these two stations is presumed to result from the Araguaia River flow spilling into the Javaés River, which is an abandoned belt of the Araguaia River. Type C floods do not display significant peaks at Aruanã (ranging between 4,500 and 5,500 m^3s^{-1}) and display slightly increasing or conservative flows (meaning that the peak discharge does not change significantly) from Aruanã to Bandeirantes, small peak decrease between Bandeirantes and Luís Alves, and can either be a slight reduction in peak discharge or maintain a similar magnitude of discharge between Luís Alves and Fazenda Telésforo due to the Javaés River (Aquino et al. 2008). Table 3.6 summarizes the models proposed by Aquino et al. and the pattern of peak discharge reduction from Aruanã to Luís Alves.

Table 3.6. Description of flood transmission models from Aquino et al. (2008) between Aruanã and Luís Alves.

Type	Description between Aruanã and Luís Alves	Example years used by Aquino et al. (2008)
A	Extreme peak floods (e.g., 7000 m^3s^{-1}), with discharge losses of about 30% between Aruanã and Luís Alves	1980, 1983
B	No major flood peaks (4,000 to 5,000 m^3s^{-1}), small increases in flow from Aruanã up to Luís Alves	1977, 1978, 1979
C	Medium peak discharge (4,500 to 5,500 m^3s^{-1}), small or no peak reduction discharge between Aruanã and Bandeirantes, and usually a slight loss of discharge between Bandeirantes and Luís Alves	1982, 1985

METHODS

Average daily discharge data were downloaded from Brazil's National Water Agency website (Agencia Nacional de Aguas) for three gaging stations along the middle

Araguaia River: Aruanã, Bandeirantes, and Luís Alves. Daily discharge measurements for all three stations are available from 1975 to 2007. The flooding period analyzed runs from November through May. Years are named for the year in which the flooding season ends in May. There are small periods of unavailable measurements within the record during the flooding period for 12 years, ranging from 15 days to about 2 months for at least one of the three stations. Average daily discharge measurements for the gauging station on the Crixas-Açu River, Jusante Rio Pintado, are available from 1980 to 2003, although the record is also not continuous with similar types of breaks during the flooding period (Agencia Nacional de Aguas).

Lag times (k) in days for the flood wave peak to travel down each reach were determined individually for each flood wave analyzed by assessing the time between peaks at the upstream and downstream stations for each reach. In determining lag times and analyzing peak reduction, the analysis was performed using the highest recorded peak discharge at Aruanã as a starting point. This was done because at times the flood wave along the Araguaia River displays multiple peaks. Thus, if the peak discharge at a downstream station occurs before the peak discharge at an upstream station, it was treated as a separate flood wave and was not used to determine how the peak upstream discharge translated downstream.

Flood wave hydrographs were analyzed for the absolute change and percent change in the peak (increase or reduction) for each flood wave between Aruanã and Bandeirantes (reach 1) and between Bandeirantes and Luís Alves (reach 2). Four years, 1991, 1992, 1997, and 2006, were not analyzed for peak discharge change due the inability to determine the peak discharge of the flood wave because discharge measurements were not available and not provided by Brazil's National Water Agency. Peak discharge change as a percent was computed using the following equation

$$\Delta Q_{pk}(\%) = \frac{Q_{pk,d,t+k} - Q_{pk,u,t}}{Q_{pk,u}} * 100 \quad (2)$$

where

$\Delta Q_{pk}(\%)$= change in peak along the reach

$Q_{pk,u,t}$= peak discharge of the flood wave (m^3s^{-1}) at the upstream station at time *t*

$Q_{pk,d,t+k}$= peak discharge of the flood wave (m^3s^{-1}) at the downstream station at time *t+k*

A negative percent change indicates a decrease in peak discharge downstream, while a positive percent change indicates an increase in peak discharge downstream. The absolute peak discharge change (in m^3s^{-1}) was computed using the following equation

$$\Delta Q_{pk} = Q_{pk,d,t+k} - Q_{pk,u,t} \quad (3)$$

The results for each year were then compared to previous flooding types described by Aquino et al. (2008).

An estimate of channel loss during the flood wave crest was made using a simplified short-term water balance approach for the years in which peak discharge reduction occurred and the discharge measurements were available. The water budget was calculated over a period of days during the flood wave crest in which daily discharge upstream was more than daily discharge downstream (i.e., over the days in which discharge loss occurred over the flood wave crest). Water budget equations determine the change in water storage of a defined control volume by examining inputs and outputs (Dunne and Leopold 1978). The water budget equation can be generalized as

$$Inputs - Outputs = \Delta Storage \quad (4)$$

For a full water budget analysis, all inputs and outputs to a storage compartment must be considered, including precipitation, runoff, evaporation, seepage to groundwater, and other aspects of the hydrological system (Dunne and Leopold 1978). For a defined river reach, a complete water balance equation is

$$\Delta S_r = time * [\, Q_u - Q_d + Q_{tr} - E \pm GW + P \pm Q_{fl}] \quad (5)$$

where

ΔS_r= volumetric change in water storage within the reach

Q_u= river discharge rate from upstream of the reach

Q_d= river discharge rate at downstream end of the reach

Q_{tr} = tributary discharge rate

E= evaporation rate from the river surface

GW= rate of groundwater fluxes to and from the channel reach

P= precipitation rate onto river

Q_{fl}= rate of water fluxes between the river channel and the floodplain

Figure 3.4 shows a diagram of the inputs and outputs described in equation 5 above. Many of the inputs and outputs for the complete water balance equation for the study reaches cannot currently be quantified. Groundwater fluxes, evaporation from the river surface, and precipitation onto the river surface have not been quantified (shown in red in Figure 3.4), although evaporation from the river surface and precipitation onto the river surface can be assumed to be negligible. There is no information on the flux rate

between the channel and the floodplain during floods (also shown in red in Figure 3.4). There are no measurements of the tributary discharges at the confluence with the Araguaia River. The Peixe River does not have a gauging station, while the Crixas-Açu River gauging station measures the discharge from 78% of the drainage area. Thus, for one of the study reaches, the tributary input can be partially quantified (shown in purple in Figure 3.4). Data is available for the blue inputs and outputs in Figure 3.4, which are the upstream and downstream discharges.

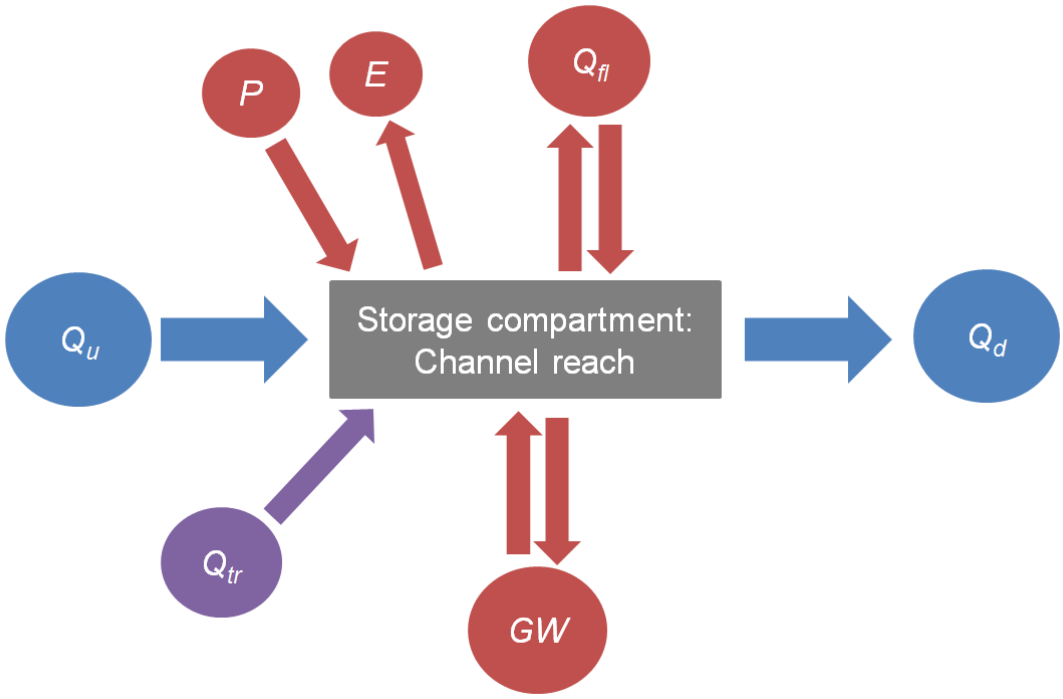

Figure 3.4. Diagram of the inputs and outputs of a full water budget equation for a channel reach. Blue inputs/outputs are quantified, purple are partially quantified, and red are currently unknown, although direct precipitation and evaporation from the river channel surface are likely small.

One method of calculating short-term channel losses, the hydrograph method, uses only the upstream discharge as an input and the downstream discharge as an output to determine channel losses (Gu and Deutschman 2001). If the upstream minus the downstream discharge is positive, it indicates that the discharge rate is less downstream and channel losses have occurred. If the upstream minus the downstream is negative, the channel is gaining discharge along the reach, and no channel losses have occurred (Gu and Deutschman 2001). A similar approach to the hydrograph method was taken due to the lack of additional data to complete a full water budget analysis. Thus, using average daily upstream and downstream discharge rate (in m^3s^{-1}) and accounting for the lag time (k) of the peak discharge, the daily volume of channel loss can be determined using

$$\Delta S_{cl} = time * [\, Q_{u,t} - Q_{d,t+k} \,] \quad (6)$$

where

ΔS_{cl} = daily volumetric channel loss for the reach (m^3)

$Q_{u,t}$ = rate of upstream discharge (m^3s^{-1}) at time t

$Q_{d,t+k}$ = rate of downstream discharge (m^3s^{-1}) at time $t+k$

The above equation was used for flood years in which peak discharge reduction occurred to calculate channel loss over the flood wave crest. Volumetric channel loss values for each day were summed over the period of discharge loss displayed in the hydrograph for the flood peak analyzed, in which discharge was less downstream compared to upstream, accounting for the lag time of the flood peak. This was done to determine the short-term channel loss that occurs over the flood wave crest. Figure 3.5 graphically demonstrates the total volumetric channel loss over the flood wave crest. The

volumetric flux was converted to loss per unit length of each river reach by dividing the volumetric flux by the length of each reach. The total volumetric channel loss underestimates the loss of water from the channel, as the tributary inputs are not quantified, but it provides a way to compare channel loss over the flood wave peak between reach 1 and reach 2 and gives a starting point for the amount of water that is likely transferred to the floodplain during the flood wave crest.

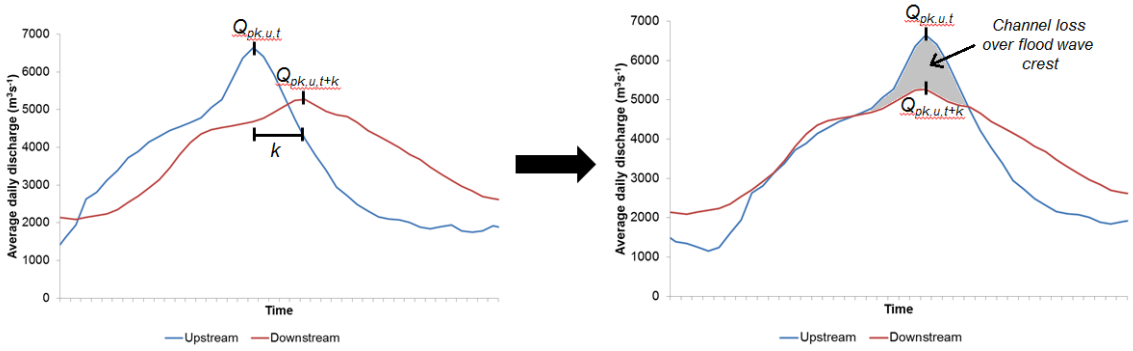

Figure 3.5. Example of the channel loss over the flood wave crest. Accounting for the lag, the volumetric difference in discharge is summed over the period of days in which downstream discharge is less than upstream discharge, represented by the gray shaded area in the right graph.

Because discharge data are available for the Crixas-Açu River at almost 80% of the total drainage area of the tributary, these data were used to compute a channel loss for reach 2 including the tributary data, for the years in which the discharge measurements were available over the flood wave crest. This resulted in calculating channel loss with the tributary data in 11 of the 21 years in which peak discharge reduction occurred in reach 2. Because the Crixas-Açu River flows into the Araguaia River approximately 12.5 km before Luís Alves, meaning that the tributary enters much closer to Luís Alves than Bandeirantes along the 64 km reach 2, the lag time used for the Crixas-Açu River was

taken to be the same lag time used for Luís Alves. Thus, the daily volumetric channel loss in reach 2 with the tributary data was found using the following equation

$$\Delta S_{cl} = time * [\, Q_{u,t} + Q_{trib,t+k} - Q_{d,t+k} \,] \quad (7)$$

where

$Q_{trib,t+k}$= rate of discharge of Crixas-Açu River (m^3s^{-1}) gauging station at time $t+k$

The daily volumetric channel loss for reach 2 with the tributary data was also summed over the period of days in which the inputs were greater than the output (i.e., channel loss was occurring) for the flood wave crest for the flood wave analyzed. These were compared to channel loss without the tributary data in reach 2, to gain a more accurate description of temporary channel loss and to provide an estimate of how much the tributary contributes to channel loss.

In addition to estimating short-term channel loss over the flood wave crest, a water budget of the entire flooding period, from 1 November to 31 May, was completed for each year in which all of the average daily discharge measurements were available. This was used to determine whether peak discharge reduction resulted in channel losses over the flooding period or only during the crest of the flood wave. Average daily discharge measurements from 1 November to 31 May were converted to volumes and then summed. In some years, discharge data were available beginning 21 November (1983) or 1 December (1990), and in these cases this date was used as a starting date instead of 1 November. The channel loss for the flooding period was calculated as

$$\Delta S_{r,fp} = V_{u,fp} - V_{d,fp} \quad (8)$$

where

$\Delta S_{r,fp}$= volumetric channel loss for the flooding period (km^3)

$V_{u,fp}$= volume of the upstream gauging station for the flooding period (km^3)

$V_{d,fp}$= volume of the downstream gauging station for the flooding period (km^3)

Positive values of $\Delta S_{r,fp}$ indicate channel loss over the flooding period, while negative values of $\Delta S_{r,fp}$ indicate that channel losses did not occur and the reach is gaining discharge over the flooding period. The flooding period water budget for reach 2 was also computed using the data from the Crixas-Açu River gauging station when available for the flooding period from November to May. The channel loss equation for the flooding period including the tributary is

$$\Delta S_{r,fp} = V_{u,fp} - V_{d,fp} + V_{t,fp} \quad (9)$$

where

$V_{t,fp}$= volume of the tributary for the flooding period (km^3)

RESULTS AND DISCUSSION

Peak discharge reduction

As expected, the average time for the peak discharge to travel downstream is longer for reach 1 compared to reach 2, as reach 1 is 170 km in length and reach 2 is 64 km in length. Average lag time of the peak discharge as it moved downstream for reach 1

is 6.2 days, with an average velocity of 0.32 m s^{-1} or 1.14 km hr^{-1}. Reach 2 average lag time is 1.8 days, resulting in an average velocity of 0.41 m s^{-1} or 1.48 km hr^{-1}.

Figure 3.6 shows the peak discharge reduction as a percentage plotted against the peak discharge measurement for the upstream station for each analyzed year. Also displayed in Figure 3.6 are the bankfull and mean maximum discharges for the upstream stations. The highest percentage of peak reduction for reach 1 occurs in 1980, when the peak discharge at Aruanã is reduced by 35.5% at Bandeirantes. There is less correlation between percent peak reduction and upstream discharge in reach 1 (Pearson's correlation coefficient (r) = 0.68) compared to reach 2 (r = 0.86), although a trend seems to exist, especially at the higher discharge rates at Aruanã (Figure 3.6). In 1996, 22.8% peak reduction occurs between Aruanã and Bandeirantes, and the peak discharge recorded (3096 m^3s^{-1}) is below bankfull discharge (3200 m m^3s^{-1}). In eight of the analyzed years, including 1984, 1988, 1993, 1994, 1995, 1998, 2001, and 2007, peak discharge increases downstream and the peak upstream discharge is at or above bankfull discharge. In 1988, the peak discharge at Aruanã is 4914 m^3s^{-1} and no peak reduction occurs between Aruanã and Bandeirantes (9.8% peak increase).

The highest measured peak reduction for reach 2 occurs in 1983, when the discharge rate at Luís Alves is 27% less than at Bandeirantes. Reach 2 displays a more uniform pattern of peak reduction in relation upstream discharge compared with reach 1, with a high correlation between peak reduction and the measured peak discharge at the upstream station (r = 0.86). In reach 2, the propensity of loss of peak discharge increases at about bankfull discharge at Bandeirantes. There is only one year, 1990, in which the bankfull discharge at Bandeirantes is exceeded (with a peak discharge of 3896 m^3s^{-1}) and no peak reduction occurs. In this year, peak discharge increases by 21% along the reach. In 1995, the peak remains almost the same along reach and is above bankfull, while in

1995 the peak increases along reach 1. In reach 2, there is only one year, 1998, in which the bankfull discharge is not exceeded at Bandeirantes and a 4% peak reduction occurs.

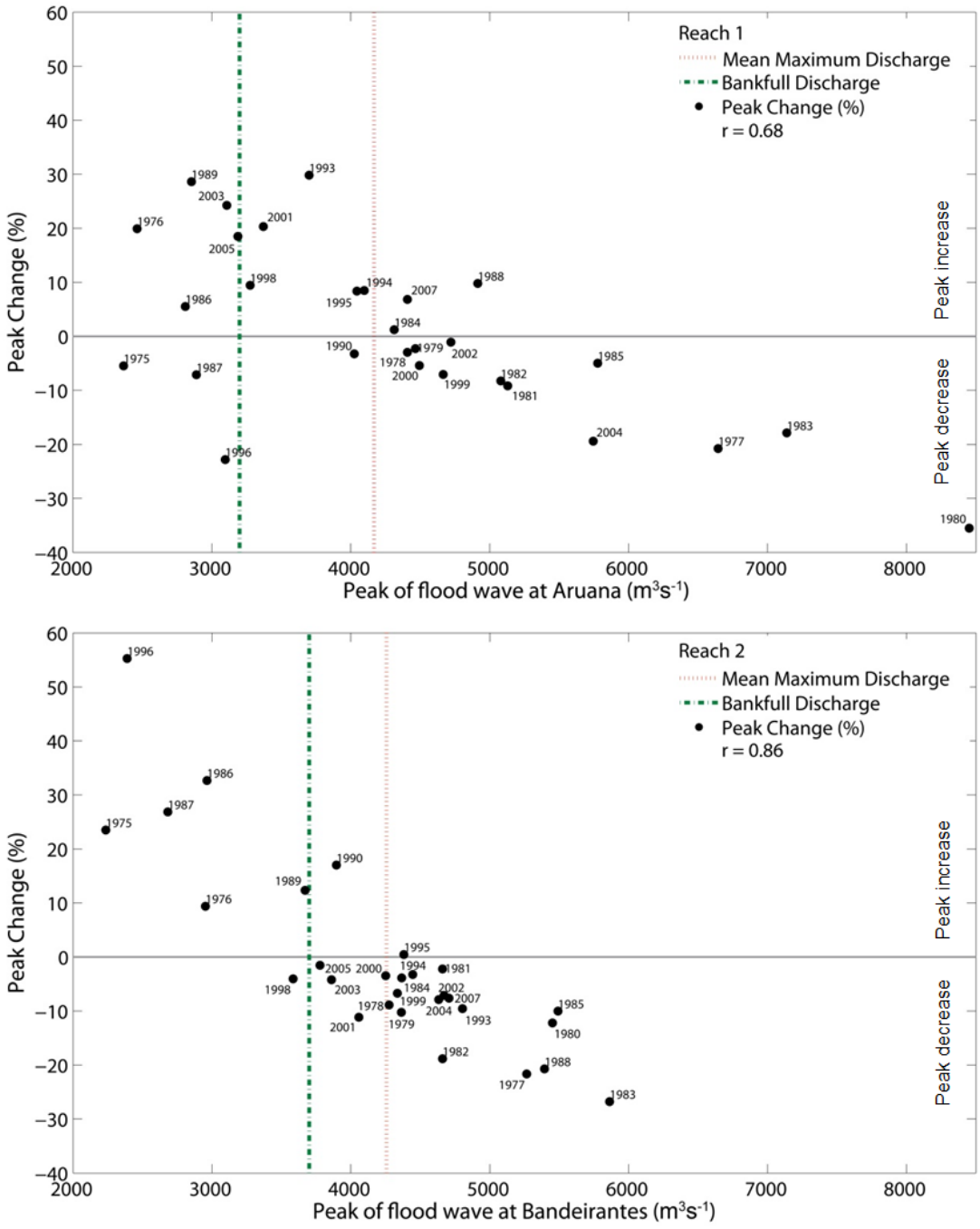

Figure 3.6: Percent peak change for reach 1 (Aruanã to Bandeirantes) and reach 2 (Bandeirantes to Luís Alves) plotted against the upstream peak discharge of the flood wave. Positive peak change indicates that the peak discharge is gaining downstream, while negative peak change indicates that the peak discharge is reduced downstream.

The absolute peak reduction (in m^3s^{-1}) in relation to upstream discharge (Figure 3.7) displays similar patterns as the percent peak reduction, but with a stronger correlation between upstream peak discharge and absolute peak reduction in reach 1 ($r = 0.80$). The percent peak change can overestimate the reduction in peak—if the peak is low, the percent change might be large while the absolute change in peak is not. For example, in reach 1 in 1996, the peak reduction as a percentage was 23%, the 2nd largest reduction after 1980. But, in terms of absolute discharge reduction, 1996 has the 5th largest peak reduction, after 1977, 1980, 1983, and 2004. Thus, it is important to characterize the absolute change as well as the percentage change in peak discharge.

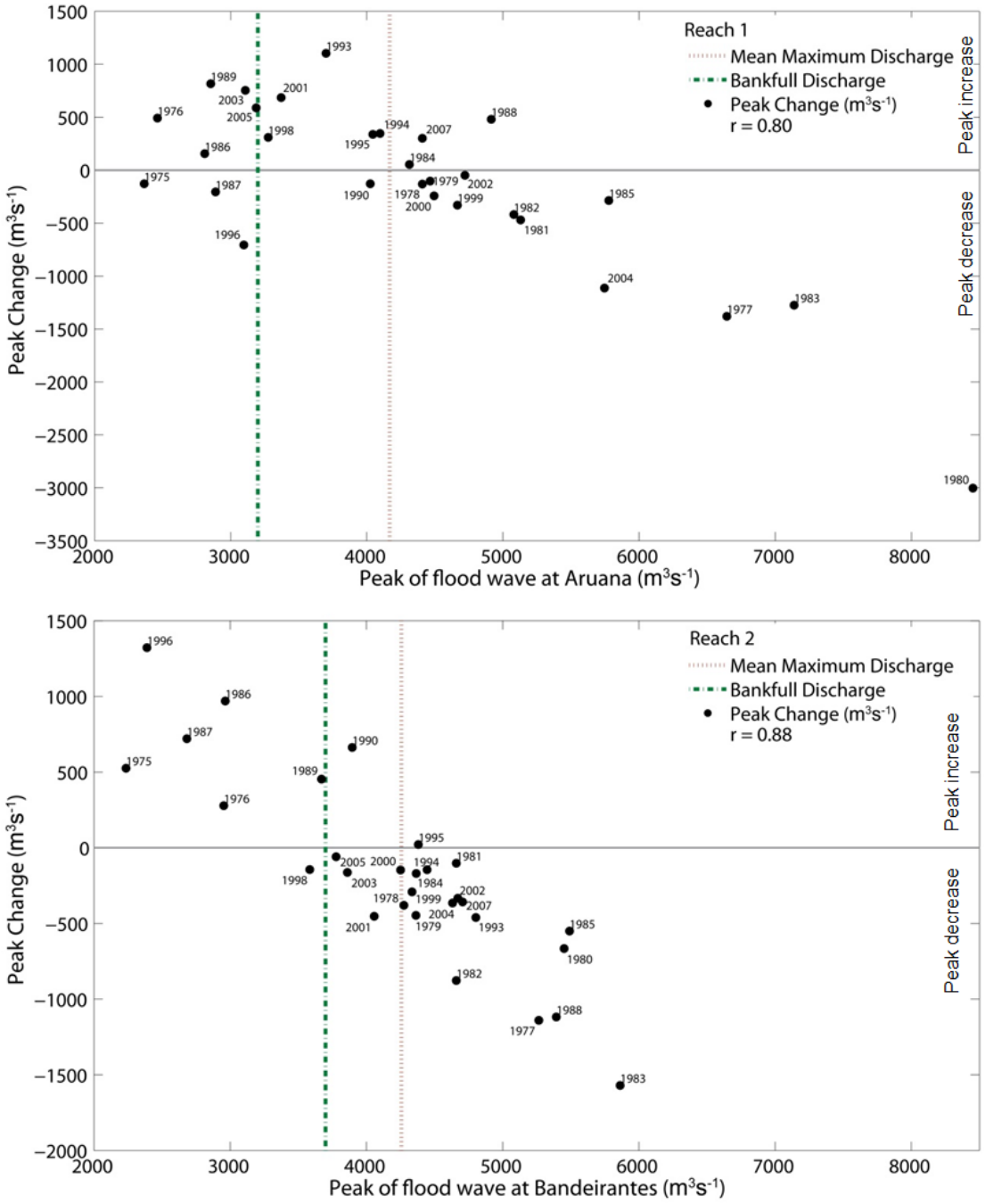

Figure 3.7. Absolute peak change for reach 1 (Aruanã to Bandeirantes) and reach 2 (Bandeirantes to Luís Alves) in m^3s^{-1} plotted against the upstream peak discharge of the flood wave. Positive peak change indicates that the peak discharge is gaining downstream, while negative peak change indicates that the peak discharge is reduced downstream.

Peak discharge reduction along the reach generally begins to occur when the upstream gauging station reaches bankfull discharge. However, the deviations from this trend, which are described above for different years, highlight the complexity of floodplain inundation. Even with an increase in peak discharge downstream, river discharge could still leaving the channel during the flood, particularly because the peak discharge reduction does not take into account the contribution of the tributaries and estimates of peak reduction are not the same as estimates of the floodplain storage during the passage of the flood wave. There are multiple ways in which river discharge can move out of the channel during flooding in addition to overbank flooding. For example, the many lakes in the middle Araguaia River, which in some cases are connected via surface water with the main river channel (see Chapter 4), provide a pathway for water to move into these lakes and the floodplain during the flood wave before the river discharge reaches bankfull discharge. In addition, the rising discharge in the river can increase the water table in the floodplain, which is a slower process relative to river discharge moving into floodplain lakes connected to the channel. These processes are characterized in equation 5 and Figure 3.4.

The complexity of the movement of water out of the river channel and onto the floodplain during flooding in different stages and at discharge levels below bankfull has been described in other tropical systems, such as the Amazon River floodplain (Mertes et al. 1995; Lesack and Melack 1995). For example, the floodplain may begin to inundate well before overbank flooding occurs due to a rising water table and breaks in floodplain drainage channel levees or the expansion of floodplain lakes, highlighting the importance of the geomorphologic controls on floodplain inundation and floodplain storage (Mertes et al. 1995). Chapter 4 describes the types of lakes in the middle Araguaia River and the pathways of surface water connection between the river and the floodplain, providing

more insight on the processes that result in peak discharge reduction and how it can occur below bankfull discharge.

Flood type characterization

Based on the analysis of peak discharge and peak discharge reduction along reaches 1 and 2, the years have been grouped and organized into types similar to Aquino et al. (Figure 3.8, Table 3.7). Type A floods demonstrate large peak discharges at Aruanã (greater than 5,000 m^3s^{-1} but upwards of 8,000 m^3s^{-1} with an average of 6,612 m^3s^{-1}) and large peak reductions along reaches 1 and 2, characterized by the years 1977, 1980, 1982, 1983, and 2004 (Figure 3.8 and example hydrograph in Figure 3.9). Type B floods have lower flood peaks, from below bankfull discharge up to about 4,000 m^3s^{-1} at Aruanã (with an average of 3,042 m^3s^{-1}), and increase in the peak discharge along both reaches, as in the years 1976, 1986, 1989, 1995 (Figure 3.8 and example hydrograph in Figure 3.10). The downstream increase in peak discharge along both reaches is the main aspect that separates this flood type from others. Type C floods have medium flood peaks (mostly 4,500 to 5,500 m^3s^{-1} at Aruanã, with an average of 4,523 m^3s^{-1}) and little to no peak reduction for reach 1, with usually a small peak reduction along reach 2 (Figure 3.8 and example hydrograph in Figure 3.11). Type D can be characterized as reach 1 and reach 2 displaying markedly different patterns of peak discharge reduction. The three other types of flood wave transmission (A, B, and C) display more similar patterns of peak reduction and peak discharge along reaches 1 and 2 (Figure 3.8 and example hydrographs in Figures 3.12 and 3.13). Type D1 floods have higher peak discharges at Aruanã (average of 4,003 m^3s^{-1}) compared with type D2 floods (average of 2929 m^3s^{-1}) and thus more absolute peak reduction. Type D2 floods have peak discharges below bankfull discharge,

indicating that the divergent patterns of reach 1 and reach 2 have smaller absolute changes in peak even though the percent change in peak may be high.

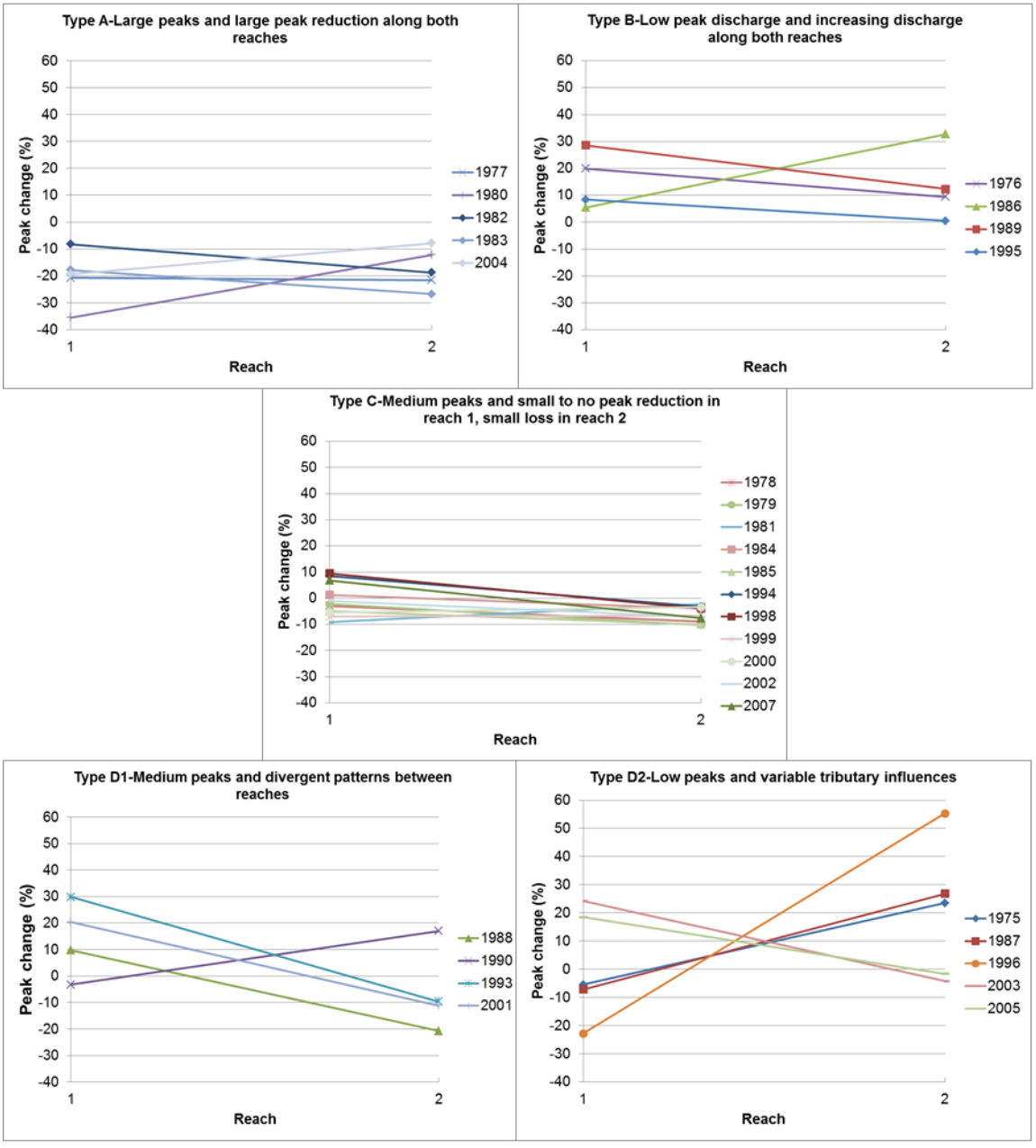

Figure 3.8. Flooding types identified through analyzing percent peak reduction. Types A, B, and C were identified previously by Aquino et al. 2008.

Table 3.7. Results of the peak discharge change analysis for reaches 1 and 2, including peak discharges for the flood wave used for analysis and flood types (n=29). NA = unavailable discharge measurements.

Year	Peak change (%)		Peak change (m^3s^{-1})		Peak of flood wave (m^3s^{-1})			Flood type
	Reach 1	Reach 2	Reach 1	Reach 2	Aruanã	Bandeirantes	Luís Alves	
1975	-5.46	23.49	-129	525	2364	2235	2760	D2
1976	19.94	9.41	491	278	2462	2953	3231	B
1977	-20.77	-21.65	-1380	-1140	6645	5265	4125	A
1978	-2.97	-8.89	-131	-380	4407	4276	3896	C
1979	-2.28	-10.25	-102	-447	4465	4363	3916	C
1980	-35.51	-12.20	-3002	-665	8453	5451	4786	A
1981	-9.16	-2.21	-470	-103	5130	4660	4557	C
1982	-8.25	-18.82	-419	-877	5079	4660	3783	A
1983	-17.87	-26.78	-1276	-1570	7139	5863	4293	A
1984	1.23	-3.87	53	-169	4314	4367	4198	C
1985	-4.97	-10.03	-287	-551	5778	5491	4940	C
1986	5.52	32.69	155	969	2809	2964	3933	B
1987	-7.13	26.85	-206	720	2888	2682	3402	D2
1988	9.79	-20.72	481	-1118	4914	5395	4277	D1
1989	28.64	12.34	817	453	2853	3670	4123	B
1990	-3.23	16.99	-130	662	4026	3896	4558	D1
1991	NA	NA	NA	NA				
1992	NA	NA	NA	NA				
1993	29.84	-9.58	1104	-460	3700	4804	4344	D1
1994	8.49	-3.26	348	-145	4097	4445	4300	C
1995	8.36	0.48	338	21	4044	4382	4403	B
1996	-22.80	55.27	-706	1321	3096	2390	3711	D2
1997	NA	NA	NA	NA				
1998	9.44	-4.02	309	-144	3275	3584	3440	C
1999	-7.07	-6.71	-330	-291	4665	4335	4044	C
2000	-5.41	-3.46	-243	-147	4493	4250	4103	C
2001	20.31	-11.14	685	-452	3372	4057	3605	D1
2002	-1.06	-7.11	-50	-332	4721	4671	4339	C
2003	24.23	-4.22	753	-163	3108	3861	3698	D2
2004	-19.39	-7.88	-1114	-365	5746	4632	4267	A
2005	18.51	-1.56	590	-59	3188	3778	3719	D2
2006	NA	NA	NA	NA				
2007	6.81	-7.61	300	-358	4407	4707	4349	C

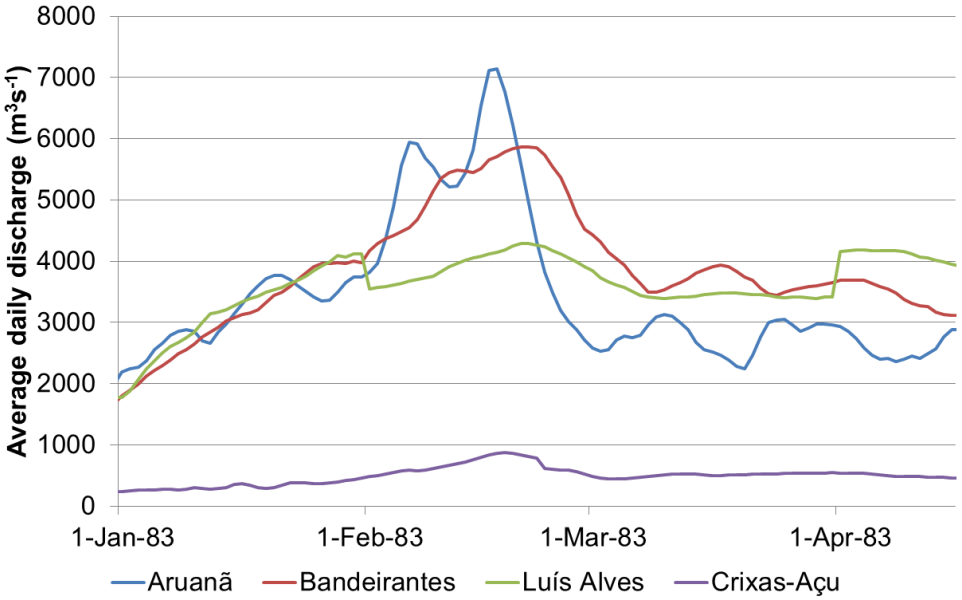

Figure 3.9. Flood wave analyzed for 1983, a type A flood.

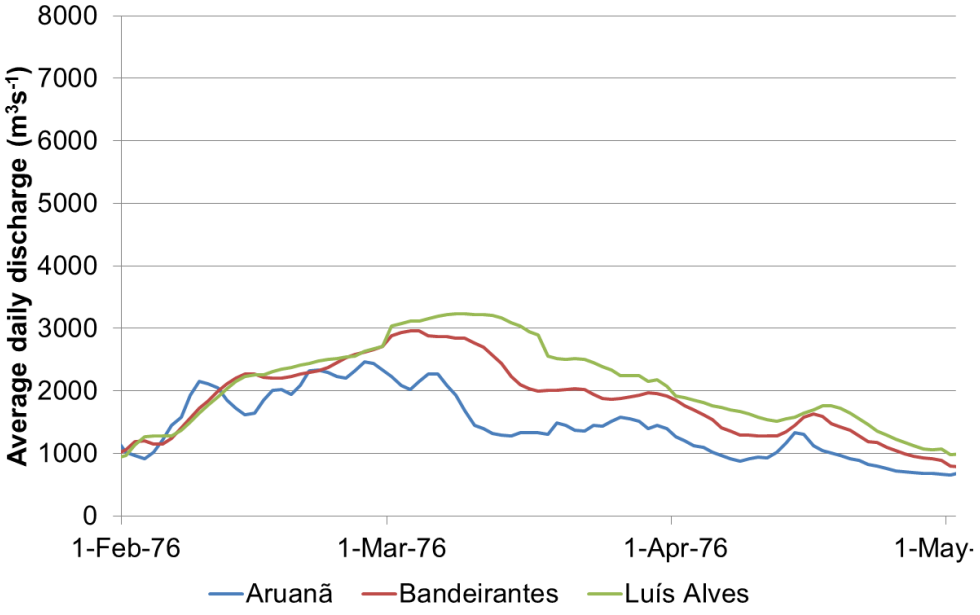

Figure 3.10. Flood wave of 1976, a type B flood. Discharge data from the Crixas-Açu River was not available for this year.

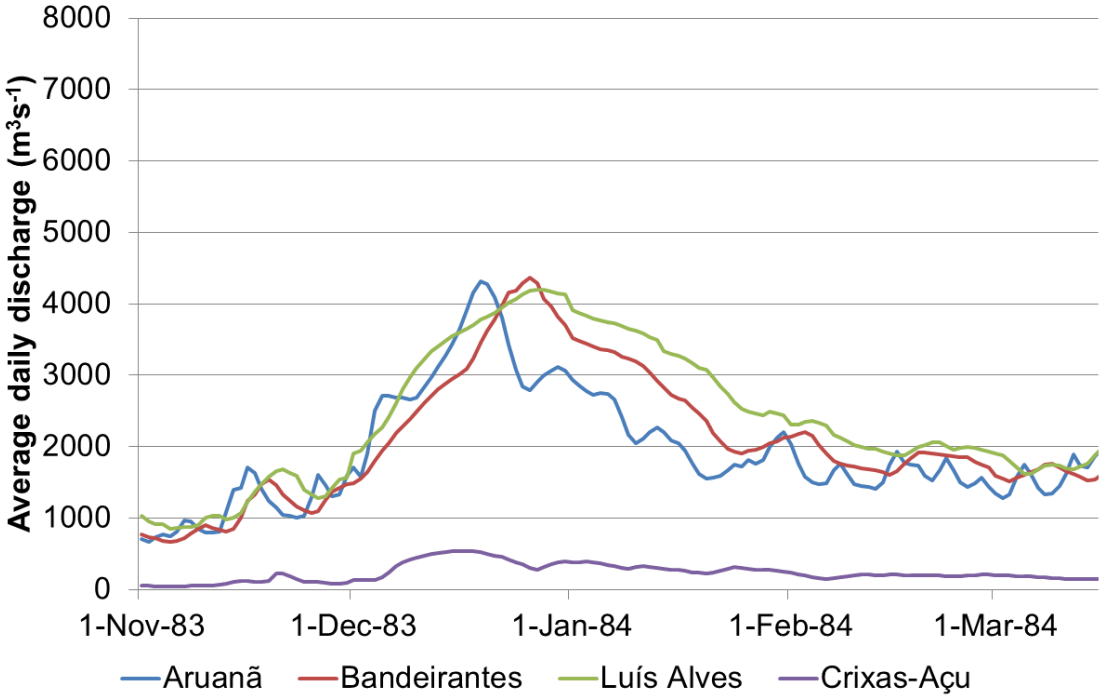

Figure 3.11. Flood wave of 1984, a type C flood.

Since type D floods display very different patterns for reach 1 and reach 2, they may be best explained by variable tributary influences. For example, in 1988 (type D1), the peak discharge at Aruanã is 4914 m^3s^{-1}, increases to 5395 m^3s^{-1}at Bandeirantes, and decreases to 4277 m^3s^{-1} at Luís Alves. Although the Peixe River's estimated mean annual discharge is about half of the estimated mean annual discharge of the Crixas-Açu River (Table 3.3), it is possible that the Peixe River watershed contributed a relatively large amount of discharge compared to the Crixas-Açu River, potentially due to variable precipitation patterns, causing the pattern of peak discharge loss to be different between reach 1 and reach 2. However, further information on precipitation and Peixe River discharge would be needed to determine whether that scenario occurred. Figure 3.10

shows the 1988 hydrograph for the three stations and includes the gauging station on the Crixas-Açu River.

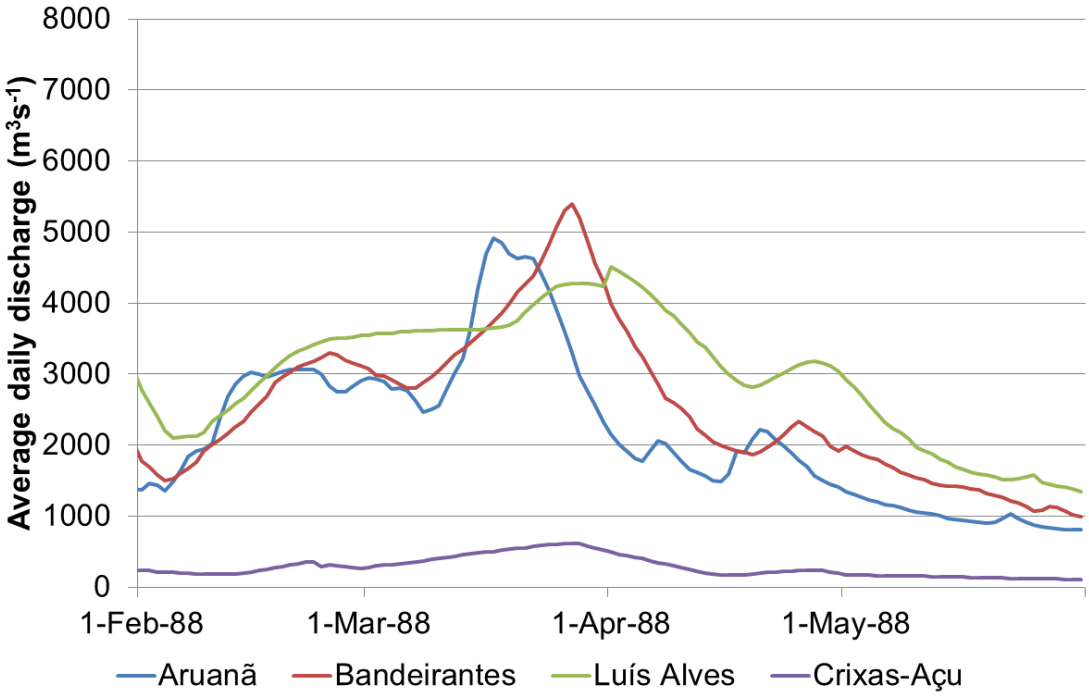

Figure 3.10. Flood wave analyzed for the year 1988, a type D1 flood.

The opposite pattern of peak reduction along the two reaches is demonstrated for another D1 flood in 1990, when the peak discharge at Aruanã is 4026 m^3s^{-1}, decreasing to 3896 m^3s^{-1} at Bandeirantes, and then increasing again to 4558 m^3s^{-1} at Luís Alves. This might be explained by a relatively small contribution by the Peixe River into reach 1 and a larger contribution by the Crixas-Açu River in reach 2. Again, more information on precipitation and Peixe River discharge would be needed for this year to substantiate that idea. The flood hydrograph is shown in Figure 3.11 for this year.

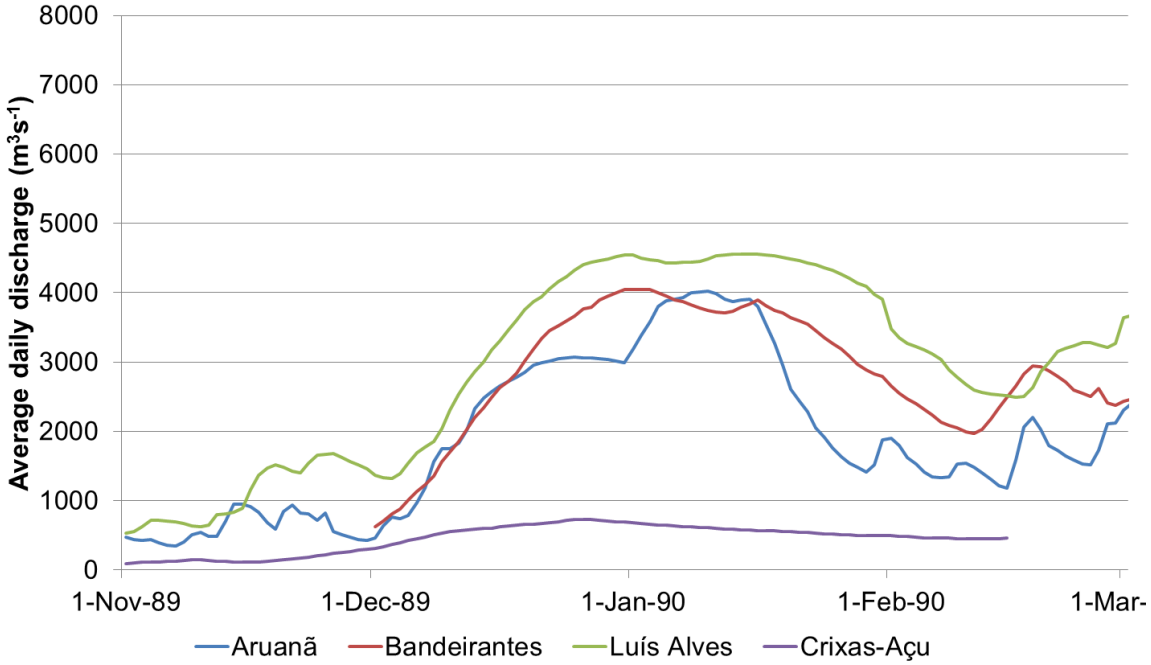

Figure 3.11. Flood wave analyzed for the year 1990, a type D1 flood.

While the types described above are in relatively good agreement with the types described in Table 3.5 by Aquino et al. (2008), the present analysis has slightly revised the flooding patterns previously described in the literature. The level of the peak discharge at Aruanã for each type has been revised to better reflect all of the years analyzed and to better group the pattern of peak discharge change along the reaches. A fourth type of flood, type D, has been added to the characteristic flooding patterns. Finally, some of the years classified by Aquino et al. (2008) have been reclassified by the present study. These differences are mainly caused by the present study using a peak values that represent the flood wave translation downstream instead of the maximum peak discharge recorded for the year at each station.

Estimation of volumetric channel loss

Taking the lag time into account, the estimate of volumetric channel loss over the flood wave crest and over the flooding period for reach 1, reach 2, and reach 2 with discharge data from the Crixas-Açu River tributary during the period of discharge loss was calculated for each available year in which peak discharge reduction occurred. Figure 3.12 and Table 3.8 show the results from channel losses over the flood wave crest. The averages for all analyzed years are 0.27 km^3 channel loss for reach 1 (n = 15 years), 0.73 km^3 channel loss for reach 2 (n = 21 years) and 1.94 km^3 for reach 2 with the tributary (n=11). The average number of days over which downstream discharge reduction occurred and volumetric channel loss was summed over the flood wave is 8.9 days for reach 1, 18.1 days for reach 2, and 32.1 days for reach 2 including the tributary. This indicates that reach 2 usually experiences more days of lower discharge compared to reach 1, whether or not the tributary estimate is included. The estimated losses per unit channel length of reach 1 and reach 2 (without the tributary) demonstrate that reach 2 loses more discharge per unit channel length (Figure 3.13). Average losses over the flood wave crest per km of channel length for the years in which peak reduction occurs is ~1,600,000 m^3km^{-1} for reach 1 and ~11,500,000 m^3km^{-1} for reach 2, indicating that loss per km of channel length is about 7 times greater in reach 2 compared to reach 1.

The largest volumetric channel loss over the flood wave crest occurred in 1996 for reach 1, when an estimated value of 0.83 km^3 is lost over a span of 17 days. The year 1996 is a type D2 flood, in which the peak discharge at Aruanã was low and the reaches displayed different patterns of peak reduction. Reach 1 displayed a 23% reduction in the peak discharge, but there was no peak reduction and no estimated channel loss for reach 2 in 1996, highlighting the difference between the reaches. The 1996 channel loss occurred when the peak discharge at Aruanã (3096 m^3s^{-1}) was below bankfull discharge (3200 m^3s^{-}

[1]), demonstrating again that channel loss over the flood peak can occur below bankfull discharge. Additional years have similar estimates of channel loss, for example in 1983 and 1977, type A floods, when 0.41 km^3 and 0.58 km^3 were lost over the flood peak. The smallest volumetric channel loss for reach 1 occurred in 1979 (0.016 km^3), which is a type C flood year, in which there was small to no peak reduction in reach 1 followed by a peak reduction in reach 2. Reach 2 channel loss in 1979 was 2.34 km^3. For reach 2 without the tributary data, the largest volumetric channel loss occurred in 1983 (type A flood), when 3.7 km^3 was lost over a span 59 days. The smallest channel loss was 0.013 km^3 in 2005, which is a type D2 flood, in which one reach increased in discharge (in this case, reach 1), and the other reach decreased in discharge (in this case, reach 2).

The results for reach 2 with the tributary data highlight the importance of accounting for the tributary contributions. When the tributary influx is included, the amount of channel loss varies between years. However, when the tributary data are included, calculations suggest at least a doubling of the estimated channel loss for every year in which measurements were available and a loss occurred. With the estimates of channel loss for the flood wave crest and for the flooding period for reach 2 with the tributary, it is important to note again that the tributary data represents about 80% of the drainage area for the tributary. Thus, the values provided represent the potential change to the water budgets that could occur if tributary data were available at the confluence with the Araguaia River. Including the tributary at 80% of the drainage area provides a way to estimate the magnitude of difference that it makes in the calculation of channel losses.

Table 3.8. Results of volumetric channel loss over the flood wave crest and channel loss per unit channel length for reaches 1 and 2 and reach 2 with tributary data. NL = no discharge loss observed for the reach; NA = unavailable discharge measurements.

Year	Peak of flood wave (m^3s^{-1})			Channel loss over flood wave crest (km^3)			Channel loss per unit channel length (m^3/km)		Flood wave type
	Aruanã	Bandeirantes	Luís Alves	Reach 1	Reach 2	Reach 2 with tributary	Reach 1	Reach 2	
1975	2364	2235	2760	0.03	NL	NA	204311	NL	D2
1976	2462	2953	3231	NL	NL	NA	NL	NL	B
1977	6645	5265	4125	0.58	1.52	NA	3418899	23699250	A
1978	4407	4276	3896	0.02	0.36	NA	114861	5624100	C
1979	4465	4363	3916	0.02	2.34	NA	94532	36595800	C
1980	8453	5451	4786	NA	2.58	NA	NA	40279950	A
1981	5130	4660	4557	0.16	0.07	NA	946842	1019250	C
1982	5079	4660	3783	0.17	1.58	4.08	999699	24678180	A
1983	7139	5863	4293	0.40	3.71	7.10	2379558	57927150	A
1984	4314	4367	4198	NL	0.04	0.34	NL	657450	C
1985	5778	5491	4940	0.10	0.44	1.88	613440	6914700	C
1986	2809	2964	3933	NL	NL	NL	NL	NL	B
1987	2888	2682	3402	0.19	NL	NL	1105920	NL	D2
1988	4914	5395	4277	NL	0.67	1.53	NL	10516500	D1
1989	2853	3670	4123	NL	NL	NL	NL	NL	B
1990	4026	3896	4558	0.22	NL	NL	1283294	NL	D1
1991				NA	NA	NA	NA	NA	
1992				NA	NA	NA	NA	NA	
1993	3700	4804	4344	NL	0.27	NA	NL	4187700	D1
1994	4097	4445	4300	NL	0.09	NA	NL	1387800	C
1995	4044	4382	4403	NL	NL	NL	NL	NL	B
1996	3096	2390	3711	0.83	NL	NL	4857205	NL	D2
1997				NA	NA	NA	NA	NA	
1998	3275	3584	3440	NL	0.10	0.80	NL	1614600	C
1999	4665	4335	4044	0.75	0.10	0.48	4426221	1572750	C
2000	4493	4250	4103	0.16	0.36	1.42	943285	5668650	C
2001	3372	4057	3605	NL	0.23	0.89	NL	3547800	D1
2002	4721	4671	4339	0.02	0.44	2.36	100122	6921450	C
2003	3108	3861	3698	NL	0.05	0.41	NL	761400	D2
2004	5746	4632	4267	0.42	0.13	NA	2458334	2097900	A
2005	3188	3778	3719	NL	0.01	NA	NL	198450	D2
2006				NA	NL	NA	NA	NL	
2007	4407	4707	4349	NL	0.33	NA	NL	5081400	C

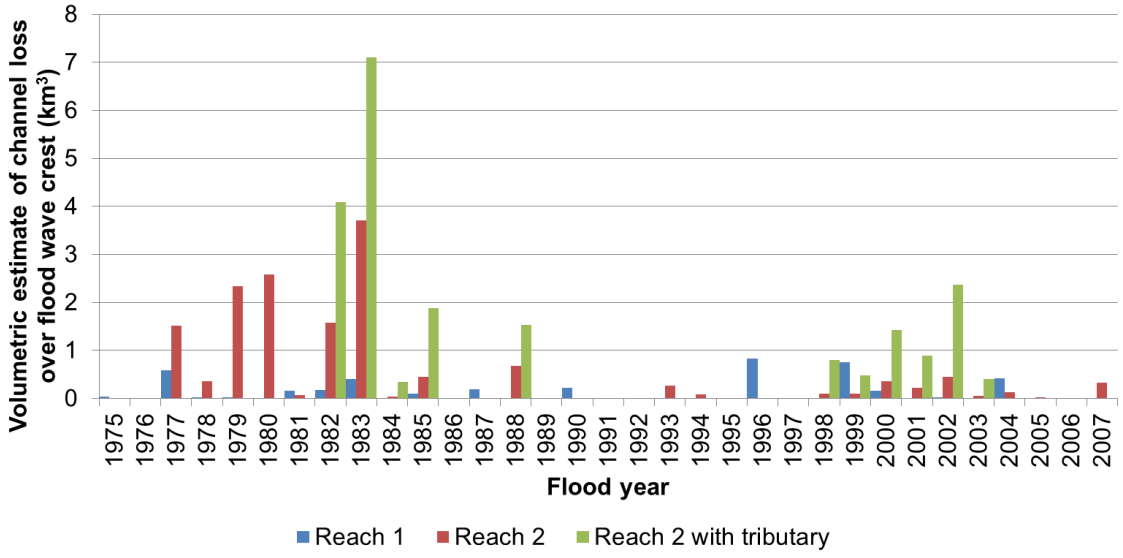

Figure 3.12. The volumetric channel loss over the flood wave crest (in km^3) for reach 1, reach 2, and reach 2 including the tributary data.

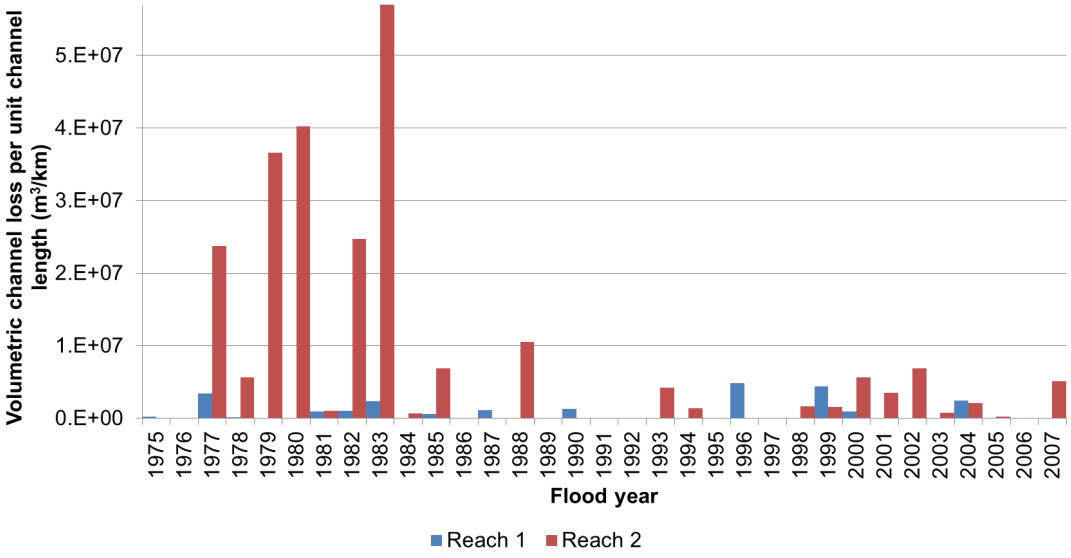

Figure 3.13. Volumetric channel loss over the flood wave crest per unit channel length (m^3km^{-1}) for reaches 1 and 2.

The channel losses over the flood wave crest can also be viewed as losses per day, with the loss normalized by the number of days over which losses occur in the flood wave crest. Figure 3.14 shows the volumetric channel loss over the flood wave crest per day, and it is clear that reach 1, reach 2, and reach 2 with the tributary have similar values of loss/day over the flood wave when normalized by the number of days of discharge loss. The average over all available years for is the same for both reaches without the tributary data (0.027 km^3/day). The reach 2 with the tributary is slightly higher, at 0.051 km^3/day. This indicates that although the absolute channel loss during the flood peak is higher in reach 2 relative to reach 1, reach 1 displays relatively the same amount of loss per day during the flood wave as reach 2, just for a shorter period of time.

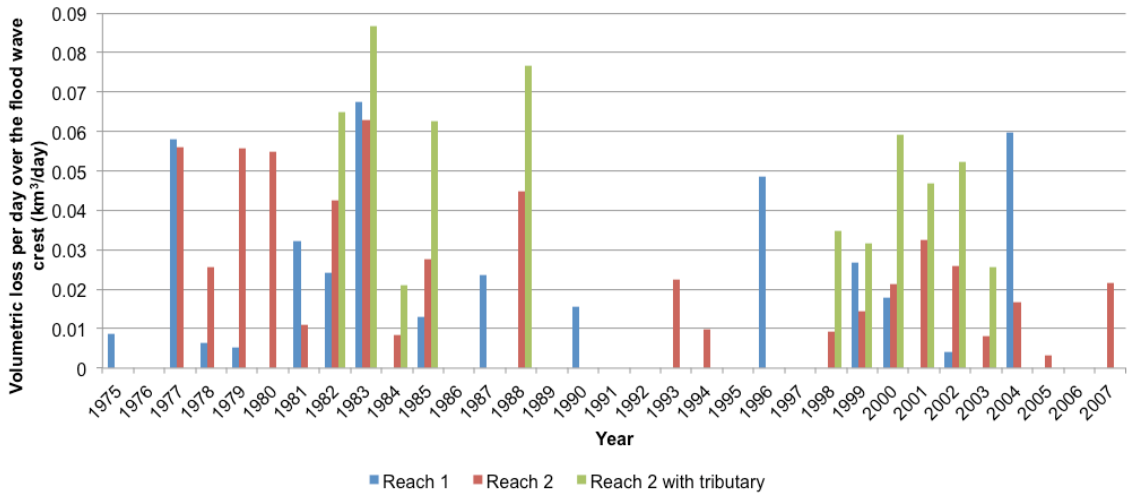

Figure 3.14. Volumetric loss per day over the flood wave crest (km^3/day) for reaches 1 and 2 and reach 2 including the tributary data.

The volumetric channel losses over the flooding period, from November to May, demonstrate that the channel losses over the flood wave crest in most cases do not result in channel loss over the entire flooding season (Figure 3.15 and Table 3.9). In Figure

3.15, negative channel loss indicates channel gains over the flood season, and positive channel loss means that channel loss occurred. Table 3.9 indicates the years analyzed and the years in which unavailable discharge measurements impeded the analysis of channel loss over the flooding period. In all years analyzed, reach 1 does not show a channel loss over the flooding period, although the Peixe River tributary is not included in this estimate. Thus, it is possible that channel loss over the flooding season could occur if Peixe River data were available. In reach 2 without the tributary, channel loss is evident in two years, 1982 and 2007, which are both type C floods. In reach 2 with the tributary data, channel loss occurs in 5 years, 1982, 1983, 1985, 2000, 2001, and 2002. The flood years of 1982 and 1983 (both type A floods) have the largest channel loss over the flooding period, with 7.5 km^3 and 5.4 km^3, respectively. Smaller losses of less than 2 km^3 occur in reach 2 with the tributary in 3 years, which are all type C floods. In 2001, there is a slight channel loss (0.03 km^3), which is a type D1 flood, in which reach 1 and 2 display different patterns of peak reduction. Thus, in reach 2 large channel losses over the entire flooding period only occur during type A floods with very high peak discharge, and smaller losses occur with type C floods, with medium peak discharges and peak discharge reduction in reach 2. The channel losses for the entire flooding season are likely stored in floodplain lakes over the dry season, lost to evaporation, or lost to groundwater beneath the floodplain.

Table 3.9. Channel loss over the flooding period, from November to May for each year in which average daily discharge measurements are available. NA = unavailable discharge measurements.

Year	Channel loss over the flooding period (km^3)			Flood wave type
	Reach 1	Reach 2	Reach 2 with tributary	
1975	-2.44	-5.64	NA	D2
1976	-4.48	-3.03	NA	B
1977	-5.37	-4.19	NA	A
1978	-6.43	-7.65	NA	C
1979	-1.01	-1.75	NA	C
1980	NA	-0.90	NA	A
1981	-7.96	NA	NA	C
1982	-6.84	0.22	7.50	A
1983	-5.53	-0.30	5.40	A
1984	-3.24	-6.54	-1.92	C
1985	-5.26	-4.91	0.77	C
1986	-6.68	-10.75	-4.05	B
1987	-3.67	-8.00	-4.33	D2
1988	-5.74	-7.26	-2.87	D1
1989	-7.01	-11.45	NA	B
1990	-9.82	-9.35	NA	D1
1991	NA	NA	NA	
1992	NA	NA	NA	
1993	NA	NA	NA	D1
1994	-10.13	-7.90	NA	C
1995	NA	NA	NA	B
1996	-0.67	-10.79	-7.29	D2
1997	NA	NA	NA	
1998	NA	NA	NA	C
1999	NA	NA	NA	C
2000	-4.81	-5.58	1.45	C
2001	-4.54	-4.70	0.03	D1
2002	-7.31	-4.38	1.92	C
2003	-7.07	NA	NA	D2
2004	-5.62	NA	NA	A
2005	NA	-5.24	NA	D2
2006	NA	NA	NA	
2007	-13.39	2.31	NA	C

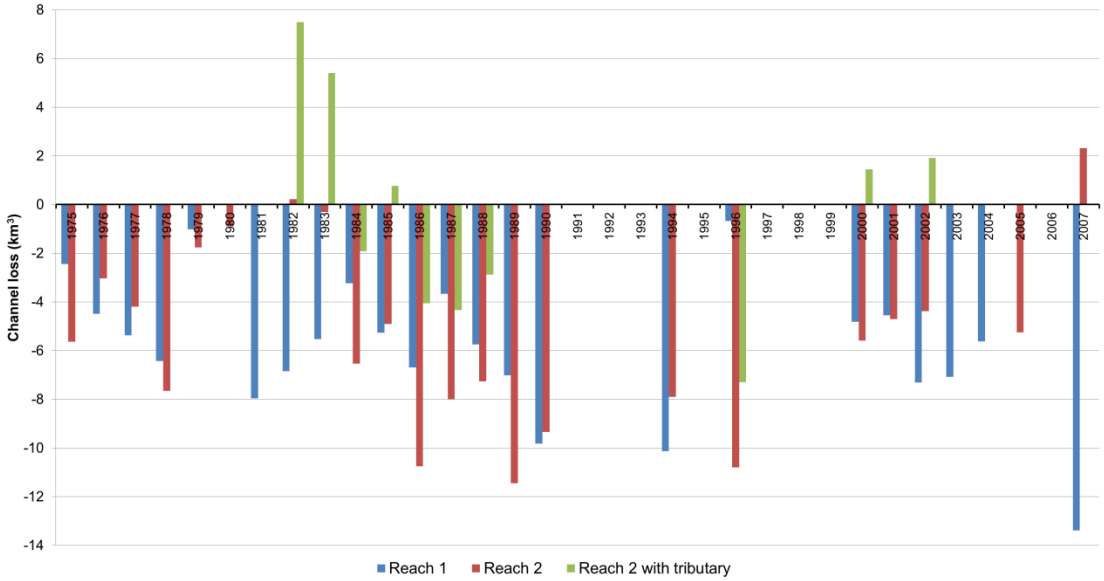

Figure 3.15. Channel loss (positive values) and channel gain (negative values) over the flooding period, from November to May, for all available years and reaches, including reach 1, reach 2, and reach 2 including tributary data.

Table 3.10 shows the years in which channel loss occurred over the entire flooding season as a percentage of the total volume of inputs (the volume of upstream discharge for reach 2; the volume of upstream discharge and tributary discharge for reach 2 with the tributary). When incorporating the tributary data, the highest loss for reach 2 is about 10% and 12% of the total discharge input, for 1982 and 1983 (type A floods), respectively. The volume of discharge that is lost as a percentage of total inputs is much smaller in the other years, which are classified as type C or type D1 floods.

Table 3.10. The loss over the flooding season for reach 2 and reach 2 with the tributary input as a percentage of the total discharge input to the reach. NL= No loss was observed; NA= discharge data were unavailable.

Year	Reach 2 channel loss as a percent of input volume (%)	Reach 2 with tributary channel loss as a percent of input volume (%)
1982	0.40	12.16
1983	NL	10.32
1985	NL	1.52
2000	NL	3.22
2001	NL	0.08
2002	NL	3.89
2007	5.51	NA

In the years in which both types of losses occur (over the flood wave crest and over the flooding period), channel loss over the flood wave crest exceeds channel loss for the flooding period in four out of six years (Table 3.11). In these years (1983, 1985, 2001, 2002), larger channel losses occur during the flood wave peaks, with the channel regaining some of this loss by the end of the flooding period. In 1982 (type A) and in 2000 (type D1), channel loss over the flood wave crest is less than channel loss over the flooding period, although in 2000 the values are very similar. In these years, it appears that losses were not exclusive to periods when upstream discharge rates exceeded downstream rates over the flood wave crest.

Table 3.11. Reach 2 with tributary channel loss over the flood wave crest compared to channel loss for the flooding period from November to May, for years in which losses occurred over the flooding period. NL= no losses observed; NA=unavailable discharge measurements.

Year	Channel loss over flood wave crest (km^3) for reach 2 with tributary	Channel loss over flooding period (km^3) for reach 2 with tributary
1982	4.08	7.5
1983	7.1	5.4
1985	1.88	0.77
2000	1.42	1.45
2001	0.89	0.03
2002	2.36	1.92

The average channel losses for each flooding type over the flood wave crest and over the flooding period are displayed in Table 3.12. The averages for the type D1 and D2 floods are not representative of the divergent patterns between reach 1 and reach 2, as in some D1 and D2 years, one reach does not have channel loss and the other reach does. Type B floods do not have measurable channel losses in any of the years. The average channel losses over the flood wave crest for types A and C reflect the peak reduction for those types of floods. For type C, there are small losses in reach 1 and a larger loss in reach 2. For type A, there are losses in reaches 1 and 2, and both reach 1 and reach 2 average losses are the highest compared to all of the types.

Table 3.12. Average channel losses for each flooding type, over the flood wave crest and over the flooding period. The first numbers in parentheses indicates the number of years in which channel losses occurred for each flood type (the number of years in which the average was calculated). The second number in parentheses indicates the number of years in which no channel losses were observed for each flood type. These numbers do not include years in which discharge measurements were unavailable. NL=no losses observed for all available years.

Flood type	Average loss over the flood wave crest (km^3)			Average loss over the flooding period (km^3)		
	Reach 1	Reach 2	Reach 2 with tributary	Reach 1	Reach 2	Reach 2 with tributary
A	0.39 (4,0)	1.90 (5,0)	5.59 (2,0)	NL	0.22 (1,3)	6.45 (2,0)
B	NL	NL	NL	NL	NL	NL
C	0.18 (7,4)	0.43 (11,0)	1.21 (6,0)	NL	2.31 (1,7)	1.38 (3,1)
D1	0.22 (1,3)	0.39 (3,1)	1.21 (2,1)	NL	NL	0.03 (1,1)
D2	0.35 (3,2)	0.03 (2,3)	0.41 (1,2)	NL	NL	NL

If the channel losses in reaches 1 and 2 are lost only to the geomorphologic floodplain, it is possible to get an estimate of the losses per area and assess whether this is a reasonable amount. For example, the 1983 (type A) channel loss over the flooding period for reach 2 with tributary data resulted in a 5.4 km^3 channel loss. If this volume was distributed only over the geomorphologic floodplain for reach 2, which is 350 km^2, a water height of 15 m would need to be stored within and across the floodplain over the entire flooding period. However, the floodplain contains many lakes formed by fluvial processes, which expand in depth and area during the flooding season (Morais et al. 2005; Chapter 4). In addition, the 1983 flood was an extreme flood, in which floodwaters likely were distributed outside of the geomorphologic floodplain (e.g., beyond the geomorphologic floodplain or in areas adjacent that area not usually flooded and are not classified as the geomorphologic floodplain) or in the Crixas-Acu River tributary floodplain prior to the confluence with the Araguaia River. These processes might also

have occurred in the type A flood of 1982. With a more moderate channel loss, such as one that occurred over the flooding period in 2000, when 1.45 km^3 of water was lost over the flooding period for reach 2 including the tributary, the height of water across the floodplain that it would need to absorb to cause the channel loss would be approximately 4 meters.

Figure 3.16 shows the discharge for each station normalized by the mean annual discharge for each station, with the color indicating the type of flood that occurred in that year (type A is red, type B is green, type C is blue, type D1 is purple, and type D2 is black). Table 3.13 shows the averages of the normalized discharge for each flood type at each station. In the figure and the table, it is clear that the high magnitude floods (particularly type A floods) result in a greater decrease in normalized peak discharge along reach 1 and reach 2. For type A floods, on average there is approximately a 56% decrease in normalized peak discharge from Aruanã to Luís Alves. For type C floods, in which flood peaks are medium high, on average there is a 36% decrease in normalized peak discharge from Aruanã to Luís Alves. The normalized peak discharge decreases only slightly for type B floods along reaches 1 and 2 (11% total), which have lower magnitudes and no estimated channel losses over the flood wave crest. Types D1 and D2 floods are difficult to characterize due to the variable reductions in peak discharge along reaches 1 and 2, but it is clear that type D2 floods have lower normalized peak discharges compared to type D2.

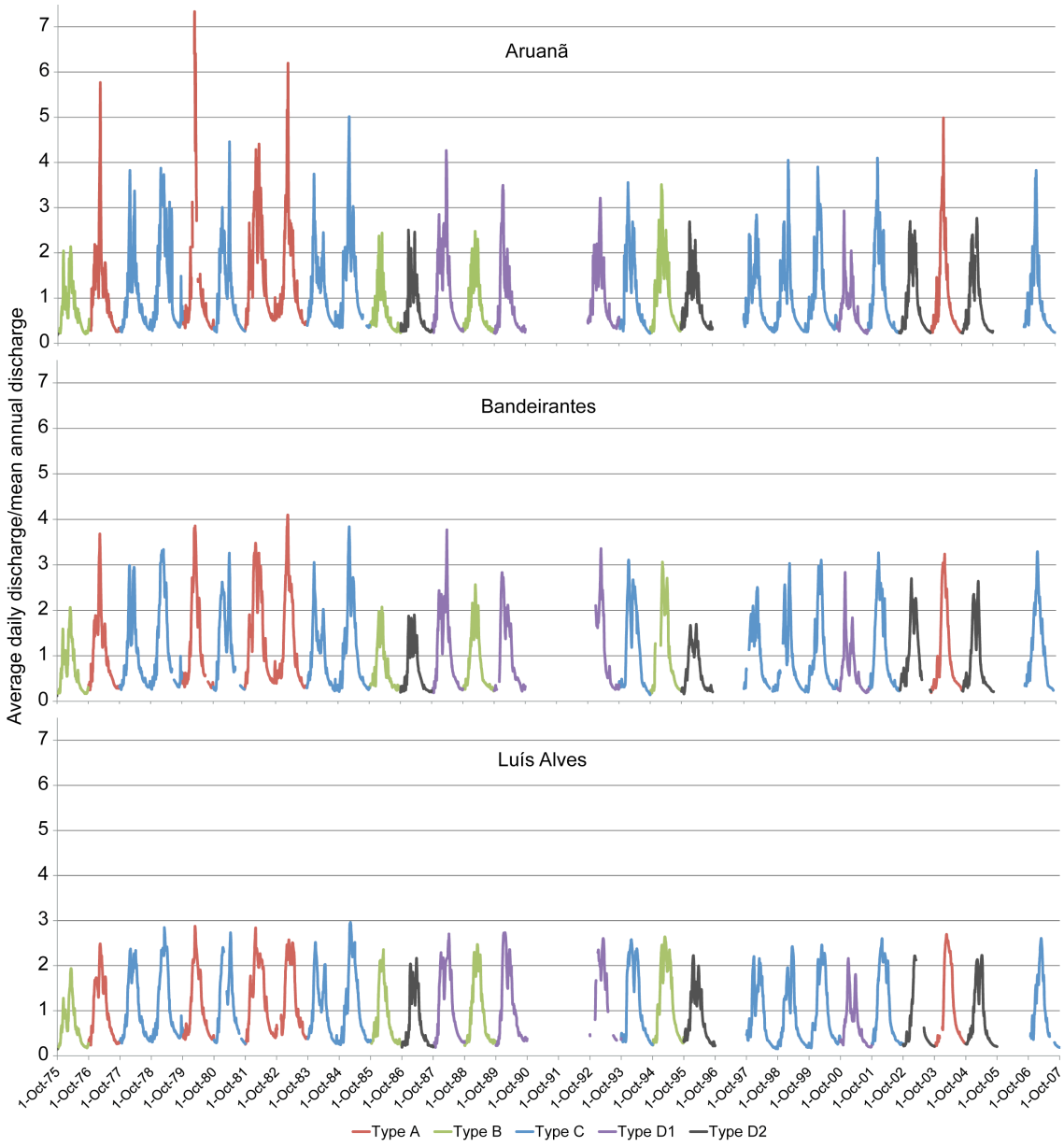

Figure 3.16. Discharges for the three gauging stations normalized by mean annual discharge. The different flood types are distinguished by color--type A is red, type B is green, type C is blue, type D1 is purple, and type D2 is black.

Table 3.13. The average peak discharge normalized by the mean annual discharge for each station and for each flood type.

Type	Average peak discharge normalized by mean annual discharge for each flood type		
	Aruanã	**Bandeirantes**	**Luís Alves**
A	5.72	3.63	2.54
B	2.63	2.45	2.34
C	3.91	3.14	2.50
D1	3.46	3.19	2.51
D2	2.53	2.10	2.07

As stated previously, it is necessary to distinguish the difference between channel losses and measurements of floodplain storage. The transfer of water to and from the floodplain during flooding occurs in many river-floodplain systems, even without an observed channel loss during peaks or during the flooding season. For example, Richey et al. (1989) estimate that a maximum of 30% of the flow in the Amazon River channel has been routed through the floodplain during the flooding season using a flood routing model, although Alsdorf et al. (2010) estimate this quantity to be about 10% using coarse resolution gravimetric data and other remotely sensed imagery over a similar study area. However, net reductions of discharge downstream are not observed (Alsdorf et al. 2010; Richey et al. 1989). In the Araguaia, movement of water onto the floodplain and back into the channel can occur without an absolute reduction of discharge downstream. The total volumetric channel loss over the flooding season can be up to 12% of the total volume of discharge inputs in reach 2 (Table 3.10), but estimates of the fluxes of water to and from the floodplain during the flooding season in the middle Araguaia River would likely be greater than the estimates of channel losses. This is because floodplain storage can occur without a net reduction of discharge rate downstream. Thus, it is difficult to

compare these channel losses to other similar systems in which floodplain fluxes have been estimated. Downstream reduction in discharge in the Upper Paraguay River as it enters the Pantanal wetland and creates a depositional fan can be as much as 50% (Assine and Silva 2009). Although this system is different than the middle Araguaia River, as described previously, peak discharge reduction in the Araguaia River can be as high as 35%, as in the 1980 type A flood.

Patterns of flooding, channel loss, and geomorphology

When comparing reach 1 and reach 2 without the tributary data, reach 1 experiences less channel loss over the flood wave crest compared to reach 2 (Figure 3.12). This could be the result of the differences in the geomorphology of the floodplain, including differences in the floodplain lakes that are connected to the main river channel. The number of floodplain lakes connected to the channel and the morphology of the floodplain likely play a strong role in channel losses over the flood wave crest by providing storage areas for the channel discharge and more opportunities for channel discharge to enter the floodplain. These aspects are further discussed in Chapter 4, which analyzes changes in floodplain lake morphometry and the changes in open water areas along the river.

Figure 3.17 summarizes the flood types and the channel losses that occur over the flood wave crest, along with the geomorphologic floodplain outlined in white on the satellite image. In reach 1, just over half of the floodplain is unit I (56%) compared to reach 2, with 24% as unit I (Table 3.4). In unit I, it is rare that the river directly contributes water to the floodplain during periods of high discharge, and is mostly inundated through the rising of the water table and smaller tributaries (Latrubesse and

Stevaux 2002). Much of the floodplain in reach 2 is unit II (73%), while only about 37% of reach 1 is unit II. In general, unit II receives more overbank flow and has more varied topography due to scroll landforms, which are created by point bar deposition as the channel migrates (Bayer 2002; Latrubesse and Stevaux 2002). This characteristic of unit II potentially provides more storage areas for river discharge. In addition, the characteristics of the sedimentary deposits differ between units I and II (see Chapter 2), with unit II having sandier sedimentary structure compared with unit I, as it is the transition zone between the high energy sandy sedimentation influenced by the channel and the low-energy fine sediment that is causing vertical accretion in unit I. It is possible that unit II is more porous due to the characteristics of its sediments, which could lead to a larger volume of water stored within the floodplain sediments and larger groundwater losses from the channel. However, more data on porosity, the average characteristics of the units in reaches 1 and 2, and groundwater characteristics would be needed to determine if this is a factor in channel loss. Further differences between units I and II and the differences between reaches are discussed in Chapter 4.

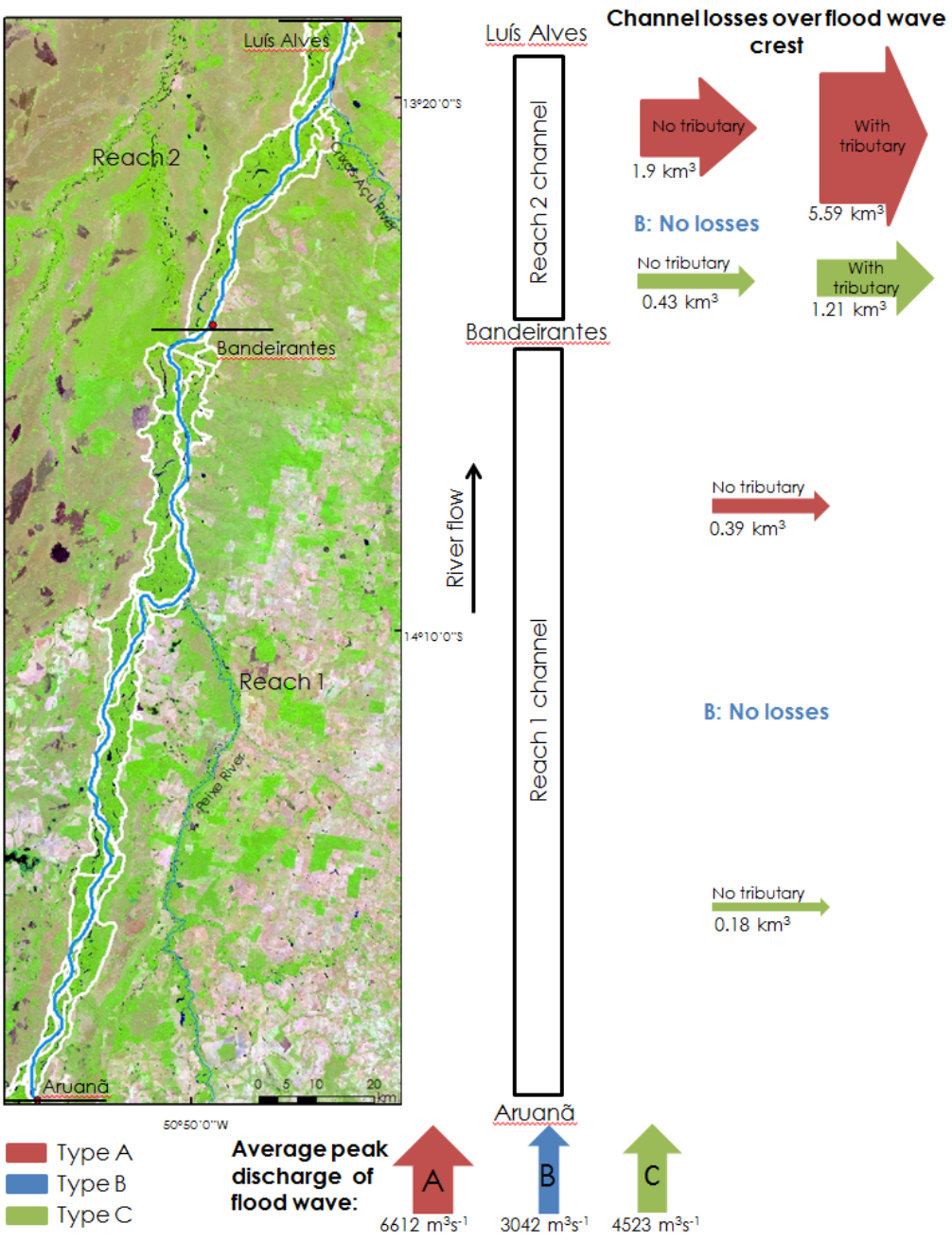

Figure 3.17. Reaches 1 and 2, showing average channel losses over the flood wave crest and average peak discharge at Aruanã. Arrow widths are proportional to the amount of channel loss or peak discharge. The geomorphologic floodplain is outlined in white in the satellite image (Landsat 5 TM, bands 5-4-3), with Roman numerals indicating units I, II, and III.

To speculate, the channel loss during peak discharge is likely due to a combination of factors. The many floodplain lakes connected to the channel provide storage areas for the river discharge (see Chapter 4), but other tropical systems have floodplains with floodplain lakes and drainage channels and do not display a reduction in downstream discharge. It could be that floodplain lakes are more frequent and more connected via surface water to the channel in the Araguaia River compared to other systems, but more research would need to be done to determine this. In addition, Woltemade and Potter (1994) showed that the intensity of the flood wave, meaning how high the peak discharge is relative to the total volume of runoff, influenced the amount of peak reduction that occurred. If the flood wave intensity was high, with a sharp peak relative to the total volume, more peak reduction downstream occurred. Although the watershed modeled by Woltemade and Potter is much smaller than the Araguaia watershed system and the flood waves modeled occur over a period of hours instead of a period of months, the processes might help explain the patterns of peak reduction and channel losses in the Araguaia River. Since the Araguaia River is located in the wet-dry tropics, with a seasonal signal of rainfall, in years with large floods (e.g, types A and C), the rise to peak discharge in hydrograph could be steeper and thus the flood over the period of months could be more intense than in other systems.

The peak discharge reduction could also be a result of the changing geomorphologic characteristics of the river system as the flood moves from the upper Araguaia River to the middle Araguaia River. Because the upper Araguaia River is constrained by bedrock in a V-shaped valley and does not have a well-developed floodplain (Latrubesse and Stevaux 2002), floods coming into the middle Araguaia River are likely more intense compared to other tropical wet-dry systems. For example, at Barra do Garças, which is at the downstream end of the upper Araguaia (see Figure 2.1), peak

flows are 16 times the minimum flows (Aquino et al. 2008). This ratio decreases to 13 at Aruanã and decreases further to 10 at Luís Alves (Aquino et al. 2008), demonstrating that peak flows are intense relative to low flows as the floods move into the middle Araguaia River. Discharges normalized by mean annual discharge decrease from Aruanã to Luís Alves (Figure 3.16), particularly during large peak discharges, showing that upstream peaks are higher relative to the mean annual discharge compared to downstream. Finally, along each reach there is only one tributary that flows into the Araguaia. This aspect of the river system may also play a role in causing net discharge reduction downstream if the tributaries are not contributing as much river discharge relative to what can be transferred to the floodplain during peak flooding. It may be that other large systems in a tropical wet-dry climate with similar geomorphologic characteristics display peak discharge reduction during flooding, but further investigation would be needed to determine this.

Understanding the flooding patterns and peak discharges on the Araguaia River are important for determining how peak discharges change downstream, as peak discharges at and above bankfull impact the geomorphology of channels and their floodplains by increasing sediment transport within the channel and delivering sediment to the floodplain. The reduction in downstream discharge would influence estimates of sediment transport within the river channel and sedimentation on the floodplain. The floods on the Araguaia River are also important for the lateral exchanges of nutrients and organisms that occur during floods and sustain the floodplain ecosystem.

Chapter 4: Changes in floodplain lakes and in the area of open water in the middle Araguaia River floodplain between the 1987 dry season and the 1988 wet season

The middle Araguaia River floodplain contains many lakes formed by fluvial processes. These lakes play an integral role in the floodplain ecosystem, providing important habitat for fish communities and phytoplankton (Nabout et al. 2006; Tejerina-Garro et al. 1998). The floodplain lakes also provide storage areas that contribute to peak river discharge reductions and temporary channel transmission losses in the middle Araguaia River. This chapter determines the change in open water area between the dry season in 1987 and the wet season in 1988 in floodplain lakes and in the middle Araguaia River floodplain along geomorphologically different channel-floodplain reaches. Determining the change in open water area provides insight into changing lake areas and which areas of the floodplain contain temporary lakes during floods in a geomorphologic context. It also allows for interpreting the connections between the floodplain and floodplain water bodies while describing the geomorphologic aspects of the floodplain that makes those connections and flow pathways possible.

Morais et al. (2005) classified the 293 lakes based on their geomorphologic formation into 10 different types between Aruanã and Luís Alves along the middle Araguaia River and found the percentages of each type based on their number: abandoned channels (4.1%), chained abandoned channels (25.6%), oxbows (4.2%), filled oxbows (5.1%), composite oxbows (6.8%), meander scroll lakes (17.8%), composite meander scroll lakes (0.7%), lakes formed by lateral accretion (12.0%), blocked valley lakes (6.1%), and levee lakes (15.7%). The authors used a dry season LandSat 5 TM image from July 1997 and a wet season LandSat 7 ETM+ image from May 2000 to

digitize the lakes, providing the area, perimeter, and other morphometric parameters for 20 lakes in the floodplain for each season. These 20 lakes were investigated because the authors also had information on their depths in the dry season and the wet season due through fieldwork. They determined whether the lakes were disconnected or connected via surface water to the river channel in each satellite image, enhancing knowledge of hydrologic connectivity between the lakes and the main river channel. The results presented in this chapter expand on the analysis by Morais et al. by analyzing changes in the same 20 lakes using different dry season/wet season imagery at a time in which the river discharge is higher than the wet season images in Morais et al. In addition, lake types that Morais et al. did not include in their previous analysis are also assessed. Investigating the changes in morphometry and connectivity in these lakes provides insights into floodplain storage and the geomorphologic controls on surface water movement, as well as being important for characterizing the diversity of habitats for aquatic organisms.

The floodplain lakes of the middle Araguaia River are similar in form and genesis to floodplain lakes in other tropical systems, such as the Amazon River and its many tributaries (Latrubesse 2012; Silva França 2002). Abandoned channel lakes are formed by channel avulsions or when secondary channels around islands become filled at the channel bifurcation. Chained abandoned channels are linked elongated lakes that have resulted from similar processes. Oxbow lakes develop through meander cut-offs, when the meander increases in sinuosity to the point where the channel cuts off the meander and an oxbow lake is created. Composite oxbows are similar in form, but are connected and resulted from multiple abandoned meanders. Filled oxbow lakes are more irregularly shaped compared to oxbow lakes because they have been subjected to sedimentation over time. Meander scroll lakes (and composite meander scroll lakes) are created by point bar

deposition as the meanders migrate downstream, leaving ridges and depressions that become filled. Levee lakes are formed by water trapped behind levees of either the main channel or abandoned channels. Lakes formed by lateral accretion occur when bars and islands accrete to the floodplain, leaving lower elevation areas between the accreted bar and the main floodplain that can be filled (Latrubesse 2012; Silva França 2002).

The present study provides estimates of the change in floodplain lakes and open water areas between the three distinct geomorphologic units of the middle Araguaia River floodplain through the use of an open water index (Xu 2006). It also identifies pathways for river discharge water movement onto the floodplain at a time of peak discharge along portions of the floodplain, as floodplain inundation occurs through various pathways, including through establishing surface connectivity with floodplain water bodies and floodplain drainage channels. Identifying different floodplain pathways has implications for the sources of water on the floodplain and the connectivity of the floodplain ecosystem, and the geomorphology of the floodplain exerts control on these processes (Mertes 1997).

As described in Chapter 2, the Araguaia River floodplain has different vegetation assemblages that correspond with the geomorphic units. In particular, unit I contains more continuous woody vegetation with a canopy, and this vegetation type is also present in unit II (Morais et al. 2008). This results in areas that are likely inundated beneath the canopy that the open water index does not detect if the river is above bankfull discharge. Thus, the change in open water area in this analysis reflects the changes in floodplain lake area and temporary areas of open water between different geomorphologic units on the floodplain, and does not represent the total area of inundation on the floodplain. This approach was taken in part due to a lack of accurate elevation data or bathymetry data for the floodplain, which impedes other methods of analysis, such as one or two dimensional

flood routing models. Elevation data from the Shuttle Radar Topography Mission (SRTM) does not reflect the ground surface and represents vegetation heights and floodplain lake water levels (Jet Propulsion Laboratory 2005). It has been shown that the SRTM resolution of 90 meters does not adequately account for smaller drainage channels and pathways of flooding in systems such as the Amazon floodplain, which is a much larger system compared to the Araguaia floodplain (Trigg et al. 2012).

STUDY AREA AND TIME PERIOD

The study area specific to this chapter includes the geomorphologic floodplain along reaches 1 and 2 described in Chapter 3. The change in open water area is also described by segments, which have previously been defined by Latrubesse et al. (2009) (Figure 4.1).

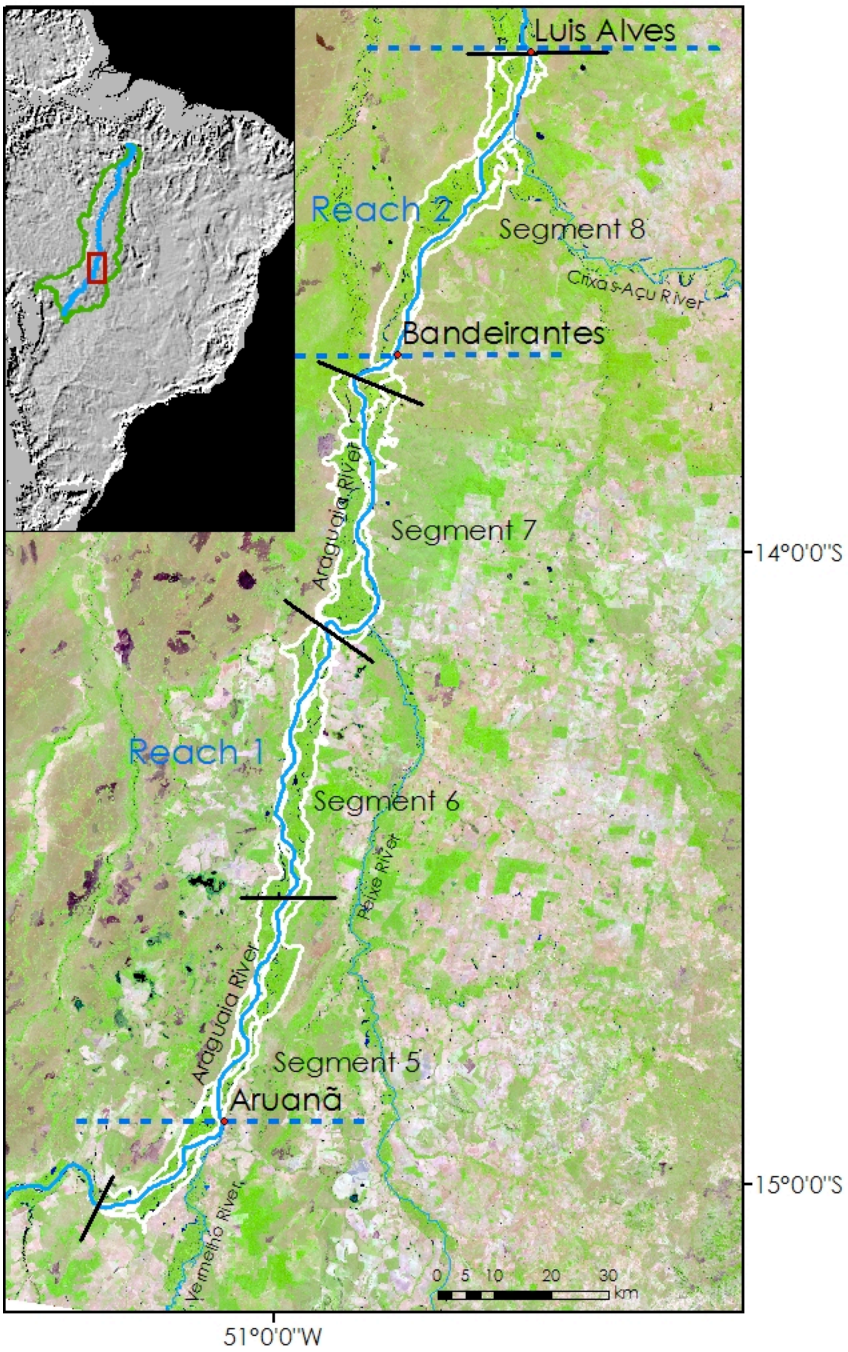

Figure 4.1. Study area, with reaches 1 and 2. The overlapping segments 5 through 8 were previously defined by Latrubesse et al. (2009). The geomorphologic floodplain is outlined in white. The background Landsat TM image is from 20 July 1987 (bands 5-4-3).

The floodplain in the study area is divided into the three geomorphologic units (Latrubesse and Stevaux 2002). The reaches and segments used for analysis are comprised of different proportions of each unit, with reach 1 and segments 5 through 7 having a majority of area that is classified as unit I, and reach 2 and segment 8 having a higher percentage of unit II floodplain compared to the other units (Table 4.1).

Table 4.1. The areas of each unit for the study reaches and study segments in km^2. The number in parentheses is the percentage of the area for each unit across the segments and reaches. Areas were found using ArcGIS and shapefiles from Latrubesse and Carvalho (2006). Areas of each unit were previously published by Morais (2006) but have been recalculated by the author.

Segment	**Unit I (km^2)**	**Unit II (km^2)**	**Unit III (km^2)**	**Total floodplain area (km^2)**
Segment 5	137 (47.9%)	115 (40.3%)	34 (11.8%)	286 (23.6%)
Segment 6	168 (70.9%)	54 (22.7%)	15 (6.5%)	238 (19.6%)
Segment 7	151 (49.9%)	135 (44.6%)	17 (5.5%)	302 (24.9%)
Segment 8	97 (24.9%)	277 (71.6%)	13 (3.4%)	387 (31.9%)
Reach	**Unit I (km^2)**	**Unit II (km^2)**	**Unit III (km^2)**	**Total floodplain area (km^2)**
Reach 1	424 (56.3%)	277 (36.8%)	52 (6.9%)	753 (67.8%)
Reach 2	89 (24.2%)	260 (72.5%)	12 (3.3%)	358 (32.2%)

Time 1 used for the analyses is in the dry season, on 20 July 1987, and time 2 is in the wet season, on 1 April 1988. The wet season images were recorded just after the peak discharge occurred at Aruanã gauging station. These images were chosen because they are relatively cloud-free and the wet season images were taken at a time of high discharge recorded at the Bandeirantes and Luís Alves stations. Table 4.2 and Figure 4.2 show the discharge at the three gauging stations in the study area at the time of the satellite images. At time 2, at Aruanã the measured discharge is below the bankfull discharge of 3200 m^3s^{-1}, but above bar-full discharge. Just before time 2, the peak discharge at Aruanã was 4914

m^3s^{-1} on 17 March, 1988, 15 days before the recorded satellite image. Thus, the peak discharge that occurred 15 days before the image was above bankfull discharge. At time 2 the measured discharge is above the bankfull discharge of 3755 m^3s^{-1} at Bandeirantes and above the bankfull discharge of 3700 m^3s^{-1} at Luís Alves. The peak discharge at Bandeirantes (5395 m^3s^{-1}) occurred 5 days before the image date on 27 March. The recorded peak discharge at Luís Alves for 1988 occurred on 1 April, the date of the wet season image.

Table 4.2. Discharge measurements at the time of the images used for analysis.

Image date	Aruanã discharge (m^3s^{-1})	Bandeirantes discharge (m^3s^{-1})	Luís Alves discharge (m^3s^{-1})
Dry season: 20 July 1987	378	398	556
Wet season: 1 April 1988	2145	3989	4511

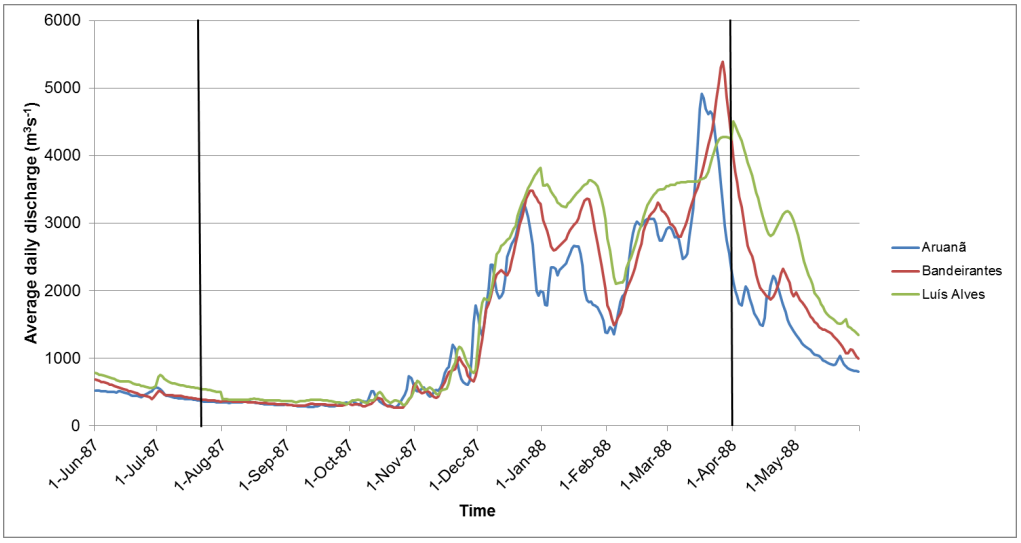

Figure 4.2. Hydrograph showing the discharge record along the dates of the images used for analysis. Black lines on the graph indicate the dates of the satellite images used for analysis.

During the flood wave of 1988, the peak discharge did not decrease between Aruanã and Bandeirantes (reach 1), increasing along the reach by 9.79%. Along reach 2, peak discharge decreased by 20.72% between Bandeirantes and Luís Alves (Chapter 3). This flood year is classified as a type D1 flood in Chapter 3, where peak discharge is above bankfull discharge and reaches 1 and 2 display divergent patterns of peak reduction.

METHODS

Landsat 5 Thematic Mapper images from two time periods were used (level L1T data, 30-meter resolution). Landsat imagery was chosen instead of MODIS imagery because most of the floodplain water bodies are narrow, and the resolution of MODIS data would not capture accurately the change in floodplain water bodies. The resolution of LandSat imagery is higher (30-meter), which allows for description of the water bodies, and it has been used in other studies of floodplain water bodies and flow pathways (Mertes et al. 1995; Trigg et al. 2012). The images used are Path/Row 223/70 (used for reach 1 and segments 5 through 7) and 223/69 (used for reach 2 and segment 8), with a total of four images used. L1T images are terrain-corrected using ground control points and a Digital Elevation Model (U.S. Geological Survey 2013). The images were projected into WGS 1984 UTM Zone 22S. Because the approach was to determine change between two times (dry season vs. wet season) using a post-classification comparison of "water" and "not water" classes, it was not necessary to correct for differences in atmospheric conditions between the images before each image was classified (Jensen 2004).

In order to systematically discern "water" from "not water" in the satellite images (subsequently referred to as water and not water, without quotations), a version of the Normalized Difference Water Index (NDWI) was used. McFeeters (1996) developed the NDWI using the green and near infra-red (NIR) spectral bands of satellite imagery:

$$NDWI = \frac{Green-NIR}{Green+NIR} \quad (10)$$

This index gives each pixel a value between -1 and 1. A value must be chosen to determine the threshold between water and not water for each pixel. McFeeters (1996) uses a threshold of 0, with water pixels values greater than zero and not water pixels (vegetation, soil, or built-up areas) less than zero. However, Ji et al. (2009) demonstrate that the threshold values are dynamic. The threshold value is influenced by the sub-pixel composition of water, vegetation, and soil or sediment. For example, a pixel of clear water will have a higher NDWI index value than a pixel with water and vegetation, or water with woody debris or suspended sediment in it. Ji et al. (2009) suggest lowering the threshold value based upon the percentage of each pixel that is not pure water.

Xu (2006) developed a variation on the NDWI, the Modified Normalized Difference Water Index (MNDWI), which better distinguished between built-up areas (e.g., cities or towns) and water features by using the middle infra-red (MIR) band instead of the NIR band. This method also has been shown to be less impacted by vegetation within each pixel of the image (Ji et al. 2009).

$$MNDWI = \frac{Green-MIR}{Green+MIR} \quad (11)$$

Pixels in the imagery on the edge of lakes and flooded areas are mixed with vegetation and soils. Thus, since the MNDWI has been shown to have less sensitivity to sub-pixel vegetation (Ji et al. 2009), it was chosen for this analysis. Eradas Imagine was used to compute the MNDWI for each of the four images, using band 5 (green) and band 2 (MIR). Figure 4.3 shows the model used to compute the index.

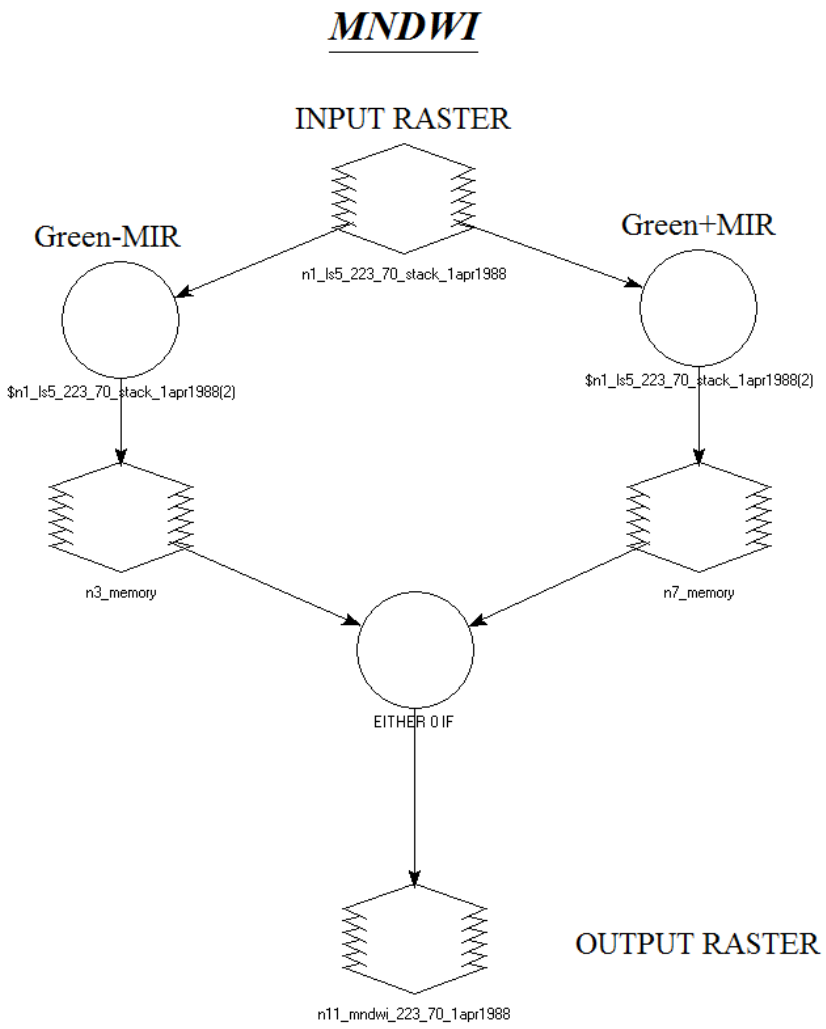

Figure 4.3. Model from Erdas Imagine used for calculating the MNDWI.

Thresholds for determining water and not water classes were determined by using a Jenks natural breaks classification with two classes. The Jenks natural breaks method minimizes the difference within classes and maximizes the difference between classes (de Smith et al. 2013). The thresholds (Table 4.3) were visually examined using the natural color satellite image to manually check that the threshold adequately distinguished between the classes. The thresholds for the images in the dry season are higher than the thresholds for the wet season images. This agrees with the concept that an index value for water without debris and sediment (dry season) will be higher than and index value for water with debris and sediment (wet season), as flood waters will likely contain more debris and sediment.

Table 4.3. Thresholds determined from Jenks Natural Breaks classification.

Image date	Path/Row	MNDWI threshold
July 20, 1987	223/70	-0.07
July 20, 1987	223/69	-0.02
April 1, 1988	223/70	-0.19
April 1, 1988	223/69	-0.13

Using ArcGIS 10.1, pixels greater than the threshold value were classified as water while the pixels less than the threshold value were classified as not water. No accuracy assessment was made of the classifications, as there was no higher resolution image available for the study dates. However, visual analysis of the classifications was made using the natural color satellite images. A change raster image from time 1 to time 2 was then created, with four classes: water to water, not water to water, water to not water, and not water to not water.

Clouds and cloud shadows, as well as a few areas of anomalies in the Landsat images, were digitized and extracted from the change rasters. Thus, the areas analyzed with change classification do not include the few areas of clouds, cloud shadows, and image anomalies. Since the water index investigates areas of open water, areas within the floodplain that have been cleared by humans have also been removed from the analysis. This results in open water areas within the natural floodplain, allowing for comparisons along the floodplain.

Shapefiles of the geomorphologic units defined by Latrubesse and Stevaux (2002) are from Latrubesse and Carvalho (2006), re-projected, and edited to reflect the 1987 river channel. The geomorphologic units for each reach and segment were related to the change rasters in ArcGIS, and area estimations and percentage change in area for each change class for each unit was identified. The 20 lakes analyzed previously by Morais et al. (2005) were analyzed for area and perimeter changes and surface water connectivity between the dry and wet seasons, and examples of the additional lake types that were not included in the Morais et al. study were also characterized in this way. Additional lakes types not included in the Morais et al. study were chosen because they are a good representation of lakes typical of each type. The number of surface water connections between floodplain lakes and the main channel (i.e., whether the floodplain lakes were connected via surface water or not) in the dry season and the wet season was recorded along the river channel. The average width of the floodplain for each segment was found by dividing the area of the floodplain by the length of the channel and was related to the area that became open water in the wet season. It should be noted again that the vegetation of the floodplain varies along with the geomorphologic unit. In particular, the gallery forests of the floodplain, most common in unit I but also present in unit II, likely

results in inundated areas beneath the canopy, particular at discharge levels that are above bankfull.

RESULTS AND DISCUSSION

The results of the change analysis over the entire study area is displayed in a from-to matrix in Table 4.4. The areas in the from-to change matrix do not include the clouds, cloud shadows, image anomalies, and cropland within the geomorphologic floodplain that were digitized and removed from the analysis. The total of the removed areas is 20.9 km^2 out of the 1212.6 km^2 of floodplain along segments 5 through 8. Thus, the area analyzed for changes between classes was 1191.7 km^2, or 98.3% of the floodplain. In Table 4.4, the water to water class indicates that the area of lake or open water is present in the dry season and the wet season. The water to not water class represents a very small area, 0.22 km^2, indicating that this transition occurs on a very small scale, as the precipitation and flooding in the wet season would probably expand the open water on the floodplain. However, this transition could occur through the infilling of floodplain lakes or the edges of floodplain lakes by sediment or vegetation. The not water to water class means that the area became open water in the wet season, which is likely caused by water table rise, precipitation onto the floodplain surface, or the distribution of river channel water due to overbank flows or surface water pathways and connections to floodplain lakes. Mechanisms for river discharge causing the not water to water transition are fully discussed below. Finally, the not water to not water class is the largest, and represents areas that remained non-water (e.g., soil, sediment, or vegetation) from the dry season to the wet season.

Table 4.4. From-to change matrix for the floodplain along segments 5 through 8, in km^2.

	1988-Wet season		
1987-Dry season	Water	Not Water	1987 Total
Water	52.16	0.22	52.38
Not Water	148.06	991.30	1139.36

Changes in the morphometry of floodplain lakes and surface water pathways of flooding

Table 4.5 shows the areas and perimeters of the floodplain lakes between the wet and the dry seasons. Also shown in Table 4.5 are the data from the 20 lakes analyzed previously by Morais et al. (2005), including measurements of lake depth between the wet season and the dry season from fieldwork. The meander scroll and composite meander scroll lakes undergo a higher percent increase in area compared to the other lake types (Table 4.4). Formosa Lake, a composite meander scroll lake, which increased in area only by 55%, is an exception to this pattern, while the other composite meander scroll and meander scroll lakes increased in area by more the 400%. Most abandoned channel lakes and blocked valley lakes had a small percent increase in area between the wet and the dry seasons compared to meander scroll lakes in both studies, although larger expansions in abandoned channel lakes such as Fuzil Lake and Piedade Lake likely reflect areas of expansion through breaks in the levees of the abandoned channel (see figures and explanation of examples below). Depth data indicates that abandoned channel and blocked valley lakes can greatly increase in depth, by as much as 5 meters (Morais et al. 2005). Levee lakes did not increase in area as much as meander scroll lakes. The lateral accretion lakes are very small, and thus increases in the percentage of their area

are more influenced by their small size. Further differences and details about the lake types are presented below using examples.

Table 4.5. Results from analyses of lake area and perimeter changes for 32 lakes along segments 5 through 8. Also included in the table are data from the study by Morais et al. (2005) on 20 of the lakes analyzed in the present study, including measurements of lake depth between the dry and wet season.

Name	Type	Area (km^2)		Percent increase in area (%)	Perimeter (km)		Morais et al. Area (km^2)		Morais et al. Perimeter (km)		Morais et al. Depth (m)	
		Dry season	Wet season		Dry Season	Wet Season	Dry Season	Wet Season	Dry Season	Wet Season	Dry Season	Wet Season
Dumbazinho	Blocked valley	0.22	0.31	39.75	4.56	7.62	0.31	0.53	7.08	8.87	0.4	3
Campos	Chained abandoned channel	0.23	0.33	46.25	8.16	9.66	0.04	0.06	1.27	1.42	2	NA
Azul	Chained abandoned channel	0.33	0.55	65.85	13.98	16.92	0.5	0.74	15.39	16.57	4.55	6
Mata Coral	Chained abandoned channel	0.16	0.43	178.73	6.57	11.36	0.16	0.3	4.95	7.98	2.65	5.7
Formosa	Composite meander scroll	0.54	0.84	55.04	19.86	21.83	0.52	0.89	16.68	17.13	2.3	3.5
Cangas	Abandoned channel	0.41	0.62	50.81	11.45	13.76	0.47	0.75	9.7	15.6	2.55	7.5
Dumba Grande	Abandoned channel	1.68	2.14	27.50	28.81	28.52	1.75	2.12	21.15	22.68	2	5.7
Rico	Abandoned channel	2.32	4.18	80.37	58.29	80.13	2.77	8.38	43.81	71.77	5.9	7.75
Saudade	Composite meander scroll	0.30	1.99	562.71	11.57	35.89	0.43	0.88	12.97	19.5	3.05	7.9
Fuzil	Abandoned channel	0.31	1.22	290.96	9.26	18.73	0.31	1.18	7.78	14.88	3.3	7.15
Landi	Blocked valley	0.02	0.06	157.21	1.44	1.91	0.03	0.04	1.2	1.24	0.95	4.45
Sao Joaquim	Abandoned channel	0.66	0.92	39.10	12.01	12.55	0.66	0.83	9.65	10.54	0.5	4.45
Cocal	Abandoned channel	2.18	6.79	211.65	42.18	91.26	2.29	5.54	31.26	43.8	2.45	5.05
Sao Jose dos Bandeirantes	Abandoned channel	0.69	2.34	239.71	16.86	43.75	0.71	1.87	11.45	20.03	4.55	6.75
Piedade	Abandoned channel	0.05	0.28	477.29	3.00	7.02	0.06	0.68	2.79	7.49	2.8	5.55
Dantas	Abandoned channel	0.20	0.46	129.76	9.82	14.60	0.21	0.62	6.83	17.79	0.3	2.7
Japones	Blocked valley	1.13	1.85	63.77	26.64	37.83	1.1	1.51	24.42	27.39	1.75	6.85
Montaria	Abandoned channel	1.30	6.22	379.15	48.10	135.78	0.82	14.19	22.57	50.82	2.6	4.55
Luis Alves	Abandoned channel	0.60	1.67	178.97	20.29	37.09	0.65	0.98	15.01	17.03	1.45	4.6
Brito	Abandoned channel	0.46	0.97	110.76	11.760	16.860	0.48	1.03	9.06	11.72	1.20	5.45
Lake 21	Oxbow	0.33	0.48	46.43	4.86	6.36						
Lake 22	Composite Oxbow	0.92	1.54	66.73	22.73	26.71						
Lake 23	Filled Oxbow	0.34	0.77	129.14	5.76	12.60						
Lake 24	Meander scroll	0.02	0.29	1146.14	0.90	8.82						
Lake 25	Lateral accretion	0.01	0.02	349.72	0.66	1.56						
Lake 26	Lateral accretion	0.04	0.05	43.90	1.68	1.86						
Lake 27	Levee lake	0.05	0.10	83.33	1.26	1.86						
Lake 28	Levee lake	0.10	0.16	53.70	1.98	2.27						
Lake 29	Levee lake	0.06	0.11	67.45	1.32	2.16						
Lake 30	Filled Oxbow	0.14	0.17	18.75	3.00	3.12						
Lake 31	Meander scroll	0.03	0.17	408.82	2.76	6.17						
Lake 32	Oxbow	0.21	0.26	25.48	4.14	4.80						

Table 4.6 shows the surface water connectivity of the floodplain lakes in the wet season, and includes the connectivity of the Morais et al. study (Table 4.6). Almost all of the abandoned channel lakes were connected to the river channel via surface water in the wet season and the dry season. The oxbow, composite oxbow, and filled oxbow lakes were not connected to the river channel in the dry or the wet season, while at least one of

the examples of meander scroll, lateral accretion, chained abandoned channel, blocked valley, and levee lakes became connected to the river channel in the wet season.

Table 4.6. Connections between the lakes and the main river channel for the 32 lakes used for analyses. Also included is the connectivity of 20 of the lakes analyzed by Morais et al. (2005).

Name	Type	Connection		Morais et al.--Connection	
		Dry season	Wet season	Dry season	Wet season
Dumbazinho	Blocked valley	No	No	Yes	Yes
Campos	Chained abandoned channel	No	No	No	No
Azul	Chained abandoned channel	No	No	No	No
Mata Coral	Chained abandoned channel	No	Yes	Yes	Yes
Formosa	Composite meander scroll	No	No	No	No
Cangas	Abandoned channel	Yes	Yes	Yes	Yes
Dumba Grande	Abandoned channel	Yes	Yes	Yes	Yes
Rico	Abandoned channel	Yes	Yes	Yes	Yes
Saudade	Composite meander scroll	No	Yes	Yes	Yes
Fuzil	Abandoned channel	Yes	Yes	Yes	Yes
Landi	Blocked valley	Yes	Yes	Yes	Yes
Sao Joaquim	Abandoned channel	No	Yes	Yes	Yes
Cocal	Abandoned channel	Yes	Yes	Yes	Yes
Sao Jose dos Bandeirantes	Abandoned channel	Yes	Yes	Yes	Yes
Piedade	Abandoned channel	Yes	Yes	Yes	Yes
Dantas	Abandoned channel	No	Yes	Yes	Yes
Japones	Blocked valley	No	No	Yes	Yes
Montaria	Abandoned channel	Yes	Yes	Yes	Yes
Luis Alves	Abandoned channel	Yes	Yes	Yes	Yes
Brito	Abandoned channel	Yes	Yes	Yes	Yes
Lake 21	Oxbow	No	No		
Lake 22	Composite Oxbow	No	No		
Lake 23	Filled Oxbow	No	No		
Lake 24	Meander scroll	No	No		
Lake 25	Lateral accretion	No	Yes		
Lake 26	Lateral accretion	No	No		
Lake 27	Levee lake	No	Yes		
Lake 28	Levee lake	No	Yes		
Lake 29	Levee lake	No	Yes		
Lake 30	Filled Oxbow	No	No		
Lake 31	Meander scroll	No	Yes		
Lake 32	Oxbow	No	No		

In Figure 4.4, Fuzil Lake (#10), an abandoned channel lake, is connected to the river channel in the wet season and the dry season. This abandoned channel lake increased from 0.31 km^2 to 1.22 km^2 in area. The perimeter changed from 9.26 km to 18.73 km. Depth measurements of this lake show that it can increase in depth by almost 4 meters (Table 4.4). In Figure 4.4, Fuzil Lake has expanded into scroll topography in unit II, likely through breaks in the abandoned channel's levees or lower elevation levee areas. Fuzil Lake has also connected to an abandoned channel lake to the southwest, providing a pathway of water from the main channel to another floodplain lake in unit II. Lakes 27, 28, and 29 are levee lakes, which expanded slightly in area between the wet season and the dry season (Table 4.4). These lakes are controlled by the levees that had formed on the sides of the channel that has now become Fuzil Lake. During the wet season, the levee lakes have become connected to Fuzil Lake, and thus the main river channel. This connection demonstrates that the levee lakes likely formed due to breaks or low areas in the abandoned channel levee. Landi Lake, #11 in Figure 4.4, is a small blocked valley lake that increased in area in the wet season from 0.02 to 0.06 km^2 and has created a pathway for open water in unit I. This lake has also been shown to greatly increase in depth from the wet season to the dry season (0.95 to 4.45 m, Table 4.4). Also noticeable in Figure 4.4 are the two areas of unit III on the right bank of the river, just south of Landi Lake. Areas that became open water in these areas of unit III reflect the processes of lateral accretion and potentially the formation of lakes formed by lateral accretion. In both sections of unit III, its center did not become open water at this particular discharge level, but the lower elevation side that became accreted to the floodplain has filled with water. This process provides a pathway for surface water from the channel into unit I.

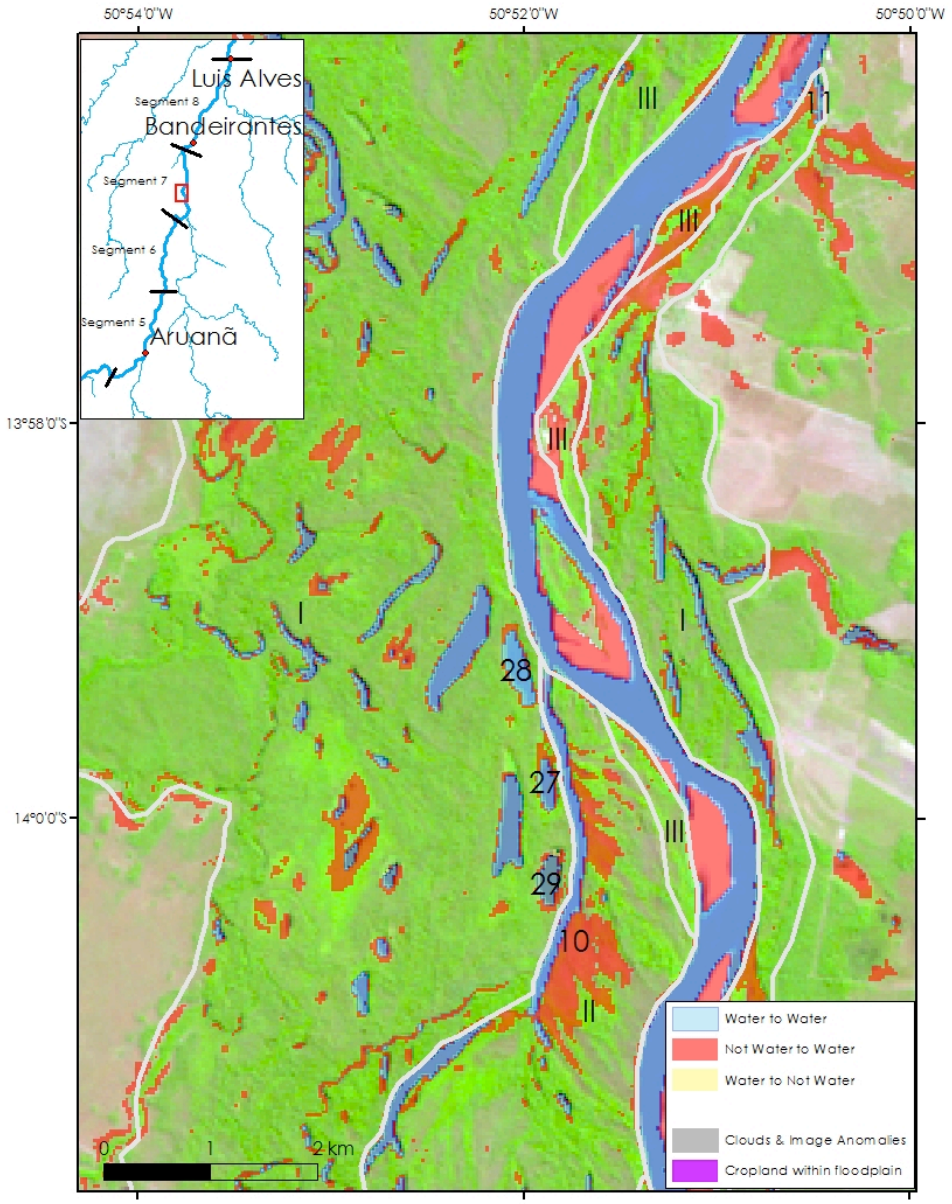

Figure 4.4. Changes between the wet season and the dry season in multiple lakes, including abandoned channel #10 (Fuzil); blocked valley #11 (Landi); levee lakes #27, # 28, # 29. Blue is water to water class, red is not water to water class, and yellow is water to not water class. Clouds and image anomalies and cropland within the floodplain are also indicated with gray and purple, respectively. Not water to not water class is shown with the background Landsat image from 20 July 1987 (bands 5-4-3). Geomorphologic units (I-III) are outlined in gray and labeled with Roman numerals, and river flow is to the north.

In Figure 4.5, Formosa Lake (#5), a composite meander scroll lake, increased slightly in area from 0.54 to 0.84 km^2 and slightly in perimeter from 19.9 to 21.8 km. The depth increase in this lake from the wet and the dry season is less than many abandoned channel lakes, increasing by about 1 m in the wet season (Table 4.4). Formosa Lake is not connected to the main river channel in the wet season or the dry season, and thus the slight increases in area of the lake could be due to water table rise or direct precipitation, or potentially by overbank flooding when the discharge is above bankfull, which it is not at this location on the river for the wet season image. The smaller increase in depth in the wet season in this lake could result from its lack of connection with the main river channel (Morais et al. 2005). The chained abandoned channel lakes in Figure 4.5, Campos (#2), Azul (#3), and Mata Coral (#4) all increased in area and perimeter. The lakes formed by lateral accretion (#25 and #26) are also shown in Figure 4.5. Lake #25, very small, thin, lake, is in unit III, and increased in area from 0.01 to 0.02 km^2 and in perimeter from 0.66 to 1.56. It also became connected to the river channel in the wet season, although it was not connected in the dry season. Lake #26, also formed by lateral accretion, is further away from the river channel in unit II and is unconnected to the river channel in the dry and wet season. It displayed a smaller increase in area compared to Lake #25, which is adjacent to the main channel and in unit III.

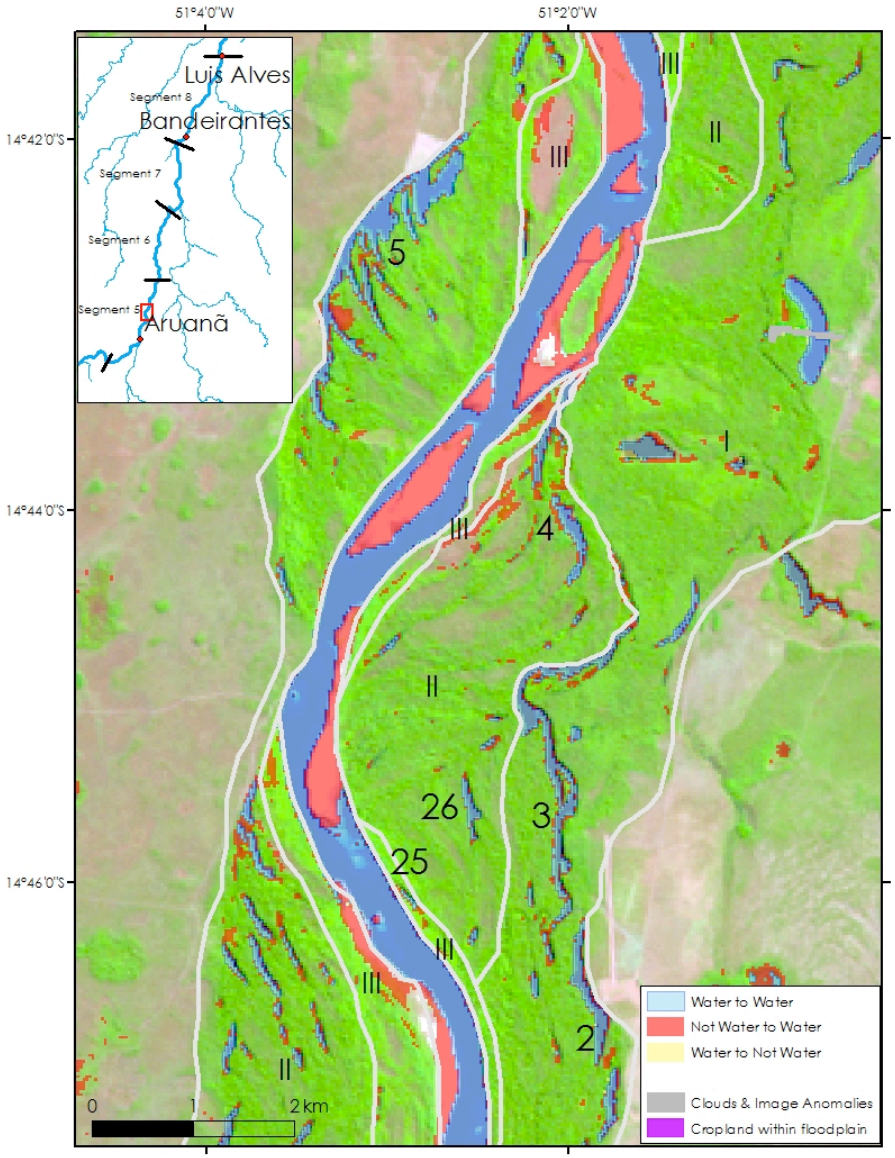

Figure 4.5. Changes between the wet season and the dry season in multiple lakes, including chained abandoned channel lakes #2 (Campos), #3 (Azul), #4 (Mata Coral); composite meander scroll #5 (Formosa Lake); and lateral accretion lakes #25, #26. Blue is water to water class, red is not water to water class, and yellow is water to not water class. Clouds and image anomalies and cropland within the floodplain are also indicated with gray and purple, respectively. Not water to not water class is shown with the background Landsat image from 20 July 1987 (bands 5-4-3). Geomorphologic units (I-III) are outlined in gray and labeled with Roman numerals, and river flow is to the north.

Figure 4.6 shows a meander scroll lake (#24) and the abandoned channel lake, Lake Cangas (#6). Lake Cangas increased in area from 0.41 to 0.62 km^2 and in perimeter from 11.45 to 13.76 km. Lake Cangas is an abandoned channel lake, and measurements of its changing depth indicate that this also increases greatly in depth (from 2.55 to 7.5 m, Table 4.4) from the dry season to the wet season, but not in area. Lake 24 is a meander scroll lake, which greatly increased in area (0.02 to 0.29 km^2) and perimeter (0.9 to 8.82 km) relative to its dry season size. Also seen in Figure 4.6 is an accreted island on the left bank of the river, across from the connection of Lake Cangas to the main channel. The secondary channel that previously separated the island from the floodplain has been filled in and vegetated, but during the wet season image this area became open water, providing a pathway of flooding between the channel and the floodplain.

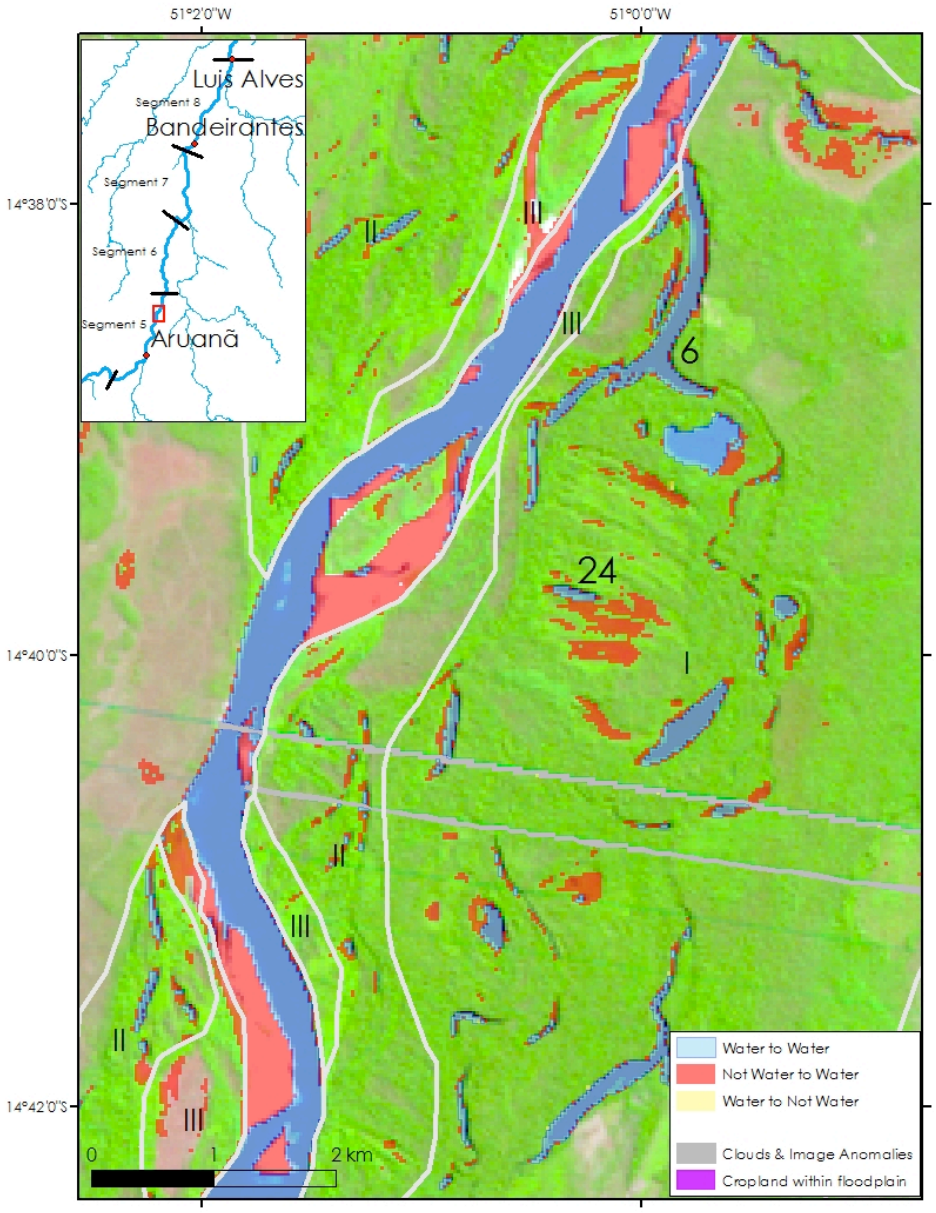

Figure 4.6. Changes between the wet season and the dry season in multiple lakes, including abandoned channel #6 (Cangas); meander scroll #24. Blue is water to water class, red is not water to water class, and yellow is water to not water class. Clouds and image anomalies and cropland within the floodplain are also indicated with gray and purple, respectively. Not water to not water class is shown with the background Landsat image from 20 July 1987 (bands 5-4-3). Geomorphologic units (I-III) are outlined in gray and labeled with Roman numerals, and river flow is to the north.

Figure 4.7 shows the abandoned channel Montaria Lake (#18) and Japones Lake, a blocked valley lake (#17). Montaria Lake has expanded from 1.30 to 6.22 km^2 in area. Montaria Lake has expanded all along its abandoned channel form and has also expanded into scroll topography. In Japones Lake, a blocked valley lake, there is no distinct pathway between it and the river channel at the time of the wet season image, but the discharge is above bankfull at this point, so water traveling on the floodplain may be masked by vegetation. Japones Lake expanded very little in area and perimeter from the wet season to the dry season, but the depth of this lake can increase greatly (by just over 5 meters (Morais et al. 2005)).

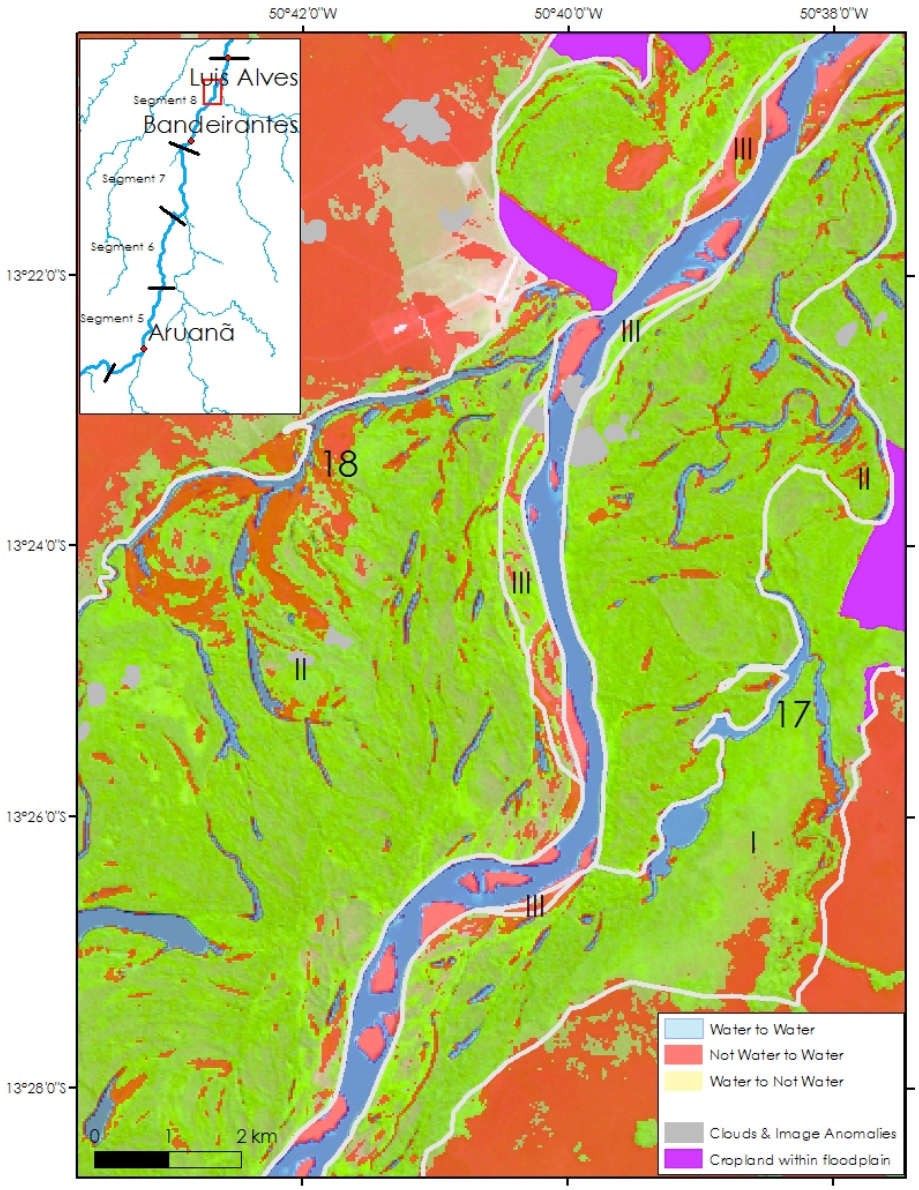

Figure 4.7. Changes between the wet season and the dry season in multiple lakes, including blocked valley #17 Japones and abandoned channel #18 (Montaria). Blue is water to water class, red is not water to water class, and yellow is water to not water class. Clouds and image anomalies and cropland within the floodplain are also indicated with gray and purple, respectively. Not water to not water class is shown with the background Landsat image from 20 July 1987 (bands 5-4-3). Geomorphologic units (I-III) are outlined in gray and labeled with Roman numerals, and river flow is to the north.

The composite oxbow Lake 22 and the abandoned channel lakes Sao Jose dos Bandeirantes (#14) and Piedade (#15) are shown in Figure 4.8. A large area west of the composite oxbow lake (Lake #22) parallel to the river channel, in which a large portion has become open water, is likely an abandoned fluvial belt of the Araguaia River. The composite oxbow lake also represents an abandoned channel of the Araguaia River. The composite oxbow lake and the abandoned fluvial belt just to the west of the composite oxbow do not have a direct connection with the channel, thus the areas that became open water in the wet season likely results from water table rise or from direct precipitation onto the floodplain. Piedade Lake (15) has increased in area a great deal relative to its dry season size, from 0.05 to 0.28 km^2. Similarly, Sao Jose dos Bandeirantes (14) increased in area from 0.69 to 2.34 km^2. In the Sao Jose dos Bandeirantes Lake, open water areas are extending into the unit II floodplain in breaks in the abandoned channel levees.

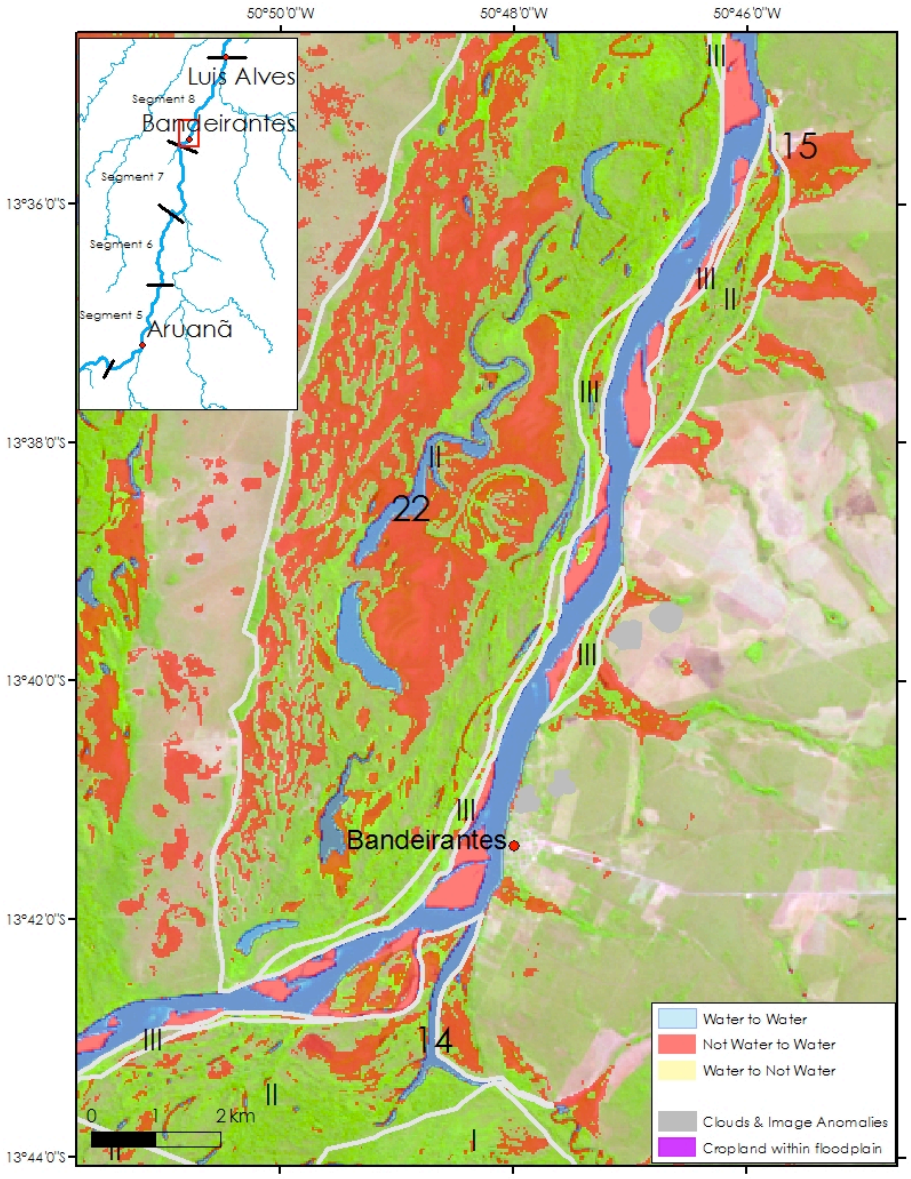

Figure 4.8. Changes between the wet season and the dry season in multiple lakes, including abandoned channels #14 (Sao Jose dos Bandeirantes), #15 (Piedade); composite oxbow lake # 22. Blue is water to water class, red is not water to water class, and yellow is water to not water class. Clouds and image anomalies and cropland within the floodplain are also indicated with gray and purple, respectively. Not water to not water class is shown with the background Landsat image from 20 July 1987 (bands 5-4-3). Geomorphologic units (I-III) are outlined in gray and labeled with Roman numerals, and river flow is to the north.

The development of different types of floodplain lakes and the influence of vertical sedimentation on the floodplain can also be seen when comparing oxbow lakes to filled oxbow lakes. For example, in Figure 4.9, Lake 21 is an oxbow lake, while Lake 21 is a filled oxbow lake. Lake 21 expanded in area from 0.33 to 0.48 km^2 (a 46% increase) and in perimeter from 4.86 to 6.36 km, while Lake 23 expanded in area from 0.34 to 0.77 km^2 (a 129% increase) and in perimeter from 5.76 to 12.6 km from the dry season to the wet season. Filled oxbows are more irregularly shaped and are oxbow lakes that have been subjected to sedimentation processes and develop into a marshier lake environment. Figure 4.9 shows that the filled oxbow lake (23) has expanded more in its perimeter along the lake, while the oxbow lake (21) has expanded mainly into the meander scar at the edges of the lake. Both of these lakes are in unit II, but the differing processes of sedimentation have resulted in a different response to lake expansion in the wet season.

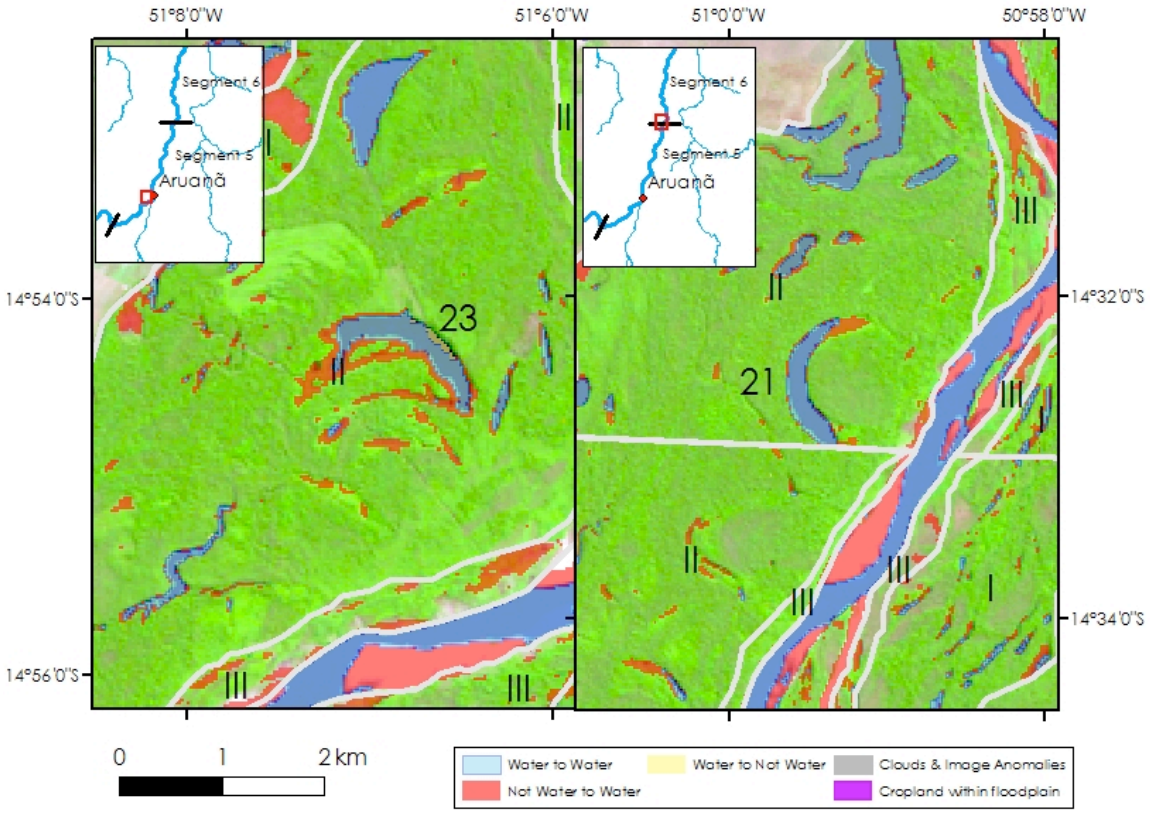

Figure 4.9. Changes between the wet season and the dry season in an oxbow lake (#21) and a filled oxbow lake (#23). Blue is water to water class, red is not water to water class, and yellow is water to not water class. Clouds and image anomalies and cropland within the floodplain are also indicated with gray and purple, respectively. Not water to not water class is shown with the background Landsat image from 20 July 1987 (bands 5-4-3). Geomorphologic units (I-III) are outlined in gray and labeled with Roman numerals, and river flow is to the east in the filled oxbow image and to the north in the oxbow image.

Figures 4.10 to 4.12 show the confluences of the three tributaries that flow into the Araguaia River along segments 5 through 8. In other tropical rivers, Landsat imagery

has been used to demonstrate areas in which sediment-rich river discharge mixes with tributary river discharge with different spectral characteristics (e.g., Mertes 1997), providing a way to determine which areas of the floodplain are influenced by local tributary waters. The change classes indicate that surface water connections do exist between tributaries and the middle Araguaia River floodplain, and qualitative assessments of the satellite imagery can inform whether tributary waters are mixing with other surface waters in the system. For example, in Figure 4.10 in the wet season satellite image, there is a slight difference in the color of the water in the Vermelho tributary compared to the main channel, although it is difficult to see mixing of surface waters with varying sediment concentration without a full analysis of spectral characteristics and measurements of sediment concentration to use for calibration. In Figure 4.11, the Peixe River tributary is flowing into the Araguaia River, and there are connections between floodplain lakes in unit II and the Peixe River. Figure 4.12 shows the Crixas-Açu River and the surface water connections between this tributary the Araguaia River floodplain, particularly to small lakes in unit II. However, in all three wet season images of the tributary confluences, it is difficult to determine mixing areas of surface waters without a more complete analysis of the imagery.

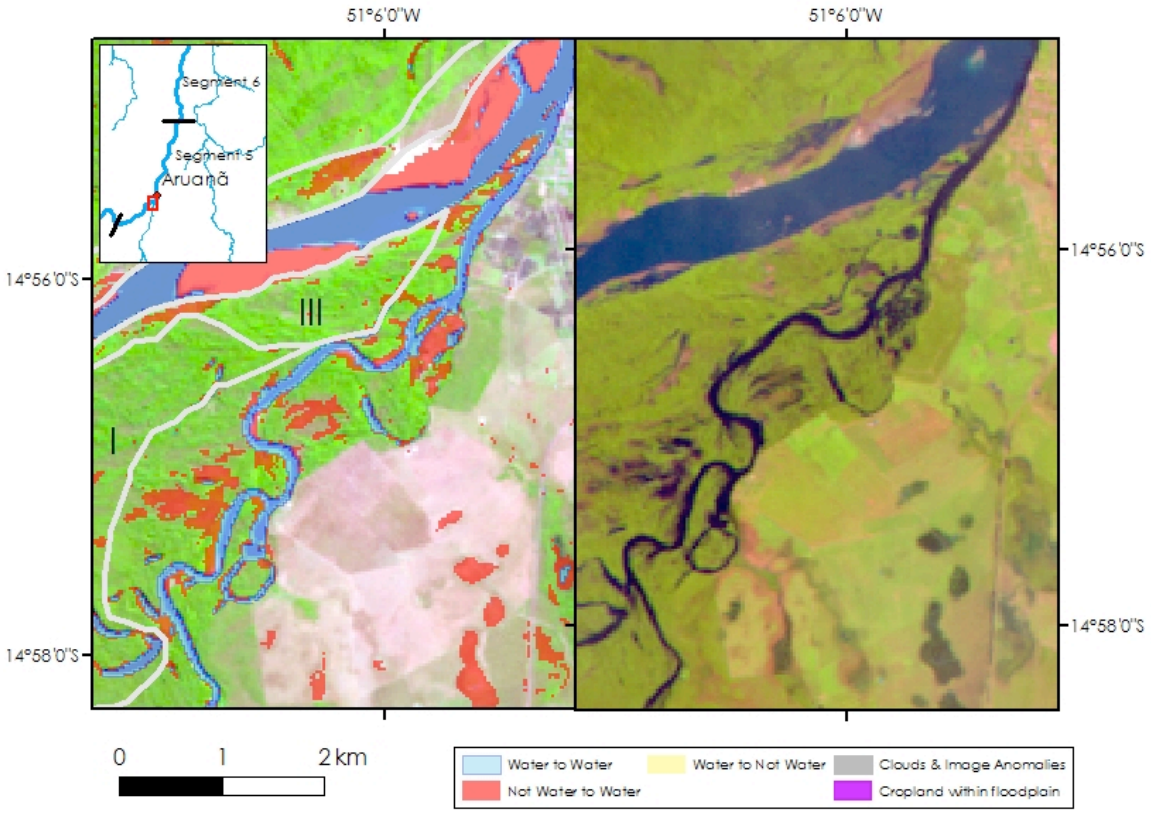

Figure 4.10. The confluence of the Vermelho River and the Araguaia River in reach 1, segment 5. The left panel is the map of change classes. Blue is water to water class, red is not water to water class, and yellow is water to not water class. Clouds and image anomalies and cropland within the floodplain are also indicated with gray and purple, respectively. Not water to not water class is shown with the background Landsat image from 20 July 1987 (bands 5-4-3). Geomorphologic units (I-III) are outlined in gray and labeled with Roman numerals. The right panel is the Landsat TM image from 1 April 1988 during the wet season (bands 5-4-3).

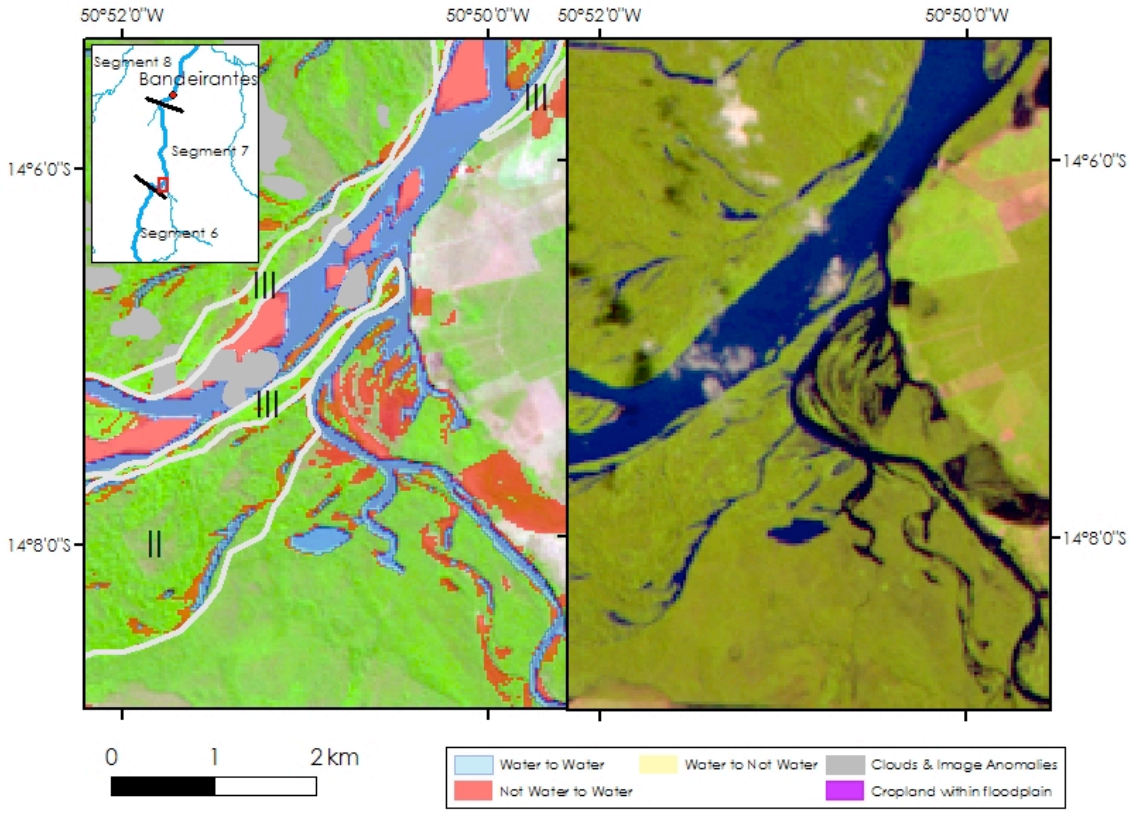

Figure 4.11. The confluence of the Peixe River and the Araguaia River in reach 1, segment 7. The left panel is the map of change classes. Blue is water to water class, red is not water to water class, and yellow is water to not water class. Clouds and image anomalies and cropland within the floodplain are also indicated with gray and purple, respectively. Not water to not water class is shown with the background Landsat image from 20 July 1987 (bands 5-4-3). Geomorphologic units (I-III) are outlined in gray and labeled with Roman numerals. The right panel is the Landsat TM image from 1 April 1988 during the wet season (bands 5-4-3).

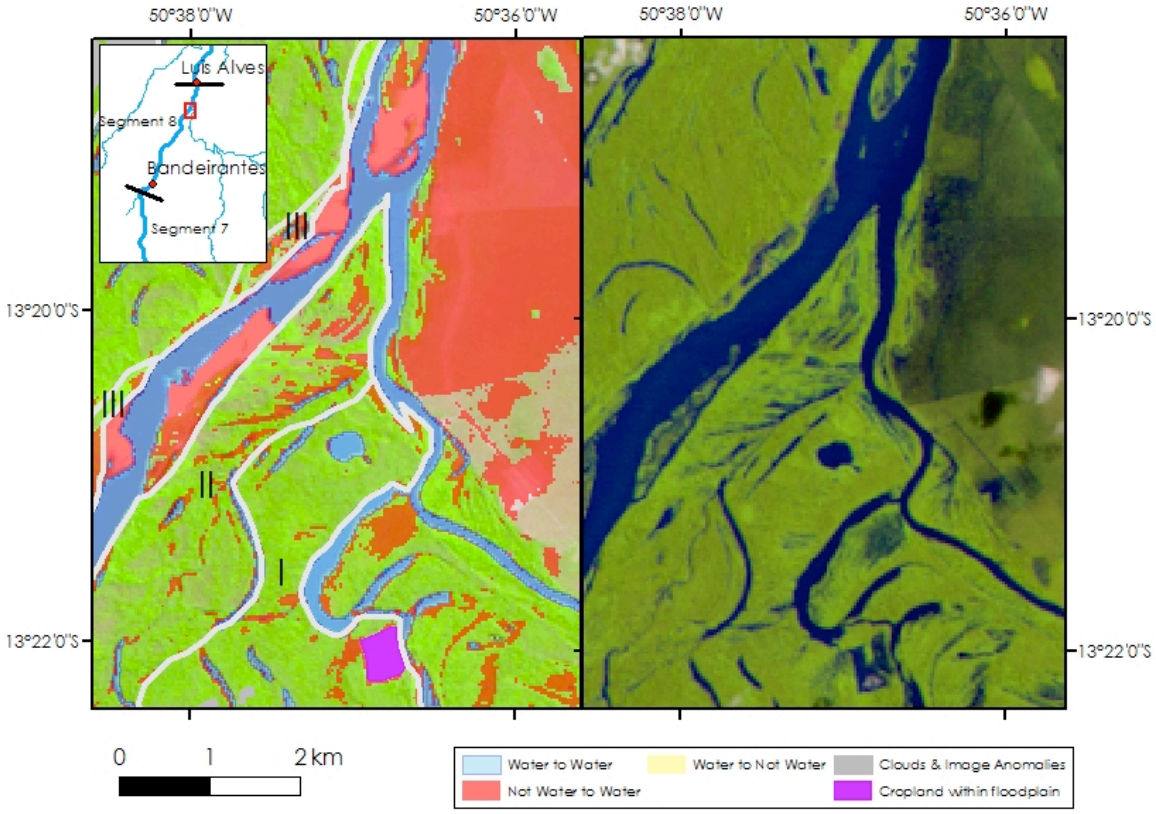

Figure 4.12. The confluence of the Crixas-Açu River and the Araguaia River in reach 2, segment 8. The left panel is the map of change classes. Blue is water to water class, red is not water to water class, and yellow is water to not water class. Clouds and image anomalies and cropland within the floodplain are also indicated with gray and purple, respectively. Not water to not water class is shown with the background Landsat image from 20 July 1987 (bands 5-4-3). Geomorphologic units (I-III) are outlined in gray and labeled with Roman numerals. The right panel is the Landsat TM image from 1 April 1988 during the wet season (bands 5-4-3).

After comparing the results in changes in area and perimeter between the present study and the same 20 lakes analyzed by Morais et al., it is clear that many of the lakes

display similar changes in area and perimeter between the wet and the dry season in both studies (Table 4.5). Because the exact date of the images used by Morais et al. is not known, the average discharge for the wet season and dry season months at the three gauging stations along the analyzed portion of the river is displayed in Table 4.7, along with the discharge measurements at the time of the images used for the present analyses. The discharge for both the wet season and the dry season images is below bankfull for all three of the gauging stations in the study area for Morais et al., while the present analysis used a wet season image in which Bandeirantes and Luís Alves are above bankfull and Aruanã is just after bankfull discharge. In addition, the dry season image in the present analysis is at a lower discharge than the discharge used by Morais et al.

Table 4.7. Average discharge for the months used for the dry season (July 1997) and the wet season (May 2000) in the analysis of lake area changes by Morais et al. (2005) and the discharge at the times used for the present analyses. Discharge data from Agencia Nacional de Aguas.

Image month	**Morais et al. (2005) Average discharge for the month (m^3s^{-1})**		
	Aruanã	**Bandeirantes**	**Luís Alves**
Dry season: July 1997	980	1130	1683
Wet season: May 2000	882	1070	1367
	Present analysis average daily discharge measurements (m^3s^{-1})		
Image date	**Aruanã**	**Bandeirantes**	**Luís Alves**
Dry season: 20 July 1987	378	398	556
Wet season: 1 April 1988	2145	3989	4511

Despite the different time periods used and the differing discharge levels between the present study and Morais et al., the few differences between the two studies in area and perimeter changes may be the result of different methods of analysis, as Morais et al.

digitized floodplain lakes, while the present study used the open water index to determine which pixels were water and which pixels were not water. In particular, the perimeter values in the present study are pixelated, extracted from the 30-meter pixel resolution Landsat images, while the Morais et al. perimeters were smoothed due to digitization. This could explain the consistently larger perimeter values in the present study compared to Morais et al. There are slight differences in the connectivity, determined by whether the lake and river channel were connected via surface water, between the river channel and the floodplain lakes in the present study compared with the Morais et al. study (Table 4.6). For example, four of the lakes (Mata Coral, Saudade, Sao Joaquim, and Dantas) are not connected to the river channel in the dry season in the present study, but were connected in the dry season in the Morais et al. study. This may reflect the lower discharge used for the dry season image in the present analysis. Morais et al. analyzed 4 out of the 10 types of lakes in the floodplain. The additional 12 lakes in the present analysis provide examples from the other 6 types of lakes in the floodplain. The measurements of depth of the lakes demonstrate that the abandoned channels and blocked valley lakes increase greatly in depth in the wet season, by as much as 5 meters in depth (Morais et al 2005). This indicates that many of these lakes expand in volume through depth, and not as much through area (Morais et al. 2005). Measurements of depth changes between the dry season and the wet season are needed for the additional 6 types of lakes described in the present analyses.

Determining changes in morphometry of floodplain lakes and pathways for surface water flow allows for an understanding of the processes of floodplain inundation and the transfer of water from the channel to the floodplain. Because movement of water onto the floodplain does not only occur during overbank floods, the results provide a way to spatially describe the movement of water onto the floodplain through various pathways

and the connectivity that is created during flooding between different surface waters. Mertes (1997) discussed the regions on the floodplain in which different surface waters mix as the "perirheic zone." This includes areas such as river water flowing into floodplain lakes, river water mixing with water on the floodplain that is present due to water table rise and groundwater saturation, and local tributary water mixing with main channel river discharge different areas of the floodplain. The mixing of surface water on the floodplain has implications for the biogeochemistry of floodplain water bodies and the continuing geomorphologic development of the floodplain (Mertes 1997; Thoms 2003). The Araguaia River floodplain lakes are similar to other tropical river-floodplain systems, such as those in the Amazon River and its tributaries, containing different types of lakes formed by fluvial processes (Latrubesse 2012). As in other studies, surface water flow pathways and potential connections between different water sources can be identified with the resolution of Landsat imagery (e.g., Trigg et al. 2012; Mertes 1995). The comparison with the Morais et al. study indicates that the floodplain lakes have similar sensitivities, measured by changes in area, despite differences in discharge level between the dry and wet seasons that were analyzed.

Variations in open water area along the river and between geomorphologic units

In addition to interpreting the changes in floodplain lakes and surface water pathways, the water index and classes also allows for comparing the changes in open water areas along the river and between geomorphologic units, including the areas of the floodplain that became open water in the wet season that are not floodplain lakes. After assessing the classes for reaches 1 and 2 and segments 5 through 8, general trends are evident (Tables 4.8 and 4.9). The area and percentages of the water to not water class is

zero or almost zero for all reaches and segments, meaning that open water areas do not usually fill in with vegetation or soil or dry up from the dry season to the wet season. The largest class is not water to not water, composing around 70 to 90% of all reaches and segments. The area of water to water class, which reflects the total area of floodplain lakes that are maintained in the wet season and the dry season, is very similar among the segments, ranging from 3.87% to 4.88% of each segment's floodplain area.

Table 4.8. Area (in km^2) and percentages of each change class for reaches 1 and 2

Reach 1	**Water to Water**	**Not Water to Water**	**Water to Not Water**	**Not Water to Not Water**
Unit I (km^2)	19.98	37.77	0.09	364.95
Unit II (km^2)	11.90	31.69	0.00	230.19
Unit III (km^2)	0.75	9.74	0.00	41.46
Total floodplain (km^2)	32.63	79.19	0.09	636.61
Unit I (% of area)	4.73	8.93	0.02	86.32
Unit II (% of area)	4.35	11.57	0.00	84.08
Unit III (% of area)	1.45	18.75	0.00	79.81
Total floodplain (% of area)	4.36	10.58	0.01	85.05
Reach 2	**Water to Water**	**Not Water to Water**	**Water to Not Water**	**Not Water to Not Water**
Unit I (km^2)	4.10	8.74	0.03	63.08
Unit II (km^2)	10.14	47.68	0.06	196.40
Unit III (km^2)	0.08	3.22	0.00	8.31
Total floodplain (km^2)	14.32	59.64	0.08	267.78
Unit I (% of area)	5.40	11.51	0.03	14.92
Unit II (% of area)	3.99	18.75	0.02	71.73
Unit III (% of area)	0.72	27.72	0.00	15.99
Total floodplain (% of area)	4.19	17.45	0.02	35.78

Table 4.9. Area (in km^2) and percentages of floodplain area of each change class segments 5 through 8.

Segment 5	Water to Water	Not Water to Water	Water to Not Water	Not Water to Not Water
Unit I (km^2)	6.66	8.79	0.03	120.94
Unit II (km^2)	3.95	8.49	0.04	102.26
Unit III (km^2)	0.41	3.90	0.00	29.40
Total floodplain (km^2)	11.02	21.18	0.07	252.59
Unit I (% of area)	4.89	6.45	0.02	88.64
Unit II (% of area)	3.44	7.40	0.03	89.13
Unit III (% of area)	1.21	11.57	0.00	87.22
Total floodplain (% of area)	3.87	7.44	0.02	88.67
Segment 6	**Water to Water**	**Not Water to Water**	**Water to Not Water**	**Not Water to Not Water**
Unit I (km^2)	8.25	15.33	0.03	144.42
Unit II (km^2)	3.07	5.40	0.00	45.41
Unit III (km^2)	0.26	3.65	0.00	11.42
Total floodplain (km^2)	11.58	24.38	0.03	201.25
Unit I (% of area)	4.91	9.12	0.02	85.95
Unit II (% of area)	5.70	10.03	0.00	84.27
Unit III (% of area)	1.72	23.79	0.00	74.49
Total floodplain (% of area)	4.88	10.28	0.01	84.83
Segment 7	**Water to Water**	**Not Water to Water**	**Water to Not Water**	**Not Water to Not Water**
Unit I (km^2)	8.09	16.88	0.03	125.87
Unit II (km^2)	5.61	18.46	0.00	107.43
Unit III (km^2)	0.14	3.56	0.00	12.60
Total floodplain (km^2)	13.85	38.90	0.03	245.90
Unit I (% of area)	5.37	11.19	0.02	83.43
Unit II (% of area)	4.27	14.04	0.00	81.70
Unit III (% of area)	0.87	21.82	0.00	77.30
Total floodplain (% of area)	4.64	13.02	0.01	82.33
Segment 8	**Water to Water**	**Not Water to Water**	**Water to Not Water**	**Not Water to Not Water**
Unit I (km^2)	4.51	9.73	0.03	71.37
Unit II (km^2)	11.11	50.38	0.06	210.57
Unit III (km^2)	0.10	3.50	0.00	9.61
Total floodplain (km^2)	15.72	63.60	0.09	291.56
Unit I (% of area)	5.27	11.36	0.03	83.34
Unit II (% of area)	4.08	18.51	0.02	77.38
Unit III (% of area)	0.73	26.48	0.00	72.79
Total floodplain (% of area)	4.24	17.14	0.02	78.60

Along the floodplain from upstream to downstream, there is an increase in the area in each segment that became open water and the percentage of the segment's floodplain that became open water. Figures 4.13 to 4.16 show the change maps for each segment, demonstrating the increase in the not water to water class in absolute area and as a percentage of each segment's floodplain moving from segment 5 to segment 8. Within the geomorphologic floodplain the area that is shown in red (not water to water) increases from Figure 4.13 to Figure 4.16. Figure 4.17 shows the cumulative area that became open water along the river, from segment 5 to segment 8, while Figure 4.18 gives the areas that became open water normalized by the floodplain area for each segment as a percentage. In segment 5, 7.4% of the floodplain area became open water, increasing to 17.1% of segment 8's floodplain area becoming open water. The average width of the floodplain increases from segment 5 to segment 8 as well, increasing from 3.66 km in segment 5 to 5.26 km in segment 8 (Figure 4.19). The average width is greater in reach 2 (5.59 km) than in reach 1 (4.43 km).

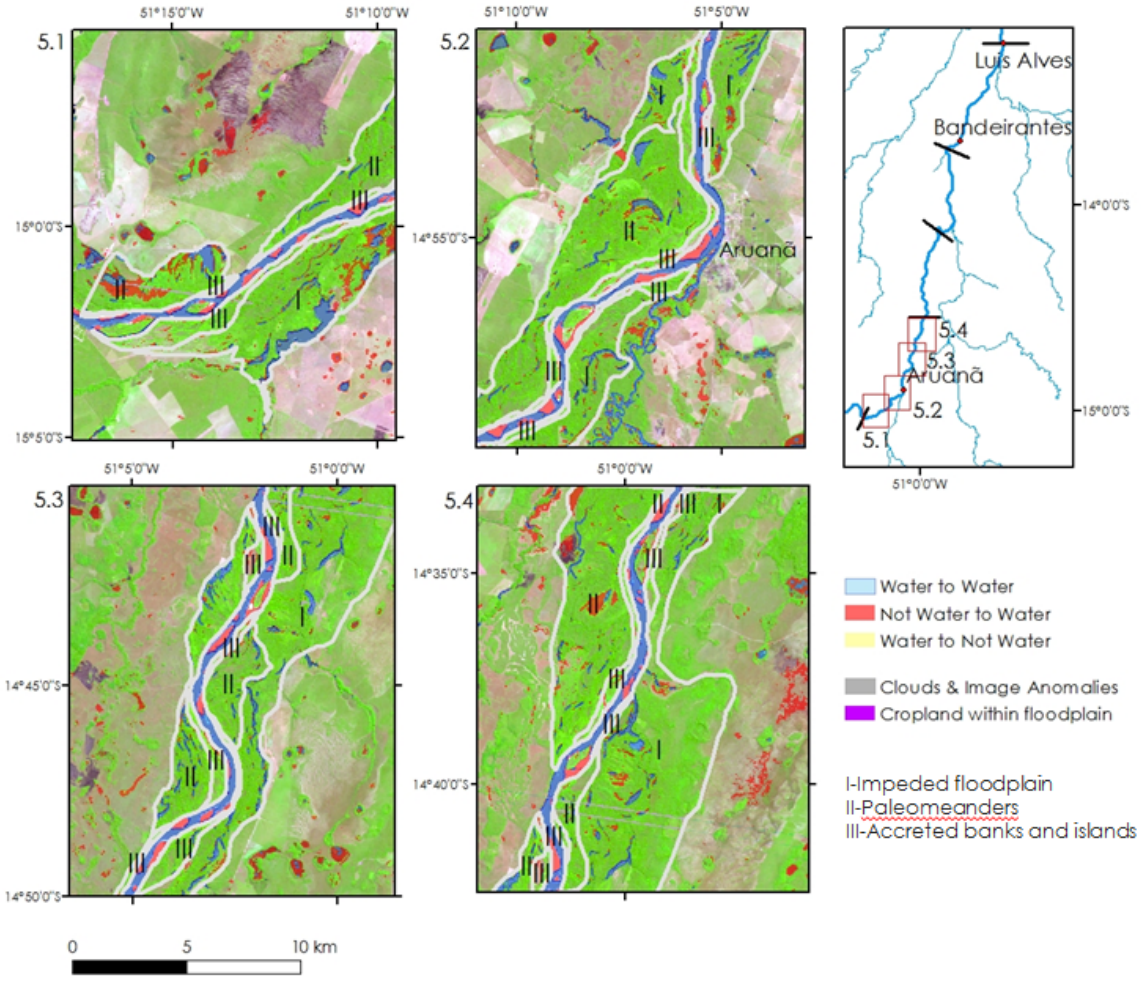

Figure 4.13. Change in open water area in segment 5. Each rectangle displays a portion of segment 5, from upstream (5.1) to downstream (5.4). Blue is water to water class, red is not water to water class, and yellow is water to not water class. Clouds and image anomalies and cropland within the floodplain are also indicated with gray and purple, respectively. Not water to not water class is shown with the background Landsat image from 20 July 1987 (bands 5-4-3). Geomorphologic units (I-III) are outlined in gray and labeled with Roman numerals, and river flow is to the north.

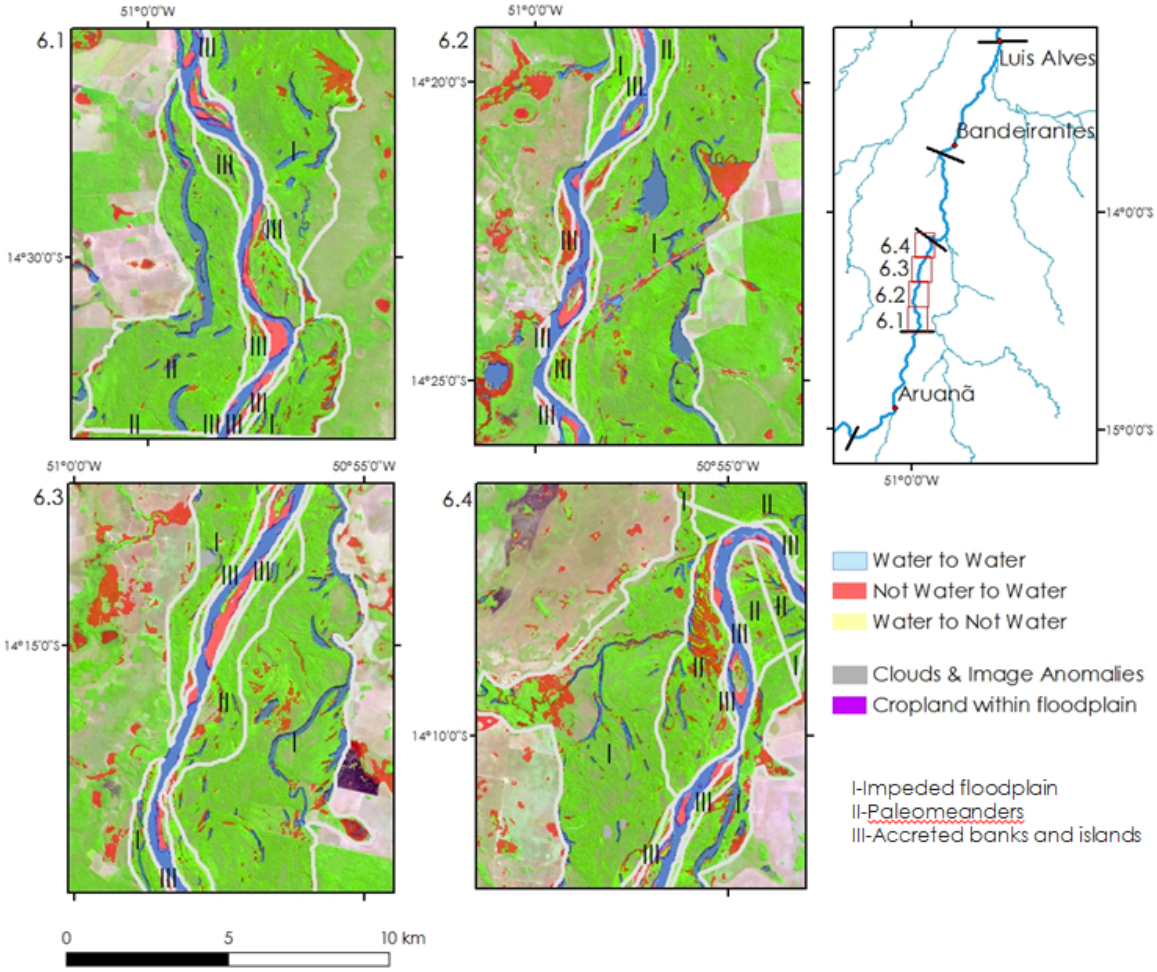

Figure 4.14. Change in open water area in segment 6. Each rectangle displays a portion of segment 6, from upstream (6.1) to downstream (6.4). Blue is water to water class, red is not water to water class, and yellow is water to not water class. Clouds and image anomalies and cropland within the floodplain are also indicated with gray and purple, respectively. Not water to not water class is shown with the background Landsat image from 20 July 1987 (bands 5-4-3). Geomorphologic units (I-III) are outlined in gray and labeled with Roman numerals, and river flow is to the north.

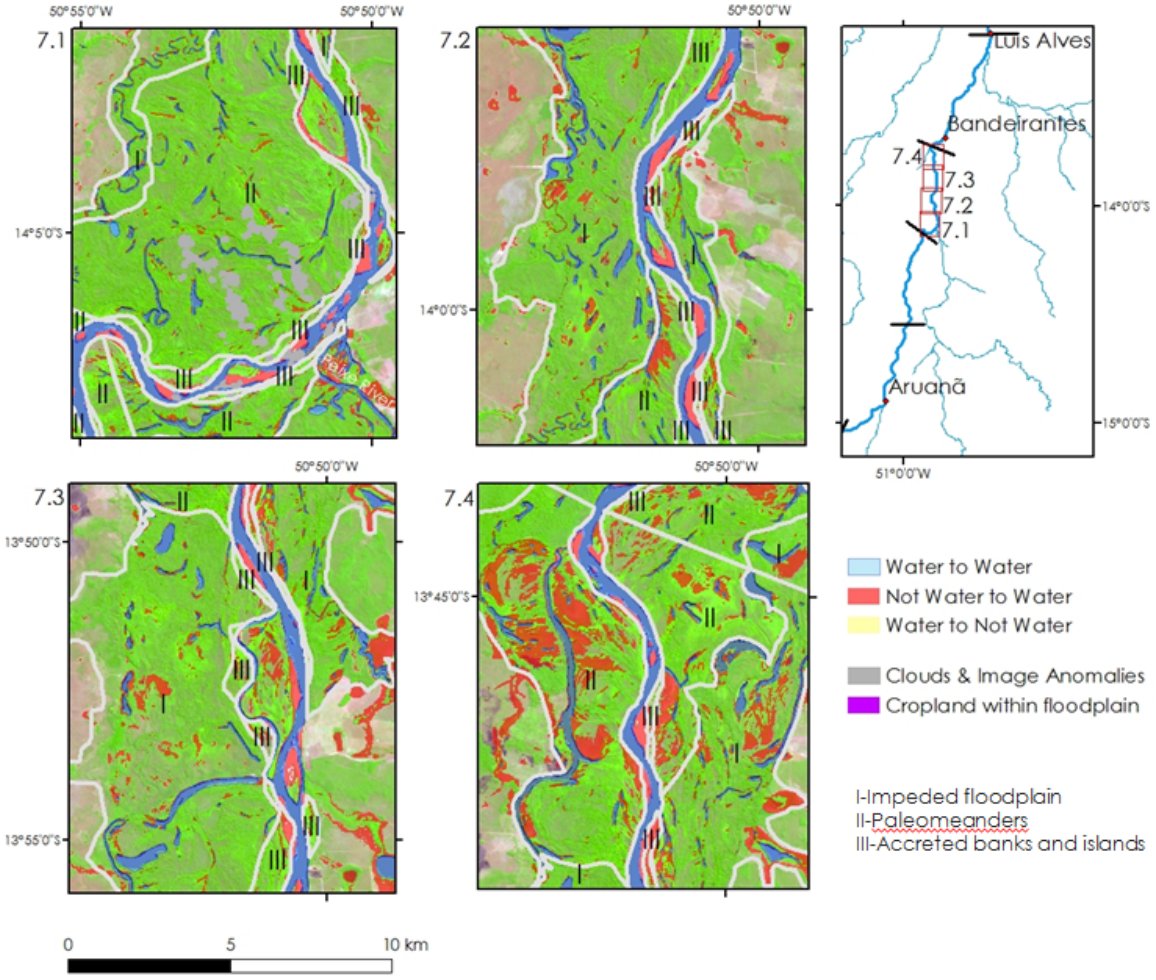

Figure 4.15. Change in open water area in segment 7. Each rectangle displays a portion of segment 7, from upstream (7.1) to downstream (7.4). Blue is water to water class, red is not water to water class, and yellow is water to not water class. Clouds and image anomalies and cropland within the floodplain are also indicated with gray and purple, respectively. Not water to not water class is shown with the background Landsat image from 20 July 1987 (bands 5-4-3). Geomorphologic units (I-III) are outlined in gray and labeled with Roman numerals, and river flow is to the north.

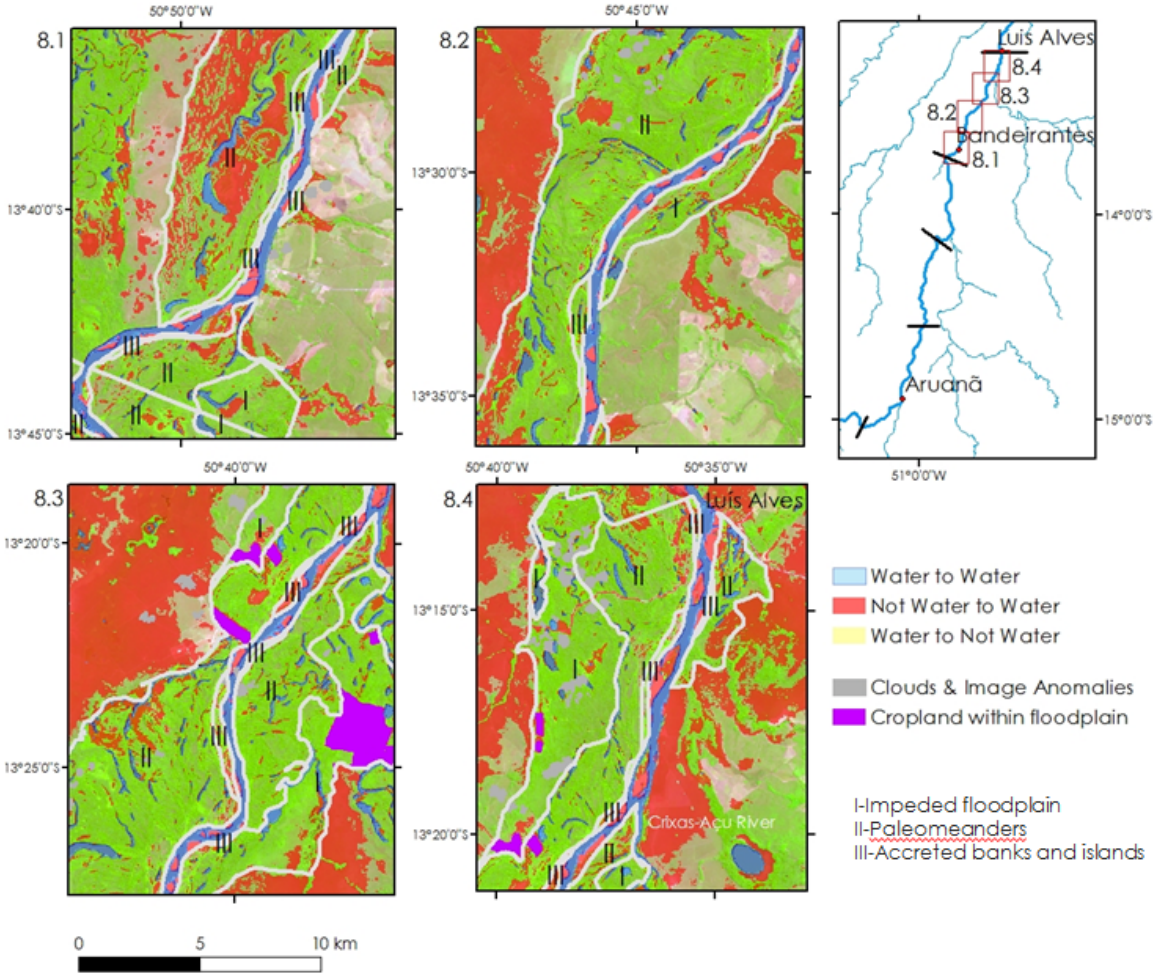

Figure 4.16. Change in open water area in segment 8. Each rectangle displays a portion of segment 8, from upstream (8.1) to downstream (8.4). Blue is water to water class, red is not water to water class, and yellow is water to not water class. Clouds and image anomalies and cropland within the floodplain are also indicated with gray and purple, respectively. Not water to not water class is shown with the background Landsat image from 20 July 1987 (bands 5-4-3). Geomorphologic units (I-III) are outlined in gray and labeled with Roman numerals, and river flow is to the north.

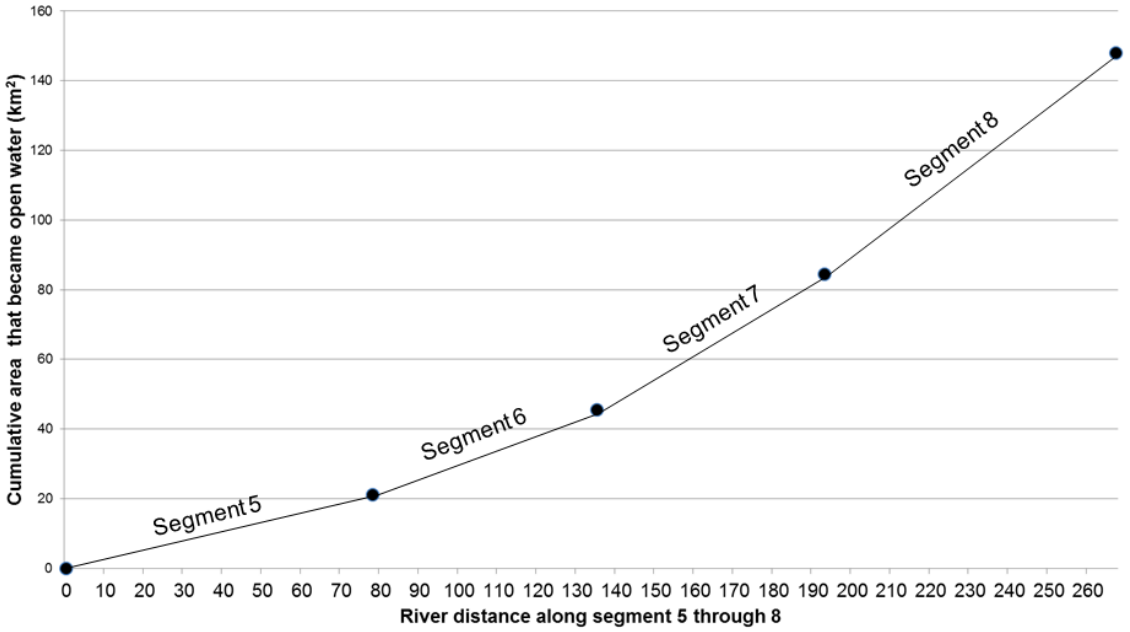

Figure 4.17. Cumulative area that became open water for each segment vs. river distance from segment 5 to 8.

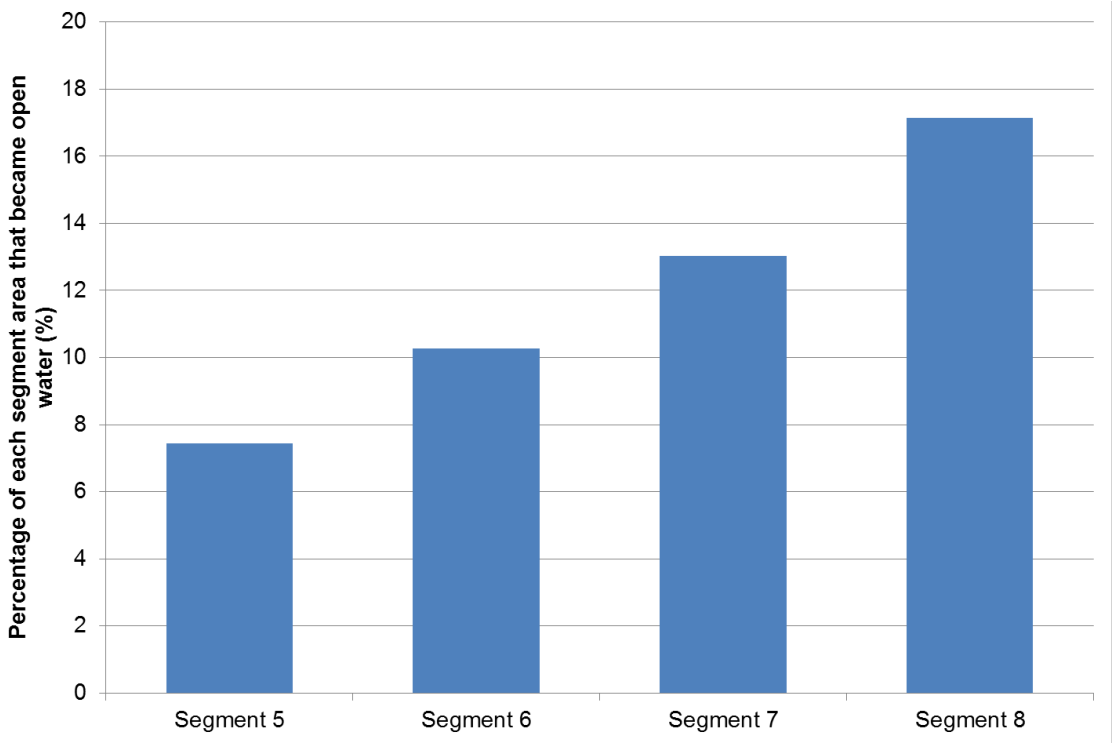

Figure 4.18. Percentage of each segment's floodplain area that became open water.

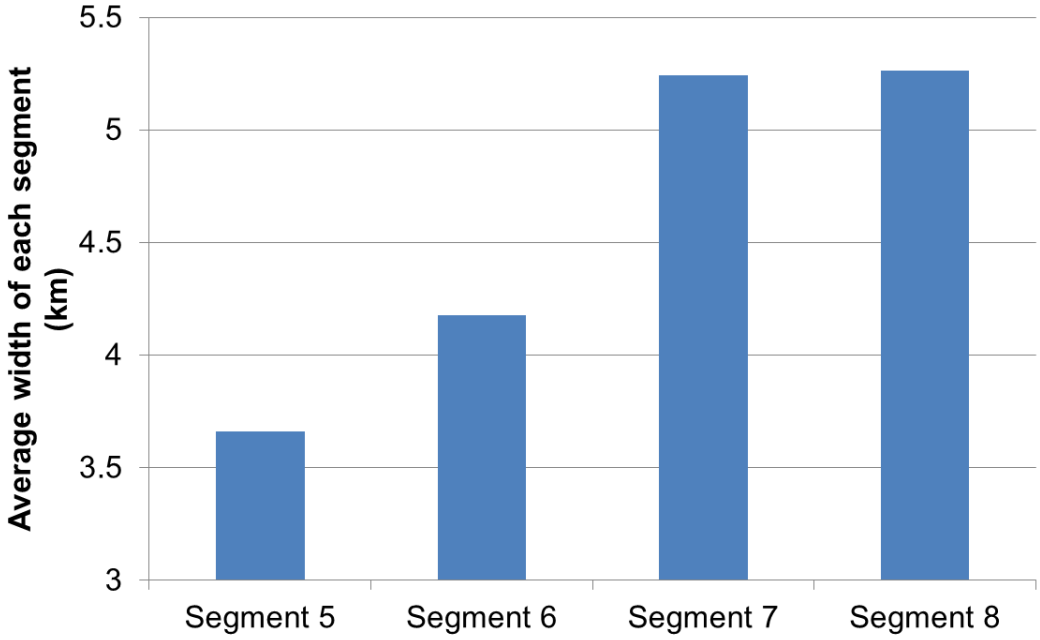

Figure 4.19. The average width of each segment analyzed.

Since the time of the wet season image is just after the peak discharge at Aruanã and is at or close to the peak discharge at Bandeirantes and Luís Alves, this trend in area that became open water change may partially reflect the passage of the flood wave along the reach. At Aruanã, the discharge at the time of the wet season image is below bankfull but above barfull, although 15 days prior to the image the river was above bankfull, peaking at 4914 m^3s^{-1}. This indicates that in segment 5, the river is not overtopping the banks in the wet season image at the Aruanã gauging station, but open water on the floodplain could be the result of overbank flooding that occurred 15 days prior to the image or through connections between floodplain water bodies and the main channel. In addition the riverAt Bandeirantes, peak discharge occurred 5 days prior to the image but is still above bankfull. Thus, overbank flooding is occurring at the time of the wet season image for Bandeirantes through Luís Alves, and likely for some distance upstream of Bandeirantes. The year 1988 is characterized as a type D1 flood (see Chapter 3), in

which reach 1 and reach 2 display divergent patterns of peak reduction. In this year, reach 2, which is encompassed by segment 8 (see Figure 4.1), displays peak discharge reduction of 20.7%, while reach 1 (segments 5-7) increases in peak discharge by 9.8%. The channel loss calculated over the flood wave crest is 0.67 km^3 for reach 2 and 1.53 km^3 for reach 2 including the tributary data, while there is no channel loss over the flood wave crest for reach 1 (Chapter 3). In addition, there are no channel losses over the flooding season, from November to May, for either reach. Thus, the greater area of "not water" to "water" change in reach 2 compared to reach 1 may also reflect a greater loss of peak discharge and channel loss to the floodplain in reach 2.

The number of lakes that are connected to the main river channel in the wet season and the dry season also likely influences the area that became open water in the wet season. Figure 4.20 shows the number lakes connected to the main river channel for each segment, in the dry season and the wet season images. These lakes include the lakes analyzed for morphometry above, but additional connections were counted beyond the 32 lakes analyzed in greater depth. Only one lake in segment 5 was connected with the main channel in the dry season, increasing to 3 connected lakes in the wet season. In segment 6, 2 floodplain lakes were connected to the main channel in the dry season, increasing to 7 in the wet season. Segment 7 shows the largest change in number of connected floodplain lakes, with 4 in the dry season and 19 in the wet season, and segment 8 also increased more than segments 5 and 6, with 4 connected lakes in the dry season and 13 connected lakes in the wet season. The higher number of lakes that became connected in the wet season could be caused by an increased number and a different distribution of lakes (e.g., more lakes closer to the channel) in the floodplain along these segments, compared to the other segments. The patterns in the number of lakes connected to the

channel may also explain the increase in the percentage of the floodplain that became open water from segment 5 to segment 8.

As demonstrated above, while there are some general trends in whether lakes expand a great deal in area in the wet season and contribute to the overall area that became open water for the segment, individual lakes display different patterns based on their morphology. In general, lakes such as abandoned channels, oxbows, and blocked valley lakes do not increase in area a great deal between the dry season and the wet season, although in the case of abandoned channels and blocked valleys they increase greatly in depth. However, the individual morphology also influences lakes of the same type, as in the case of Fuzil Lake (in segment 7) and Piedade Lake (segment 8), which are abandoned channel lakes that increased more in area compared with the other abandoned channel lake examples (see Table 4.5). Although each segment has a similar proportion of its floodplain covered by floodplain lakes in the dry season (seen through the similar percentages of floodplain area of the open water to open water class, Table 4.9), Figure 4.20 demonstrates that more floodplain lakes are connected to the main river channel in segments 7 and 8 than in segments 5 and 6, in the dry season and in the wet season. The number of lakes connected to the channel in the wet season and the dry season for reaches 1 and 2 is displayed in Table 4.10, along with the number of connected lakes normalized by channel length for each reach. While the normalized number of connected lakes is very similar between reaches 1 and 2, reach 2 is slightly higher than reach 1. The absolute number of lakes in Table 4.6 for reach 1 is much larger than for reach 2, as reach 1 is 170 km in length and reach 2 is 64 km in length.

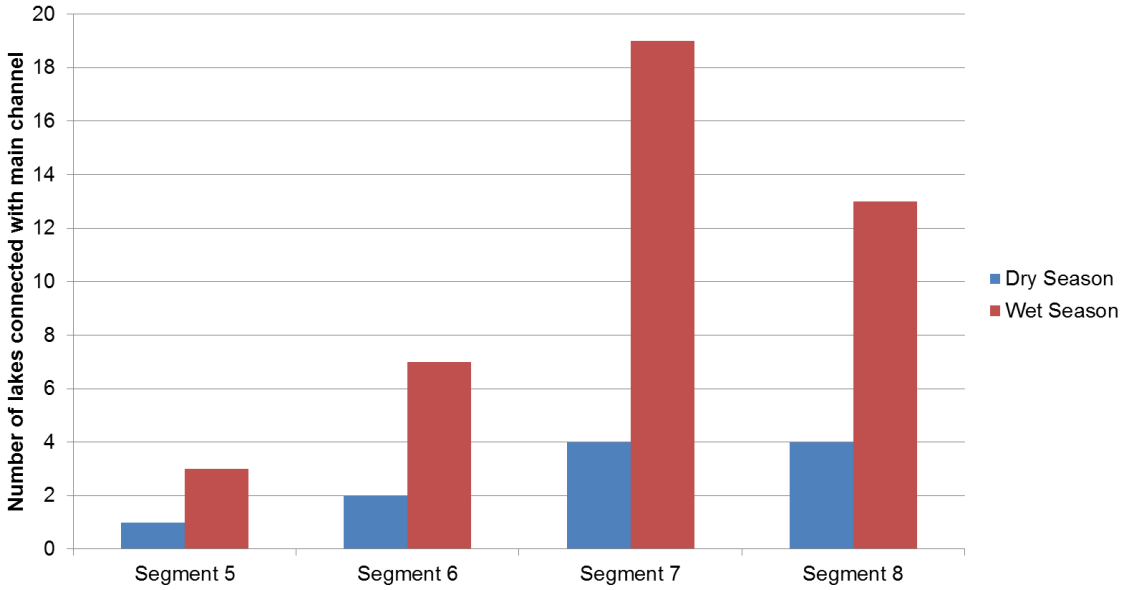

Figure 4.20. Number of connections between floodplain lakes and the main channel for each segment, in the wet season and the dry season.

Table 4.10. Number of connections between floodplain lakes and the main channel for reaches 1 and 2 and normalized by channel length (km) in the wet season and the dry season.

Reach	Number of connected floodplain lakes		Number of connected floodplain lakes per km of channel	
	Dry Season	Wet Season	Dry Season	Wet Season
1	7	27	0.0412	0.1588
2	3	12	0.0469	0.1875

The characteristics of the geomorphologic units and the proportion of each geomorphologic unit in the segments also likely influence the amount of open water area that is created on the floodplain in the wet season. Figure 4.21 shows the percentages of the each unit's area that became open water for each segment. The percentage of total floodplain area that became open water is the highest in unit III, the plain of accreted

banks and islands, in all of the segments. Unit III is the closest to the river channel and is the most influenced by channel processes (Latrubesse and Stevaux 2002). In all analyzed areas the percentage of water to water class is the lowest in unit III, demonstrating that unit III contains very few to no floodplain lakes like in the other two units, as it is a narrow band adjacent to the channel and is the most recently formed by fluvial processes (Tables 4.8 and 4.9). Units I and II have more floodplain lakes and a higher percentage of open water area that is maintained in dry season and the wet season (water to water class). Unit II has a higher percentage of its area that became open water in the wet season compared with unit I across all segments (Figure 4.21). The morphology in unit II is more pronounced than in unit I, which may influenced this difference. As the channel has migrated over time, point bar deposition in the convex side of meanders has resulted in meander scrolls, creating ridges and depressions within unit II, which can vary in elevation at times by up to 2 meters (Bayer 2002). These forms and the morphology in unit I are less pronounced because it has developed into a marshy environment due to the vertical accretion of fine, low energy sediment (Bayer 2002). Meander scroll lakes, among the additional types such as oxbow lakes, are a more common feature of unit II, although they can also be found in unit I (Morais et al. 2005). Blocked valley lakes and chained abandoned channel lakes are common in unit I (Morais et al. 2005). As seen in the descriptions of changes in lake morphometry, meander scroll lakes usually expand more in area than abandoned channel lakes and blocked valley lakes, although there are exceptions. This difference between open water areas between unit I and unit II may also influence the higher percentage of unit II that became open water. In addition, the characteristics of the sedimentary deposits of unit I and unit II, such as unit II being composed of more sandy sediment compared to unit I (Bayer 2002; see Chapter 2 description), may also play a role, although further information on these differences

would be needed to determine whether the differences in sedimentary deposits influence the difference in open water area between units I and II.

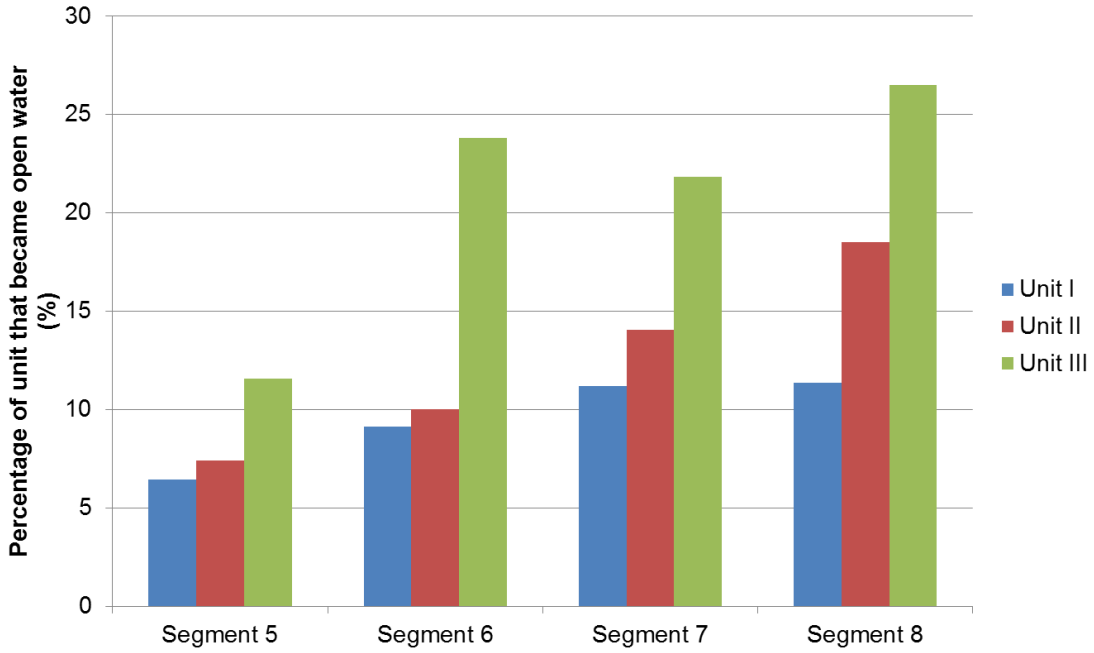

Figure 4.21. Percentage of each unit that became open water in segments 5 through 8. Unit III has the highest percentage of its area that became open water, followed by unit II and then unit I.

The higher percentage of the floodplain that became open water in segments 7 and 8 compared with segments 5 and 6 also could be influenced by the proportion of the geomorphologic units in each segment, along with the connections with floodplain lakes. Figure 4.22 plots the percentage of each segments area that is classified as each geomorphologic unit along with the percentage of the segment that became open water. The proportions of units I and II are pretty similar between segment 5 and segment 7, although the percentage of the floodplain area that became open water is 7.4% for segment 5 and 13.0% for segment 7. This indicates that the proportion of the

geomorphologic units may not influence the percentage of the floodplain that becomes open water in the wet season. However, from segment 6 to segment 8, the proportion of the floodplain that is unit I decreases, while the proportion of the floodplain that is unit II increases. There is also an increase in the percentage of the floodplain that became open water from segment 6 to segment 8.

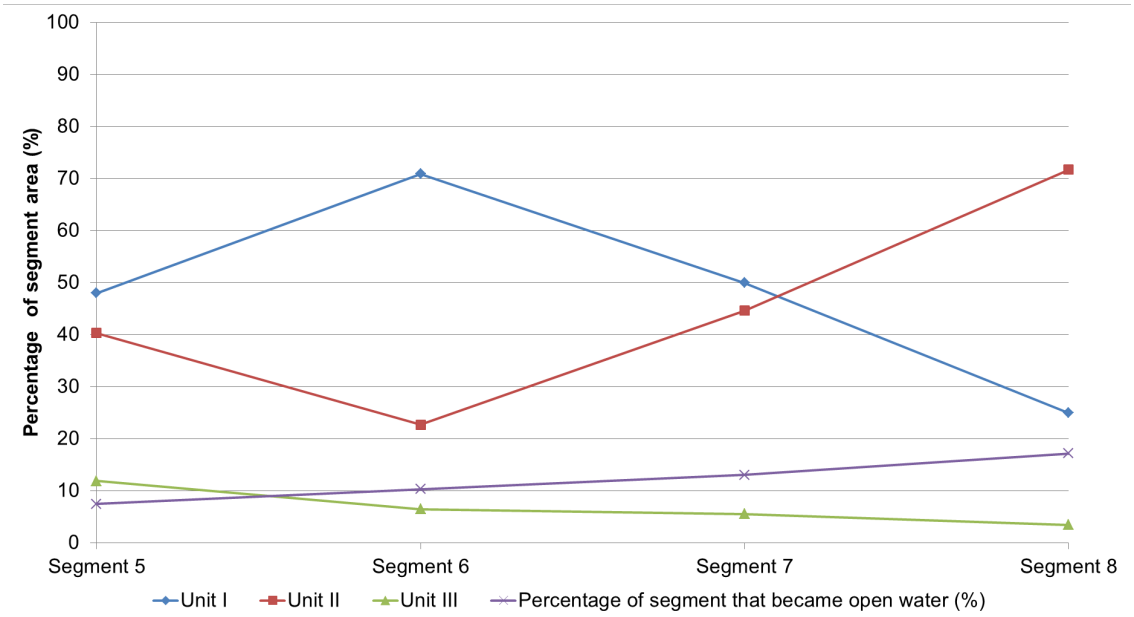

Figure 4.22. The percentage of each segment area that is each geomorphologic unit (I-III) plotted along with the percentage of the segment area that became open water.

The estimates of open water areas using the water index do not give estimates of the area of inundation, as this measurement is impeded by the canopy vegetation, but the water index can determine the changes in floodplain lakes and some of the surface water connections between the channel and the floodplain. Additional studies using different remote sensing data have investigated inundated areas, but the resolution of these data many times are not high enough to determine the spatial changes in lakes and the small

surface water pathways connecting the channel and floodplain lakes. For example, Hamilton et al. (2002) determine inundation patterns in the middle Araguaia River region, including the Bananal Island, finding large seasonal variations in inundation that align with the wet season. Hamilton et al. use passive microwave remote sensing with a spatial resolution of 27 km, while the width of the floodplain of the middle Araguaia River can be as small as 2 km or as large as 10 km. Accurate modeling of the floodplain environment requires adequate information on elevation for the floodplain, which is not available for the Araguaia River, but it has been applied in similar regions, such as the Upper Paraguay Basin (Paz et al. 2011).

Integrating peak reduction, channel losses, and assessments of lake morphometry and open water areas

After analyzing lake morphometry and the changes in open water areas along the river and between geomorphologic units in Chapter 4, the hydrologic analyses in Chapter 3 can be better explained, highlighting the need to place hydrologic analyses in a geomorphologic context. The changes in open water from the dry season in 1987 to the wet season in 1988 can be related to the patterns of channel losses and peak discharge reduction described in Chapter 3. It is clear that during the flooding season, the floodplain lakes expand in area and in depth, providing areas for storing the channel losses discussed in Chapter 3. Reach 2 had a greater percentage of its area that became open water compared to reach 1, with 17.5% of area that became open water compared to 10.6% in reach 1(Table 4.4). This difference provides support for the finding that reach 2 without the tributary data displays more channel losses compared to reach 1 without the tributary data, although different patterns of peak reduction and channel loss occur in different flooding years. In addition, the number of lakes that are connected to the main

river channel per kilometer of channel length is slightly higher for reach 2 compared with reach 1 (Table 4.6), which could contribute to higher channel losses in reach 2. Channel loss over the flood wave crest and peak reduction for reach 1 (which includes segments 5-7) may occur mostly in segment 7, as there are more lakes connected to the main river channel in the wet and dry season in this segment compared with segments 5 and 6. As described in Chapters 3 and 4, the different proportions of the geomorphologic units in reaches 1 and 2, particularly the increase in the proportion of unit II in reach 2, may influence greater channel losses and an increase in area that became open water in reach 2.

The year 1988 is a D1 flood type, and the reaches have displayed divergent patterns of peak reduction, with no channel losses for reach 1, a 0.67 km^3 loss for reach 2, and a 1.53 km^3 loss for reach 2 including the tributary data over the flood wave crest. The open water areas of reach 2 does not reflect the area of inundation, thus channel losses that occur during peak discharge in reach 2 could also be beneath the vegetation. In the change maps in Chapter 4 (e.g., Figure 4.16), areas adjacent to the river became open water but are not within the geomorphologic floodplain. This demonstrates that the area that channel losses could move into might be larger than the geomorphologic floodplain. Therefore, assessments in Chapter 3 of the height of water (e.g., 4 meters in the year 2000 and 15 meters in the year 1983) that would need to be stored in and on the area of the geomorphologic floodplain are likely overestimated, because additional areas adjacent to the channel and beyond the geomorphologic floodplain are not included.

Chapter 5: Conclusion

Summary of Analyses

This thesis adds to the literature on large tropical river systems by assessing hydrological patterns of flooding and changes in floodplain lakes and open water areas in a geomorphologic context. It has also contributed to previous knowledge of the main river draining the Brazilian *Cerrado*, shedding light on floodplain dynamics and the hydro-geomorphology of the channel-floodplain system. The geomorphology of the middle Araguaia River and its floodplain exerts physical controls on flooding patterns and the surface water connectivity between the river and floodplain lakes, and the spatial heterogeneity of the system provides a variety of ecological habitats.

In Chapter 3, analysis of peak discharge reduction and upstream discharge rate indicate that reductions in peak discharge are more prevalent during higher magnitude floods. Estimates of short-term channel losses during flooding peaks for reaches 1 and 2 allow for comparison of channel loss patterns between reaches, and the addition of tributary data for reach 2 provides an assessment of the contributions of tributaries to channel loss. Differing geomorphologic characteristics between reaches 1 and 2 likely influence the different patterns of peak reduction and channel loss between the two reaches, with reach 2 displaying larger channel losses compared to reach 1. Channel losses over the flood wave crest are not usually maintained for the duration of the flooding season, indicating that channel losses during peak discharge are temporary and the river regains these losses before the end of the flooding season. The analyses of flood wave types indicate that flood waves can be characterized into types displaying similar characteristics. The characterization of flooding patterns into different types mostly agrees with types described in previous literature.

In Chapter 4, the analyses of changes in floodplain lakes, pathways of surface water, and open water areas provides a geomorphologic context for the changes that are caused by annual flooding. The geomorphologic classification of the lakes, which is based on the process of formation, controls how lake morphometry changes from the wet season to the dry season. For example, abandoned channel lakes expand less in area from the dry season to the wet season compared to meander scroll lakes. The results of lake area and perimeter changes between the dry season of 1987 and the wet season of 1988 are similar to previous analyses using different study time periods. The similarities suggest that the floodplain lakes respond similarly to different river discharge levels, although data on depth measurements are unavailable for the years used by the present analyses. Changes in open water areas along the floodplain indicate that a greater percentage of the area of unit III, which is situated closest to the river channel and is most influenced by channel processes, became open water compared to units I and II. A greater percentage of the area of unit II became open water compared to unit I, which may be explained by the variable topography characteristic of unit II. The number of surface water connections along the river between the floodplain lakes and the main river channel varies, and these variations may help to explain the patterns of peak reduction and channel losses described in Chapter 3.

The net peak discharge reduction along the middle Araguaia River occurs during flooding despite large increases in drainage area and the input of tributaries. This has been observed mostly in arid systems or in systems with different geomorphologic characteristics. However, it may be that tropical wet-dry systems are understudied and peak discharge reduction during flooding in large river systems is more common than what is displayed in available literature. The many floodplain lakes that are connected to the river channel provide storage areas for channel losses during the flood wave, which

likely contributes to reduced peak discharge. The upper section of the Araguaia River flows on bedrock in a V-shaped valley, and the middle Araguaia River flowing through an alluvial floodplain. These geomorphologic differences between the upper and middle section may contribute to the loss of peak discharge observed along the middle Araguaia River by creating a high intensity flood wave at the upstream end of the middle Araguaia River, which reduces in peak discharge as it moves downstream due to floodplain storage. The strong seasonality of the tropical wet-dry climate also may play a role in causing peak discharge reduction by contributing to high intensity flood waves. Only one tributary flows into reach 1 and reach 2 of the Araguaia River, and these tributaries may not contribute very much river discharge relative to the amount of water that can be transferred to the floodplain during flooding. If this were the case, it could also contribute to peak discharge reduction along the main channel. Further work is needed, however, to fully explain the reasons for the hydrologic patterns of flooding displayed in the middle Araguaia River.

FUTURE WORK

In the future, a more complete characterization of the water budget described in Chapter 3 would result in more accurate measurements of channel loss. Estimates of groundwater fluxes could be made using various methods, for example with piezometers to determine the groundwater flow field, among other methods (e.g., Kalbus et al. 2006). Information on the water holding capacity of the floodplain could be explored by characterizing grain size and porosity, and measurements of precipitation and evaporation could be integrated into the water budget analysis. In addition, stage measurements could be made in floodplain lakes to characterize the relationship between river discharge rise

and changes in floodplain lakes. Assessments of the fluxes of water between the floodplain and the channel could be undertaken through modeling efforts. The full contributions of the tributaries could be modeled and included in main river channel modeling and water budget equations. Assessments of channel slope along the two reaches could potentially provide more information on additional geomorphologic greater channel losses occur in reach 2 compared with reach 1.

To enhance the analysis of changes in lake morphometry and open water areas, the same analysis should be done at similar discharge levels for each segment and reaches. This would allow for a controlled comparison between the segments, without the stage of the river influencing the analysis and the results. The analyses using Landsat data could also be compared with coarse resolution MODIS data, as MODIS data has a higher temporal resolution compared with Landsat. However, the coarser spatial resolution of MODIS would mean that small, thin floodplain lakes and surface water pathways would not be recognized. In addition, satellite imagery with a higher resolution than Landsat, such as GeoEye imagery, could be employed to better describe the spatial variations in lake morphometry and open water areas. The influence of floodplain vegetation should be further explored in future analyses, as vegetation type influences which areas become open water and the pathways that water has to travel onto the floodplain.

Future research on the Araguaia River should also expand on analyses of the impacts of land use change on the hydrology and geomorphology described in Chapter 2. The Appendix describes future research that will be conducted to determine floodplain sedimentation rates over the past 100 years, which encompasses the period of the rapid increase in land clearing within the watershed. This research could provide insight into whether land use changes have impacted floodplain sedimentation rates.

Appendix: Fieldwork conducted to determine floodplain sedimentation rates

Floodplain sedimentation is important for the delivery of nutrients and sediment to the floodplain ecosystem associated with the middle Araguaia River (Aquino et al. 2009). Researchers have estimated the rate of bedload and suspended sediment transport within the channel in the middle Araguaia River, but the rate of sediment delivery to the floodplain is currently unknown (Aquino et al. 2009; Latrubesse et al. 2009). Sediment cores collected in the floodplain of the Araguaia River in July 2012 will be analyzed using lead-210 geochronology, which can determine floodplain sedimentation rates over the past 100 years and has been used in other tropical watersheds (Aalto and Nittrouer 2012; Aalto et al. 2003). The research will also provide insight into whether the floodplain sedimentation rate has changed along with the increase in large-scale land clearing beginning in the 1970s.

Lead-210 is produced in the atmosphere by radioactive decay of radon-222 and falls out onto sediments through precipitation at a constant rate (Aalto et al. 2012; Stokes and Walling 2003). It then decays with a half-life of about 22 years and allows for dating sediments deposited in the last 100 years (Aalto et al. 2012; Stokes and Walling 2003). Lead-210 measured within sediment can be divided into two types: unsupported or excess lead-210, which comes from fallout from the atmosphere, and lead-210 produced in situ due to local decay of radium-226 (Stokes and Walling 2003). Measurements of unsupported lead-210 are used for dating because the unsupported portion indicates the portion in the sediment that the river has deposited from an upstream location. Unsupported lead-210 more readily associates itself with fine sediments, and thus

determining the grain size of sediments through grain size analysis is integral to measuring lead-210 within sediment cores (He and Walling 1996).

Lead-210 geochronology has been applied to the analysis of sedimentation rates in other tropical rivers. For example, Aalto et al. (2003) determined the sedimentation rates of the Beni and Mamore River floodplains in northern Bolivia. Evidence indicated that sedimentation pulses coincided with increases in precipitation and runoff due to wet La Niña conditions, although the geomorphic location of these samples was not fully described. Lead-210 geochronology has also been utilized for determining sediment accumulation of the Strickland River floodplain in Papua New Guinea and for small watersheds in Fiji (Aalto et al. 2008; Terry et al. 2011).

FIELDWORK DESCRIPTION

Fieldwork was conducted from July 24 to July 27, 2012 near the town of Aruanã (Figure A1). Fifteen short cores (<1 meter) were collected, and GPS points were recorded on a Garmin Etrex unit (accuracy of ±10 m) (Table A1). Cores were taken from levees, island levees, island interiors, a floodplain lake, and in the floodplain of Vermelho River tributary (Figure A1). In addition, a grab sample of sediment deposited during the last flood was taken to calibrate the lead-210 age model. Cores were transported to the Geology and Physical Geography lab at the Universidade Federal de Goiás (UFG), in Goiânia, Brazil.

Figure A1. Locations of cores (C1-C15) and grab sample (G1) during fieldwork in July 2013. Image shown is Landsat 5 Thematic Mapper, bands 5-4-3, from June 20, 2011. Geomorphic units (unit I-impeded floodplain; unit II-paleomeanders; unit III-accreted banks and islands; unit IV-tributary floodplains) are also noted in the figure.

Table A1. Locations of cores (C1-C15) and grab sample (G1) near Aruanã from fieldwork conducted in July 2012.

ID	Location	
C1	14° 50’ 17” S	51 °5’ 29.3” W
C2	14° 50’ 15.3” S	51° 5’ 26.7” W
C3	14° 51’ 29.9” S	51° 5’ 26.7” W
C4	14° 51’ 38.2” S	51° 5’ 23.5” W
C5	14° 52’ 10.6” S	51° 5’ 40” W
C6	14° 53 ’2.4” S	51° 5’ 43.2” W
C7	14° 56’ 49.1” S	51° 9’ 11” W
C8	14° 56’ 49.1” S	51° 9’ 10.9” W
C9	14° 56’ 49.6” S	51° 9’ 9.9” W
C10	14° 56’ 36.8” S	51° 8’ 54.6” W
C11	14° 56’ 33.8” S	51° 8’ 11.9” W
C12	14° 56’ 31.5” S	51° 5’ 51.4” W
C13	14° 56’ 9.4” S	51° 5’ 41.3” W
C14	14° 55’ 39.1” S	51° 5’ 21.4” W
C15	14° 55’ 39.1” S	51° 5’ 21.4” W
C16	14° 55’ 14.8” S	51° 5’ 2.2” W
C17	14° 55’ 14.9” S	51° 5’ 2.5” W

At the physical geography lab at UFG, the cores were split and photographed. One-centimeter increment samples were taken at various locations along the cores, focusing on the areas with the most clay content. The samples were weighed, dried at 100º C for 24 hours, and then weighed again after drying. They were then packaged and shipped to the University of Texas at Austin physical geography laboratory. The samples will be analyzed for lead-210 content with an ORTEC alpha spectrometer available in the University of Texas at Austin physical geography labs. Samples from sediment cores will also be used for grain size analysis. Figure A2 shows photos of the cores that were taken and will be analyzed in the future.

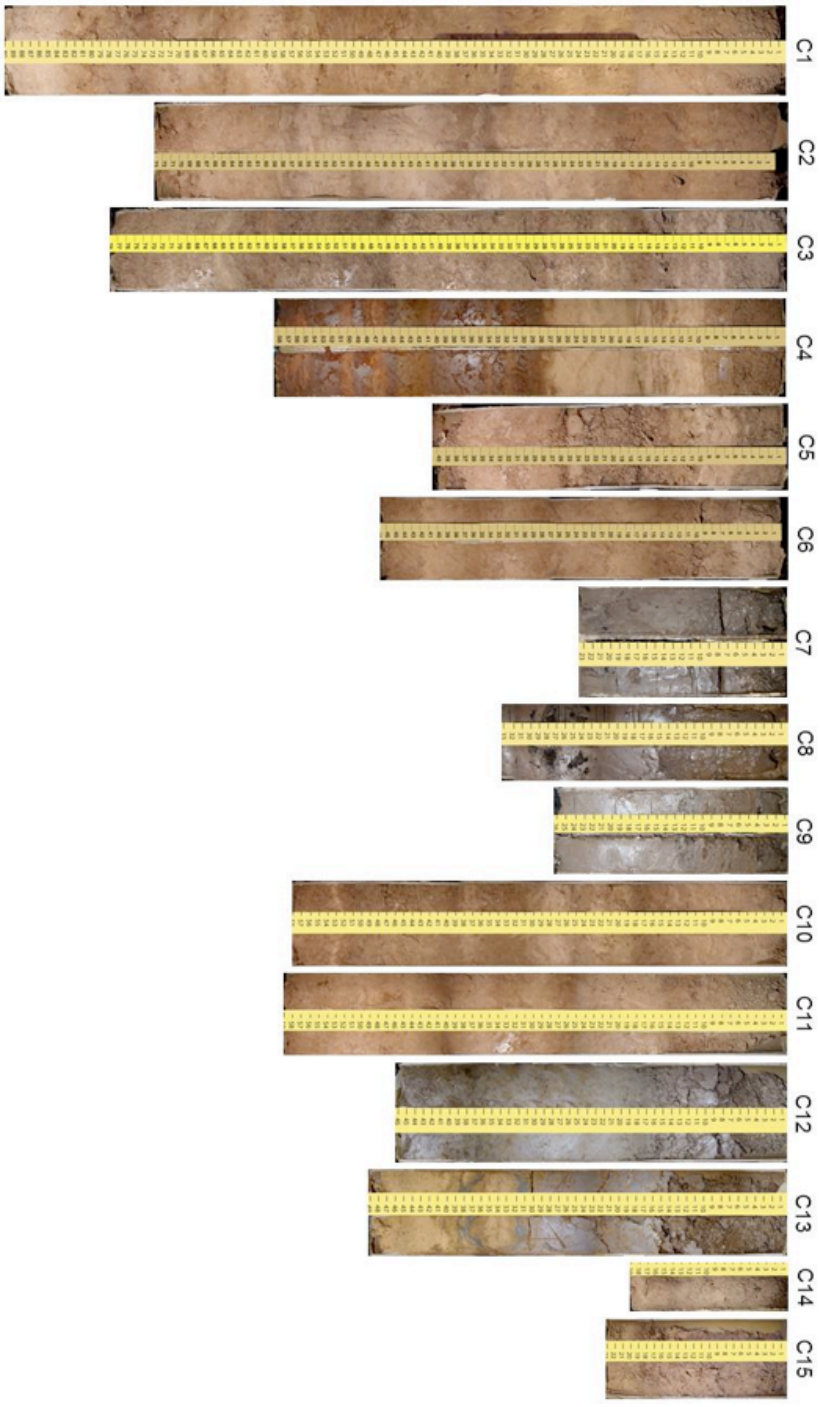

Figure A2. Photos of cores collected in July 2013 that will be used for lead-210 analysis. Numbers above cores correspond to the number in the map in figure A1.

References

Aalto, R., J.W. Lauer, and W.E. Dietrich. 2008. "Spatial and Temporal Dynamics of Sediment Accumulation and Exchange Along Strickland River Floodplains (Papua New Guinea) over Decadal-to-centennial Timescales." *Journal of Geophysical Research* 113: 1–22.

Aalto, R., L. Maurice-Bourgoin, T. Dunne, D.R. Montgomery, C.A. Nittrouer, and JL Guyot. 2003. "Episodic Sediment Accumulation on Amazonian Flood Plains Influenced by El Nino/Southern Oscillation." *Nature* 425: 493–497.

Aalto, R., and C.A. Nittrouer. 2012. "210Pb Geochronology of Flood Events in Large Tropical River Systems." *Philosophical Transactions of the Royal Society A: Mathematical, Physical and Engineering Sciences* 370: 2040–2074.

Agencia Nacional de Aguas. "Discharge Data." www.ana.gov.br.

Alsdorf, D., S. C. Han, P. Bates, and J. Melack. 2010. "Seasonal Water Storage on the Amazon Floodplain Measured from Satellites." *Remote Sensing of Environment* 114: 2448–2456.

Amoros, C., and G. Bornette. 2002. "Connectivity and Biocomplexity in Waterbodies of Riverine Floodplains." *Freshwater Biology* 47: 761–776.

Anderson, B.G., I.D. Rutherfurd, and A.W. Western. 2006. "An Analysis of the Influence of Riparian Vegetation on the Propagation of Flood Waves." *Environmental Modelling & Software* 21: 1290–1296.

Aquino, S., E.M. Latrubesse, and E.E. de Souza Filho. 2008. "Relações Entre o Regime Hidrológico e Os Ecossistemas Aquáticos Da Planície Aluvial Do Rio Araguaia." *Acta Scientiarum. Biological Sciences* 30: 361-369.

Aquino, S., E.M. Latrubesse, and M. Bayer. 2009. "Assessment of Wash Load Transport in the Araguaia River (Aruanã Gauge Station), Central Brazil." *Latin American Journal of Sedimentology and Basin Analysis* 16: 119–128.

Aquino, S., E.M. Latrubesse, and E.E. Souza Filho. 2009. "Caracterizacão Hidrológica e Geomorfológica Dos Afluentes Da Bacia Do Rio Araguaia." *Revista Brasileira de Geomorfologia* 10: 43-54.

Assine, M.L., and A. Silva. 2009. "Contrasting Fluvial Styles of the Paraguay River in the Northwestern Border of the Pantanal Wetland, Brazil." *Geomorphology* 113: 189–199.

Bayer, M. 2002. "Diagnostico dos processos de erosao/assoreamento na planicie aluvial do rio Araguaia, entre Registro do Araguaia (GP) e Cocalinho (MT)". Universidade Federal de Goiás.

Bonnet, M.P., G. Barroux, J.M. Martinez, F. Seyler, P. Moreira-Turcq, G. Cochonneau, J.M. Melack, et al. 2008. "Floodplain Hydrology in an Amazon Floodplain Lake (Lago Grande de Curuaí)." *Journal of Hydrology* 349: 18–30.

Bravo, J. M., D. Allasia, A. R. Paz, W. Collischonn, and C. E. M. Tucci. 2012. "Coupled Hydrologic-Hydraulic Modeling of the Upper Paraguay River Basin." *Journal of Hydrologic Engineering* 17: 635–646.

Castro, S.S., and J.P. Queiroz Neto. 2010. "Soil Erosion in Brazil from Coffee to the Present-day Soy Bean Production." In *Natural Hazards and Human-exacerbated Disasters in Latin-America: Special Volumes of Geomorphology*, edited by E.M. Latrubesse, 1st ed, 195–221. Developments in Earth Surface Processes 13. Amsterdam, The Netherlands; Boston, MA: Elsevier.

Charlton, R. 2007. *Fundamentals of Fluvial Geomorphology*. 1st ed. London: New York: Routledge.

Chen, J. L., C. R. Wilson, and B. D. Tapley. 2010. "The 2009 Exceptional Amazon Flood and Interannual Terrestrial Water Storage Change Observed by GRACE." *Water Resources Research* 46: 1-10.

Coe, M. T., E. M. Latrubesse, M. E. Ferreira, and M. L. Amsler. 2011. "The Effects of Deforestation and Climate Variability on the Streamflow of the Araguaia River, Brazil." *Biogeochemistry* 105: 119–131.

Costa, M. H, A. Botta, and J. A Cardille. 2003. "Effects of Large-scale Changes in Land Cover on the Discharge of the Tocantins River, Southeastern Amazonia." *Journal of Hydrology* 283: 206–217.

De Smith, M.J., M.F. Goodchild, and P.A. Longley. 2013. *Geospatial Analysis*. 4th ed. Winchelsea, UK: The Winchelsea Press.

Dingman, S. L. 2008. *Physical Hydrology*. Waveland PressInc.

Dunne, T., and L.B. Leopold. 1978. *Water In Environmental Planning*. Macmillan.

Ferreira Jr., P.D., and P.T.A. Castro. 2005. "Nest Placement of the Giant Amazon River Turtle, Podocnemis Expansa, in the Araguaia River, Goiás State, Brazil." *AMBIO: A Journal of the Human Environment* 34: 212–217.

Ferreira, M.E., L.G. Ferreira, E.M. Latrubesse, and F. Miziara. 2008. "High Resolution Remote Sensing Based Quantification of the Remnant Vegetation Cover in the Araguaia River Basin, Central Brazil." In *Geoscience and Remote Sensing Symposium, 2008. IGARSS 2008. IEEE International*, 4: IV–739.

Frappart, F., K. Do Minh, J. L'Hermitte, A. Cazenave, G. Ramillien, T. Le Toan, and N. Mognard-Campbell. 2006. "Water Volume Change in the Lower Mekong from Satellite Altimetry and Imagery Data." *Geophysical Journal International* 167: 570–584.

Frappart, F., F. Seyler, J.M. Martinez, J.G. León, and A. Cazenave. 2005. "Floodplain Water Storage in the Negro River Basin Estimated from Microwave Remote Sensing of Inundation Area and Water Levels." *Remote Sensing of Environment* 99: 387–399.

Gu, R., and M. Deutschman. 2001. "Hydrologic Assessment of Water Losses in River." *Journal of Water Resources Planning and Management* 127: 6–12.

Hamilton, S.K. 2010. "Biogeochemical Implications of Climate Change for Tropical Rivers and Floodplains." *Hydrobiologia* 657: 19–35.

Hamilton, S.K., S.J. Sippel, and J.M. Melack. 2002. "Comparison of Inundation Patterns Among Major South American Floodplains." *Journal of Geophysical Research* 107: 1-14.

He, Q., and D. E. Walling. 1996. "Interpreting Particle Size Effects in the Adsorption of 137Cs and Unsupported 210Pb by Mineral Soils and Sediments." *Journal of Environmental Radioactivity* 30: 117–137.

Jensen, J.R. 2004. *Introductory Digital Image Processing*. 3rd ed. Prentice Hall.

Jet Propulsion Laboratory. 2005. "Shuttle Radar Topography Mission." http://www2.jpl.nasa.gov/srtm/faq.html#penetration.

Ji, L., L. Zhang, and B. Wylie. 2009. "Analysis of Dynamic Thresholds for the Normalized Difference Water Index." *Photogrammetric Engineering and Remote Sensing* 75: 1307–1317.

Junk, W.J. 2004. "The Flood Pulse Concept: New Aspects, Approaches and applications-An Update." In *Symposium on the Management of Large Rivers for Fisheries Volume 2*, 117–140.

Junk, W.J., P.B. Bayley, and R.E. Sparks. 1989. "The Flood Pulse Concept in River-Floodplain Systems." In *Proceedings of the International Large River Symposium*, 110–127. Can. Spec. Publ. Fish. Aquat. Sci. 106. D.P. Dodge.

Kalbus, E., F. Reinstorf, and M. Schirmer. 2006. "Measuring Methods for Groundwater? Surface Water Interactions: a Review." *Hydrology and Earth System Sciences Discussions* 10: 873–887.

Klink, C.A., and R.B. Machado. 2005. "Conservation of the Brazilian Cerrado." *Conservation Biology* 19: 707–713.

Knighton, A.D., and G.C. Nanson. 1994. "Flow Transmission Along an Arid Zone Anastomosing River, Cooper Creek, Australia." *Hydrological Processes* 8: 137–154.

Lange, J. 2005. "Dynamics of Transmission Losses in a Large Arid Stream Channel." *Journal of Hydrology* 306: 112–126.

Latrubesse, E. M. 2012. “Amazon Lakes.” In *Lakes and Reservoirs*, edited by L. Bengtsson, R. Herschy, and R. Fairbridge, 13–26. Springer Verlag.

Latrubesse, E.M. 2008. “Patterns of Anabranching Channels: The Ultimate End-member Adjustment of Mega Rivers.” *Geomorphology* 101: 130–145.

Latrubesse, E.M., M.L. Amsler, R.P. De Morais, and S. Aquino. 2009. “The Geomorphologic Response of a Large Pristine Alluvial River to Tremendous Deforestation in the South American Tropics: The Case of the Araguaia River.” *Geomorphology* 113: 239–252.

Latrubesse, E.M., and T.M. de Carvalho. 2006. “Geomorfologia Do Estado de Goiás e Distrito Federal.” Série Geologia e Mineração. Goiânia – Goiás: Governo do Estado de Goiás.

Latrubesse, E.M., and E. Franzinelli. 2002. “The Holocene Alluvial Plain of the Middle Amazon River, Brazil.” *Geomorphology* 44: 241–257.

Latrubesse, E.M., and J.C. Stevaux. 2002. “Geomorphology and Environmental Aspects of the Araguaia Fluvial Basin, Brazil.” *Zeitschrift Fur Geomorphologie* 129: 109–127.

———. 2006. “Características Físico-bióticas e Problemas Ambientais Associados à Planície Aluvial Do Rio Araguaia, Brasil Central.” *Revista Geociências* 5: 65–73.

Latrubesse, E.M., J.C. Stevaux, and R. Sinha. 2005. “Tropical Rivers.” *Geomorphology* 70: 187–206.

Lee, H., R.E. Beighley, D. Alsdorf, H.C. Jung, C.K. Shum, J. Duan, J. Guo, D. Yamazaki, and K. Andreadis. 2011. “Characterization of Terrestrial Water Dynamics in the Congo Basin Using GRACE and Satellite Radar Altimetry.” *Remote Sensing of Environment* 115: 3530–3538.

Leopold, L.B., M.G. Wolman, and J.P. Miller. 1964. *Fluvial Processes in Geomorphology*. Series of Books in Geology. San Francisco: W. H. Freeman.

Lesack, L.F.W., and J.M. Melack. 1995. “Flooding Hydrology and Mixture Dynamics of Lake Water Derived from Multiple Sources in an Amazon Floodplain Lake.” *Water Resources Research* 31: 329–345.

Li, C., Z. Yang, G. Huang, Q. Tan, and Y. Cai. 2011. “Analysis of the Net Water Loss in the Main Reach of the Yellow River.” *International Journal of Environment and Pollution* 45: 249–267.

Manyari, W.V, and O.A. de Carvalho Jr. 2007. “Environmental Considerations in Energy Planning for the Amazon Region: Downstream Effects of Dams.” *Energy Policy* 35: 6526–6534.

Marchetti, Z.Y., E.M. Latrubesse, M.S. Pereira, and C.G. Ramonell. 2013. "Vegetation and Its Relationship with Geomorphologic Units in the Parana River Floodplain, Argentina." *Journal of South American Earth Sciences*.

Marinho, G. V., S. S. de Castro, and A. B. de Campos. 2006. "Hydrology and Gully Processes in the Upper Araguaia River Basin, Central Brazil." *Zeitschrift Fur Geomorphologie* 145: 119–145.

McFeeters, S.K. 1996. "The Use of the Normalized Difference Water Index (NDWI) in the Delineation of Open Water Features." *International Journal of Remote Sensing* 17: 1425–1432.

Mertes, L.A.K. 1997. "Documentation and Significance of the Perirheic Zone on Inundated Floodplains." *Water Resources Research* 33: 1749–1762.

Mertes, L.A.K., D.L. Daniel, J.M. Anderies, B. Nelson, L.A. Martinelli, and B.R. Forsberg. 1995. "Spatial Patterns of Hydrology, Geomorphology, and Vegetation on the Floodplain of the Amazon River in Brazil from a Remote Sensing Perspective." *Geomorphology* 13: 215–232.

Montero, J.C., and E.M. Latrubesse. 2013. "The Igapó of the Negro River in Central Amazonia: Linking Late-successional Inundation Forest with Fluvial Geomorphology." *Journal of South American Earth Sciences*.

Morais, R.P., S. Aquino, and E.M. Latrubesse. 2008. "Controles Hidrogeomorfológicos Nas Unidades Vegetacionais Da Planície Aluvial Do Rio Araguaia, Brasil." *Acta Sci. Biol. Sci.* 30: 411-421.

Morais, R.P., L.G. Oliveira, E.M. Latrubesse, and R.C. Diogenes Pinheiro. 2005. "Morfometria de Sistemas Lacustres Da Planície Aluvial Do Médio Rio Araguai a." *Acta Sci. Biol. Sci.* 27: 203–213.

Morais, R.P.A. 2006. "Planície Aluvial Do Médio Araguaia: Processos Geomorfológicos e Suas Implicações Ambientais." Universidade Federal de Goiás.

Myers, N., R.A. Mittermeier, C.G. Mittermeier, G.A.B. da Fonseca, and J. Kent. 2000. "Biodiversity Hotspots for Conservation Priorities." *Nature* 403: 853–858.

Nabout, J. C., I. S. Nogueira, and L. G. Oliveira. 2006. "Phytoplankton Community of Floodplain Lakes of the Araguaia River, Brazil, in the Rainy and Dry Seasons." *Journal of Plankton Research* 28: 181–193.

Nanson, G.C., and A.D. Knighton. 1996. "Anabranching Rivers: Their Cause, Character and Classification." *Earth Surface Processes and Landforms* 21: 217–239.

Paz, A. R., J. M. Bravo, D. Allasia, W. Collischonn, and C. E. M. Tucci. 2010. "Large-Scale Hydrodynamic Modeling of a Complex River Network and Floodplains." *Journal of Hydrologic Engineering* 15: 152–165.

Paz, A.R. da, W. Collischonn, C.E.M. Tucci, and C.R. Padovani. 2011. "Large-scale Modelling of Channel Flow and Floodplain Inundation Dynamics and Its Application to the Pantanal (Brazil)." *Hydrological Processes* 25: 1498–1516.

Pinheiro, R.T. 2007. "Avifauna Do Corredor de Biodiversidade Do Araguaia: Distribuição e Conservação Na Área de Proteção Ambiental Ilha Do Bananal/ Cantão." Edited by S. Merlin, D. Rezende, L. E. B. Leal, E. K. Pareja, and A. S. Pinto. *Revista Carbono Social* 1: 65–71.

Puckridge, J. T., F. Sheldon, K. F. Walker, and A. J. Boulton. 1998. "Flow Variability and the Ecology of Large Rivers." *Marine and Freshwater Research* 49: 55–72.

Richey, J.E., L.A.K. Mertes, T. Dunne, and R.L. Victo. 1989. "Sources and Routing of the Amazon River Flood Wave." *Global Biogeochemical Cycles* 3: 191–204.

Sano, E., R. Rosa, J. Brito, and L. Ferreira. 2010. "Land Cover Mapping of the Tropical Savanna Region in Brazil." *Environmental Monitoring and Assessment* 166: 113–124.

Sholtes, J., and M. Doyle. 2011. "Effect of Channel Restoration on Flood Wave Attenuation." *Journal of Hydraulic Engineering* 137: 196–208.

Silva França, A.M. da. 2002. "Ordenamento geomofologico dos sistemas lacustres da planicie aluvial do Rio Araguaia." Goiânia – Goiás: Universidade Federal de Goiás.

Tejerina-Garro, F.L., R. Fortin, and M.A. Rodríguez. 1998. "Fish Community Structure in Relation to Environmental Variation in Floodplain Lakes of the Araguaia River, Amazon Basin." *Environmental Biology of Fishes* 51: 399–410.

Terry, J.P., R. Lal, and Sitaram Garimella. 2011. "Assessing the Utility of 210Pb Geochronology for Estimating Sediment Accumulation Rates on River Floodplains in Fiji." *Singapore Journal of Tropical Geography* 32: 102–114.

The Ramsar Convention on Wetlands. 1997. "Information Sheet on Ramsar Wetlands."

Thoms, M.C. 2003. "Floodplain–river Ecosystems: Lateral Connections and the Implications of Human Interference." *Geomorphology* 56: 335–349.

Tockner, K., F. Malard, and J. V. Ward. 2000. "An Extension of the Flood Pulse Concept." *Hydrological Processes* 14: 2861–2883.

Trigg, M.A., P.D. Bates, M.D. Wilson, G. Schumann, and C. Baugh. 2012. "Floodplain Channel Morphology and Networks of the Middle Amazon River." *Water Resources Research* 48: 1-17.

Trigg, M.A., M.D. Wilson, P.D. Bates, M.S. Horritt, D.E. Alsdorf, B.R. Forsberg, and M.C. Vega. 2009. "Amazon Flood Wave Hydraulics." *Journal of Hydrology* 374: 92–105.

U.S. Geological Survey. 2013. "Frequently Asked Questions About the Landsat Missions." http://landsat.usgs.gov/descriptions_for_the_levels_of_processing.php.

Valente, C.R., and E.M. Latrubesse. 2012. "Fluvial Archive of Peculiar Avulsive Fluvial Patterns in the Largest Quaternary Intracratonic Basin of Tropical South America: The Bananal Basin, Central-Brazil." *Palaeogeography, Palaeoclimatology, Palaeoecology* 356–357: 62–74.

Valente, C.R., E.M. Latrubesse, and L.G. Ferreira. 2013. "Relationships Among Vegetation, Geomorphology and Hydrology in the Bananal Island Tropical Wetlands, Araguaia River Basin, Central Brazil." *Journal of South American Earth Sciences*.

Wohl, E. 2007. "Hydrology and Discharge." In *Large Rivers: Geomorphology and Management*, edited by A. Gupta, 29–44. Chichester, England; Hoboken, NJ. John Wiley & Sons.

Wohl, E., A. Barros, N. Brunsell, N.A. Chappell, M. Coe, T. Giambelluca, S. Goldsmith, et al. 2012. "The Hydrology of the Humid Tropics." *Nature Climate Change* 2: 655-662.

Wolman, M.G., and J.P. Miller. 1960. "Magnitude and Frequency of Forces in Geomorphic Processes." *The Journal of Geology* 68: 54–74.

Woltemade, C.J., and K.W. Potter. 1994. "A Watershed Modeling Analysis of Fluvial Geomorphologic Influences on Flood Peak Attenuation." *Water Resources Research* 30: 1933–1942.

Xu, H. 2006. "Modification of Normalised Difference Water Index (NDWI) to Enhance Open Water Features in Remotely Sensed Imagery." *International Journal of Remote Sensing* 27: 3025–3033.

Zwarts, L., N. Cisses, and N. Diallo. 2005. "Hydrology of the Upper Niger." In *The Niger, a Lifeline: Effective Water Management in the Upper Niger Basin*, edited by L. Zwarts, P. van Beukering, B. Kone, and E. Wymenga, 15–40. Lelystad, Netherlands: RIZA.